A STUDY OF TEMPERATURE CYCLING EFFECT ON THE VISCOELASTIC BEHAVIOUR OF NATURAL RUBBER

CHULEEKORN TANGJAI

A THESIS SUBMITTED IN PARTIAL FULFILLMENT
OF THE REQUIREMENTS FOR
THE DEGREE OF MASTER OF SCIENCE
(POLYMER SCIENCE AND TECHNOLOGY)
FACULTY OF GRADUATE STUDIES
MAHIDOL UNIVERSITY
2004

ISBN 974-04-5289-2
COPYRIGHT OF MAHIDOL UNIVERSITY

Copyright by Mahidol University

A STUDY OF TEMPERATURE CYCLING EFFECT ON THE VISCOELASTIC BEHAVIOUR OF NATURAL RUBBER

Chuleekorn T.
.....
Ms. Chuleekorn Tangjai
Candidate

C. Deeprasertkul
.....
Lect. Chudej Deeprasertkul,
Ph.D.
Major advisor

.....
Asst. Prof. Krisda Suchiva,
Ph.D.
Co-advisor

P. Tangboriboonrat
.....
Assoc. Prof. Pramuan Tangboriboonrat,
Ph.D.
Co-advisor

Rassmidara Hoonsawat
.....
Assoc. Prof.Rassmidara Hoonsawat,
Ph.D.
Dean
Faculty of Graduate Studies

Darapond T.
.....
Lect. Darapond Triampo
Ph.D.
Acting Chair
Master of Science Programme in
Polymer Science and Technology
Faculty of Science

Copyright by Mahidol University

A STUDY OF TEMPERATURE CYCLING EFFECT ON THE VISCOELASTIC BEHAVIOUR OF NATURAL RUBBER

was submitted to the Faculty of Graduate Studies, Mahidol University
for the degree of Master of Science (Polymer Science and Technology)

on

September 24, 2004

Chuleekorn. T.
.....
Ms. Chuleekorn Tangjai
Candidate

C. DEEPRASERTKUL
.....
Lect. Chudej Deeprasertkul,
Ph.D.
Chair

.....
Asst. Prof. Krisda Suchiva,
Ph.D.
Thesis Defence Committee

Sahasithiwat Somboon
.....
Mr. Somboon Sahasithiwat
Ph.D.
Thesis Defence Committee

P. TANGBORIBOONRAT
.....
Assoc. Prof. Pramuan Tangboriboonrat,
Ph.D.
Thesis Defence Committee

.....
Assoc. Prof. Rassmidara Hoonsawat,
Ph.D.
Dean
Faculty of Graduate Studies
Mahidol University

.....
Prof. Amaret Bhumiratana
Ph.D.
Dean
Faculty of Science
Mahidol University

Copyright by Mahidol University

ACKNOWLEDGEMENTS

The author would like to express her sincere gratitude to her advisor, Dr. Chudej Deeprasertkul, for his excellent supervision, inspiring guidance and encouragement throughout this research. She is grateful to Assoc. Prof. Dr. Pramuan Tangboriboonrat and Asst. Prof. Dr. Krisda Suchiva for their invaluable advice and helpful criticism. She is also thankful to Dr. Somboon Sahasithiwat for his helpful suggestions and comments for completion of this thesis.

She would like to thank Department of Chemistry, Faculty of Science, Mahidol University for the use of rubber mixer, two rolls mill, hydraulic hot press, tensile tester and dynamic mechanical analyser (DMA). She also would like to thank all the members of Chudej and Pramuan laboratory for their deeply-touched assistance and their helps in various way. For financial support during this research, she is so grateful to Faculty of Science, Mahidol University.

Finally, she takes this opportunity to express her gratitude to her lovely family for encouragement, understanding and giving her the best thing.

Chuleekorn Tangjai

Copyright by Mahidol University

A STUDY OF TEMPERATURE CYCLING EFFECT ON THE VISCOELASTIC BEHAVIOUR OF NATURAL RUBBER

CHULEEKORN TANGJAI 4436295 SCPO/M

M.Sc. (POLYMER SCIENCE AND TECHNOLOGY)

THESIS ADVISORS: CHUDEJ DEEPRASERTKUL, Ph.D., KRISDA SUCHIVA, Ph.D., PRAMUAN TANGBORIBOONRAT, Ph.D.

ABSTRACT

Rubber is employed as an engineering material for dynamic absorption applications such as a bridge bearings and an automobile parts. The repeated change in temperature in a cycle affects the viscoelastic behaviour of rubber. Therefore, relaxation behaviour under a temperature cycling process was investigated. Natural rubber (NR), with a high relaxation rate, was chosen as a model in this study. Important factors such as initial strain and crosslink density were controlled in order to simplify the investigation. The micro-tension apparatus was built in order to study the relaxation behaviour in the water environment because the heat conductivity in water is better than in air.

The relaxation behaviour of unfilled NR under the temperature cycling process was firstly investigated. William-Landel-Ferry theory was employed in this study in order to verify that both change in entropy and reduction in the internal viscosity could be considered as the explanation for the relaxation behaviour when the temperature was raised. However, the stress was dramatically decreased when the temperature was immediately reduced during the temperature cycling process. The difference in mobility of the rubber chains due to the non-equilibrium temperature over the rubber system caused a breakdown of physical interaction between elastomer-elastomer. Therefore, the stress relaxation behaviour could be accelerated by performing temperature cycling process. Cycling temperature repeatedly could reduce a large number of elastomer-elastomer interactions. Not only might physical interaction between elastomer and elastomer be diminished but chemical interaction might also be reduced when the temperature gradient of the temperature cycling is high enough. The effect of time interval of the temperature cycling on the relaxation behaviour was also studied. Only time interval in the second step of temperature cycling should be concerned when the rubber was operated under temperature cycling. Furthermore, the relaxation behaviour of the carbon black filled NR under temperature cycling was also studied. The reduction in stress due to the temperature cycling process was governed equally by the break down in elastomer-elastomer interaction, elastomer-filler interaction and filler-filler interaction. The temperature cycling technique was also employed to study the interaction between elastomer and filler in carbon black filled NR prepared by incorporating carbon black into latex NR (NR-Mast). The results indicated that the elastomer interacted with carbon black by the physical linkage.

KEY WORDS: STRESS RELAXATION BEHAVIOUR/ TEMPERATURE CYCLING/ VISCOELASTICITY

Copyright by Mahidol University

113 pp. ISBN 974-04-5289-2

การศึกษาสมบัติการหยุ่นหนืดของยางธรรมชาติภายใต้สภาวะการขึ้นลงของอุณหภูมิอย่างปั่นวัฏจักร (A STUDY OF TEMPERATURE CYCLING EFFECT ON THE VISCOELASTIC BEHAVIOUR OF NATURAL RUBBER)

ชุลีกร ตั้งใจ 4436295 SCPO/M

วท.ม. (วิทยาศาสตร์และเทคโนโลยีพอลิเมอร์)

คณะกรรมการควบคุมวิทยานิพนธ์: ชูเดช ดีประเสริฐกุล, Ph.D., กฤษฎา สุชีวะ, Ph.D., ประมวล ตั้งบริบูรณ์รัตน์, Ph.D.

บทคัดย่อ

ปัจจุบันยางได้นำไปใช้งานทางด้านวิศวกรรม โดยนำไปใช้งานทางด้านการรับแรงทางพลศาสตร์ ซึ่งสามารถเห็นได้ทั่วไปในชีวิตประจำวัน เช่น ยางรองคอสะพาน และ ยางที่เป็นส่วนประกอบยานยนต์ การเปลี่ยนแปลงอุณหภูมิในสภาวะการขึ้นลงของอุณหภูมิอย่างเป็นวัฏจักร ส่งผลต่อพฤติกรรมการหยุดหนืดของยาง ดังนั้นในงานวิจัยนี้จึงศึกษาผลของการขึ้นลงของอุณหภูมิอย่างปั่นวัฏจักรต่อพฤติกรรมการหยุ่นหนืดของยาง โดยเลือกศึกษายางธรรมชาติ ซึ่งมี relaxation rate สูง และศึกษาปัจจัยต่างๆที่ส่งผลต่อพฤติกรรมการ relax ตัวของยาง เช่น ระยะดึงยืดเริ่มต้น และ crosslink density ซึ่งในงานวิจัยนี้ศึกษาผลของการขึ้นลงของอุณหภูมิอย่างปั่นวัฏจักรต่อพฤติกรรมการหยุ่นหนืดของยางในน้ำ โดยใช้เครื่อง micro-tension ทำการทดสอบ

ดังนั้นเพื่อการเข้าใจผลที่เกิดขึ้นจากการศึกษาผลของการขึ้นลงของอุณหภูมิอย่างปั่นวัฏจักรต่อพฤติกรรมการหยุ่นหนืดของยางธรรมชาติ จึงทำการศึกษาผลที่เกิดขึ้นกับ WLF theory พบว่าผลที่เกิดขึ้นเป็นผลอันเนื่องมาจากการแข่งขันระหว่าง Entropy effect กับ การลดลงของ Internal viscosity โดยการเปลี่ยนแปลงอุณหภูมิในสภาวะการขึ้นลงของอุณหภูมิอย่างเป็นวัฏจักรจะทำให้ stress ลดลง อันเนื่องมาจากการทำลายแรงยึดเหนี่ยวทางกายภาพระหว่าง ยางกับยาง ดังนั้นการเปลี่ยนแปลงอุณหภูมิในสภาวะการขึ้นลงของอุณหภูมิอย่างเป็นวัฏจักรจะเร่งการ relax ตัวของยางมากขึ้น และยิ่งจำนวนการขึ้นลงของอุณหภูมิอย่างเป็นวัฏจักรมากขึ้นการทำลายแรงยึดเหนี่ยวทางกายภาพระหว่างยางกับยางมากขึ้นด้วย นอกจาก นี้การทำลายแรงยึดเหนี่ยวทางเคมียังสามารถเกิดขึ้นได้ เมื่ออุณหภูมิในสภาวะการขึ้นลงของอุณหภูมิอย่างเป็นวัฏจักร หรือ Temperature gradient มากพอ และพบว่าเวลาช่วงที่มีอุณหภูมิสูงของสภาวะการขึ้นลงของอุณหภูมิอย่างเป็นวัฏจักร ส่งผลต่อพฤติกรรมการหยุดหนืดของยาง โดยทั่วไปการใช้งานยางมักมีการเติมสารเติมแต่งเพื่อเพิ่มความแข็งแรง เช่น เขม่าดำ หรือที่เรียกว่า carbon black จากการศึกษาผลของการเปลี่ยนแปลงอุณหภูมิในสภาวะการขึ้นลงของอุณหภูมิอย่างเป็นวัฏจักรในยางที่มีการเติมเขม่าดำ พบว่าพฤติกรรมการหยุ่นหนืดของยางจะถูกควบคุมโดยแรงยึดเหนี่ยวระหว่างยางกับยาง แรงยึดเหนี่ยวระหว่างยางกับเขม่าดำ และ แรงยึดเหนี่ยวระหว่างเขม่าดำกับเขม่าดำ ซึ่งผลของการขึ้นลงของอุณหภูมิอย่างเป็นวัฏจักร จะส่งผลต่อแรงยึดเหนี่ยวระหว่างยางกับยาง แรงยึดเหนี่ยวระหว่างยางกับเขม่าดำ และ แรงยึดเหนี่ยวระหว่างเขม่าดำกับเขม่าดำ ในสัดส่วนที่เท่ากัน และจากผลการศึกษาสามารถพิสูจน์ได้ว่าการเตรียมยางที่เติมเขม่าดำ โดยวิธี masterbatch แรงยึดเหนี่ยวระหว่างยางกับเขม่าดำน่าจะเป็นแบบกายภาพเป็นส่วนใหญ่

Copyright by Mahidol University

113 หน้า ISBN 974-04-5289-2

CONTENTS

Page

ACKNOWLEDGEMENTS……..……..iii

ABSTRACT……...iv

LIST OF TABLES……...x

LIST OF FIGURES……...….xii

LIST OF ABBREVIATIONS…….……...xvii

CHAPTER

1 INTRODUCTION……..……1

2 LITERATURE REVIEW……..……5

2.1 Theory of rubber like elasticity……..5

2.1.1 Thermodynamics of elastomer deformation……...5

2.1.2 Statistical theory of rubber deformation……..…7

2.2 Theory of linear viscoelasticity……..12

2.2.1 The Maxwell Model……...13

2.2.2 Zener Model……...15

2.3 Dynamic Mechanical Properties……19

2.3.1 Effect of strain amplitude on the dynamic mechanical properties of carbon black filled elastomer……..……..21

2.3.2 Effect of carbon black on the dynamic mechanical properties of elastomer……...……22

2.3.3 Effect of oil on the dynamic mechanical properties of elastomer…….22

2.3.4 Effect of crosslink density on the dynamic mechanical properties……23

2.3.4.1 Chemical method……...23

2.3.4.2 Physical method…….25

2.4 Stress relaxation behaviour…….26

2.4.1 Measurement of stress relaxation…….27

Copyright by Mahidol University

CONTENTS (Continued)

Page

2.4.1.1 Physical relaxation…….27
2.4.1.2 Physical relaxation…….29
2.4.2 Effect of temperature on the stress relaxation behaviour……...29
2.4.3 Effect of temperature cycling on the stress relaxation behaviour…….32
2.5 The mechanism of carbon black reinforcement…….34
2.5.1 Bound rubber model…….35
2.5.2 Mechanical interaction model…….35
2.5.3 Physical interaction model…….36
2.5.4 Chemical interaction model…….36
2.6 Mechanism of elastomer deformation……...37
2.6.1 Chain breakage……...38
2.6.2 Molecular slippage……38
2.6.3 Filler-filler linkage breakdown……..39
2.6.4 Sulphur linkage breakdown……39

3 OBJECTIVES OF THIS STUDY……....40

4 MATERIALS AND METHODS…….41
4.1 Apparatus…….. 41
4.2 Materials and Chemical Additives……42
4.3 Preparation of rubber sheet from high ammonia natural rubber latex (NR)……...44
4.3.1 Preparation of rubber sheet from natural rubber latex……..44
4.3.2 Preparation of CB/NR masterbatch……..44
4.4 Preparation of rubber compound……..45
4.5 Cure Characteristic Measurement……..48
4.6 Compression Moulding……49

Copyright by Mahidol University

CONTENTS (Continued)

Page

4.7 Physical properties measurement……..50
4.8.1 Total solid content……..…….50
4.8.2 Dry rubber content…….....50
4.7.3 Density Measurement…….……..51
4.7.4 Crosslink density measurement ……..…….51
4.8 Rheological properties measurement ……..……..54
4.9 Mechanical properties measurement ……..…...…..55
4.9.1 Dynamic mechanical analysis…….…….55
4.9.2 Micro-tension apparatus…….……...56
5 RELAXTION BEHAVIOUR OF ELASTOMER……..……..……57
5.1 Effect of crosslink density on the relaxation behaviour……59
5.2 Effect of initial strain on the relaxation behaviour……60
5.3 Effect of water on the stress relaxation behaviour…….……....61
5.4 Effect of carbon black on the relaxation behaviour……..……..63
5.4.1 Amount of carbon black……...63
5.4.2 Surface area of carbon black……64
6 EFFECT OF THE TEMPERATURE CYCLING ON STRESS RELAXATION BEHAVIOUR OF ELASTOMER…….…….……..……..66
6.1 Effect of temperature cycling on the stress relaxation behaviour of unfilled natural rubber……..……66
6.2 Effect of temperature gradient in temperature cycling condition on the stress relaxation behaviour of unfilled natural rubber..……..78
6.3 Effect of time interval in temperature cycling condition on the stress relaxation behaviour of unfilled natural rubber…….84
6.3.1 Time interval in the first step of temperature cycling……...84
6.3.2 Time interval in the second step of temperature cycling……..87

Copyright by Mahidol University

CONTENTS (Continued)

Page

6.4 Effect of the temperature cycling process on the stress relaxation behaviour of carbon black filled natural rubber……..88
7 CONCLUSIONS……..……..101
REFERENCE……..……....103
APPENDIX ...……....108
BIOGRAPHY……..…….113

Copyright by Mahidol University

LIST OF TABLES

Table Page

2.1 Parameters characterizing temperature dependence of a_T……...31
for various polymer systems
4.1 Trade mark of the instrument are used throughout this study……41
4.2 The chemical reagents are used throughout this study……42
4.3 The materials and chemical additives are used throughout this study……43
4.4 The rubber formulations of different type of interaction
between CB and NR……44
4.5 The rubber formulations with different amount of carbon black……46
4.6 The rubber formulations with different amount of sulfur……...46
4.7 The rubber formulations with different type of carbon black……46
4.8 The mixing condition of different type of interaction
between CB and NR used in this study……...47
5.1 DMA testing condition for study of the effect of temperature
cycling on dynamic mechanical behaviour of elastomer……58
5.2 The surface area of the different type of CB……...64
6.1 The temperature cycling steps for unfilled NR……..….67
6.2 Log a_T of unfilled natural rubber at a specific temperature……70
6.3 The temperature cycling steps for unfilled NR……...78
6.4 The temperature cycling steps for unfilled NR of
the changing time in the region at 25 °C……...…..85
6.5 The temperature cycling steps for unfilled NR of
the changing time in the region at 50 °C……87
6.6 The step of the temperature cycling process for the investigation
the effect of amount of CB in temperature cycling processes on
the stress relaxation behaviour……89

Copyright by Mahidol University

LIST OF TABLES (Continued)

Table Page

6.7 The temperature cycling step for the investigation the effect of interaction between CB and rubber under temperature cycling processes……..96

Copyright by Mahidol University

LIST OF FIGURES

Figure Page

2.1 Maxwell model……...13
2.2 Zener model……15
2.3 Sinusoidally varying simple shear: strain and stress decomposed into in-phase and out-of-phase components……...19
2.4 Stress relaxation of natural rubber at 30°C and 50% elongation at various cross-link densities……28
2.5 Comparison between creep behaviour of rubber when the temperature is cycled between 40°C and 60°C and the long term creep of rubber at 40°C at a fix stress that results in an approximate initial 50% pre-strain……...33
2.6 The stress relaxation of NR after 5% extension with an intermediate temperature change……34
4.1 Internal mixer 0.5L……..45
4.2 Two rolls mill……..45
4.3 Brabender……47
4.4 Schematic design of the oscillating disk rheometer……48
4.5 Rheometer cure curve……49
4.6 Wabash Genesis Series Hydraulic Press, G30H……49
4.7 Electronic Densimeter (MD-200S Mirage)……51
4.8 INSTRON extensometer……52
4.9 Dimensions of the tensile specimen……52
4.10 Stress-strain behaviour of unfilled NR……53
4.11 The reduced stress (Φ) against the inverse of extension ratio (λ^{-1}) of NR-2.5S……53
4.12 Mooney Shearing Disk Viscometer……..54
4.13 Dynamic Mechanical Analyser (DMA)……55
4.14 Micro-tension……56

Copyright by Mahidol University

LIST OF FIGURES (Continued)

Figure Page

5.1 The effect of CB loading in the effect of temperature cycling on dynamic mechanical properties……58
5.2 The relationship between the relaxation rate (sec^{-1}) and the crosslink density of unfilled NR……....60
5.3 The relationship between calculated long term relaxation rate and initial strain (%) of unfilled NR…..……..61
5.4 The relationships between stress relaxation and time of unfilled NR determined in water medium and in air medium…….……62
5.5 The relationships between relaxation rate at specific time of unfilled NR for both determined in water medium and in air medium……...62
5.6 The relationships between stress relaxation rate (sec^{-1}) and different amounts of carbon black (phr)……..63
5.7 The relationship between calculated long term relaxation rate and surface area of carbon black……65
6.1 The stress relaxation of unfilled NR as a function of time under the temperature cycling condition……68
6.2 Stress relaxation rate of unfilled NR at different temperature……69
6.3 The relationship between $(T - T_r) / \log a_T$ and $T - T_r$ of unfilled NR……..…..69
6.4 The stress relaxation of unfilled NR at 50 % elongation under the temperature cycling condition from 25 °C to 50 °C and then back to 25 °C in the water environment……..70
6.5 The relationship between calculated relaxation rate at 50°C from temperature cycling condition and calculated relaxation rate at 50°C using WLF approach……..71
6.6 The relationship between calculated relaxation rate at 25°C from temperature cycling condition and calculated relaxation rate at long term 25°C…….……...72

Copyright by Mahidol University

LIST OF FIGURES (Continued)

Figure Page

6.7 Comparison between the stress relaxation behaviour at 50°C from temperature cycling condition and the stress relaxation behaviour at long term 25°C……..73
6.8 Comparison between the stress relaxation behaviour at 25°C from temperature cycling condition and the stress relaxation behaviour at long term 25°C……...74
6.9 The stress relaxation of unfilled NR as a function of time under the temperature cycling condition…….75
6.10 The relationship between calculated relaxation rate at 50°C from temperature cycling condition and number of cycles……..76
6.11 The relationship between calculated $R_{25L/25C}$ from temperature cycling condition and number of cycles……...76
6.12 The stress relaxation of unfilled NR at 50% elongation under the temperature cycling from 25°C to 40°C and then back to 25°C in the water environment…….....78
6.13: The stress relaxation of unfilled NR at 50% elongation under the temperature cycling from 25°C to 50°C and then back to 25°C in the water environment……79
6.14 The stress relaxation of unfilled NR at 50% elongation under the temperature cycling from 25°C to 60°C and then back to 25°C in the water environment……79
6.15 The stress relaxation of unfilled NR at 50% elongation under the temperature cycling from 25°C to 80°C and then back to 25°C in the water environment……....80
6.16 The relationship between R_{600} and the temperature gradient (°C)……...80
6.17 The stress relaxation of unfilled NR as a function of time under the temperature cycling condition……..82

Copyright by Mahidol University

LIST OF FIGURES (Continued)

Figure Page

6.18 The relationship between $R_{\Delta s}$ and the temperature gradient (°C)……82
6.19 The relationship between relaxation rate (sec^{-1})
and the temperature gradient (°C)……..…...83
6.20 The relationship between $R_{25L/25C}$ and the temperature gradient (°C)…..……84
6.21 The relationship between calculated $R_{\Delta S}$ and time (min)……..85
6.22 The relationship between calculated relaxation rate (sec^{-1}) and (min)……..86
6.23 The relationship between calculated log $R_{25L/25C}$ and time (min)……..…86
6.24 The relationship between calculated log $R_{25L/25C}$ and time (min)……88
6.25 The stress relaxation of unfilled NR as a function of time
under the temperature cycling condition…….….89
6.26 The stress relaxation of NR-10CB as a function of time
under the temperature cycling condition……..90
6.27 The stress relaxation of NR-30CB as a function of time
under the temperature cycling condition……..……..90
6.28 The stress relaxation of NR-60CB as a function of time
under the temperature cycling condition……..91
6.29 The relationship between calculated relaxation rate (sec^{-1})
at 25°C in the first step of the temperature cycling
process and the amount of CB (phr)……..…91
6.30 The relationship between calculated relaxation rate (sec^{-1})
at 50°C in the second step of the temperature cycling process
and the amount of CB (phr)…….….92
6.31 The relationship between calculated $R_{(C/T)}$ in the first step
of the temperature cycling process and the amount of CB (phr)…….93
6.32 The relationship between calculated $R_{(C/T)}$ in the second
step of the temperature cycling process and the amount of CB (phr)……..…93

Copyright by Mahidol University

LIST OF FIGURES (Continued)

Figure Page

6.33 The relationship between calculated $R_{\Delta S}$ under the temperature cycling process and the amount of CB (phr)……....94
6.34 The relationship between calculated $R_{25L/50C}$ under the temperature cycling process and the amount of CB (phr)……..94
6.35 The relationship between calculated R_f under the temperature cycling process and the amount of CB (phr)……95
6.36 The stress relaxation of NR-Conv as a function of time under the temperature cycling condition……..97
6.37 The stress relaxation of NR-Mast as a function of time under the temperature cycling condition……..97
6.38 Comparison between the relaxation rate at 25°C in the first step of the temperature cycling condition and the different type of interaction between CB and rubber……..98
6.39 Comparison between the relaxation rate at 50°C in the second step of the temperature cycling condition and the different type of interaction between CB and rubber……..99
6.40 Comparison between the relaxation rate at 25°C in the third step of the temperature cycling condition and the different type of interaction between CB and rubber……..…99

Copyright by Mahidol University

LIST OF ABBREVIATIONS

ASTM	= The American Society of Testing Materials
CB	= Carbon black
DCP	= Dicumyl peroxide
DRC	= Dry rubber content
DMA	= Dynamic Mechanical Analyser
MBTS	= 2-mercaptobenzothiazole disulfide
max	= Maximum
min	= Minute
NR	= Natural rubber
phr	= Parts per hundred rubber
6PPD	= N-1,3-dimethylbutyl-N'-phenyl p-phenylenediamine
r.p.m.	= Revolutions per minute
sec.	= Second
TMTD	= Tetramethylthiouram disulfide
TSC	= Total solid content
v/v	= Volume by volume
w/v	= Weight by volume
w/w	= Weight by weight
ZnO	= Zinc oxide

Copyright by Mahidol University

CHAPTER 1
INTRODUCTION

The rubber product is widely applied in many manufacture such as tire, belt, hose, footwear, ball and cables. The component of tire such as tread, sidewall, inner liner can be produced by Natural rubber (NR), Styrene butadiene rubber (SBR) and Butyl rubber (IIR). The source of rubber is first known as the large forest tree of Hevea brasiliensis which occurs in the southern equatorial region of America. The use of rubber for waterproofing garments was first noted by Pizarro in 1540. In 1826. Faraday found an empirical formula of (C_5H_8) for natural rubber [1,2]. In 1910, Harries, Pickles discovered the structure formulation of natural rubber in the cis-1,4 configuration [2] whose the molecular weight is in the region of million. Natural rubber is known to contain not only cis-1,4-polyisoprene but a few percentage non-rubber material such as proteins, carbohydrates and lipids. Proteins in natural rubber have been regarded as reactive substance to produce branching by reaction with abnormal groups [3] and act as an essential component to lead the outstanding properties of natural rubber [4]. However, Ichikawa found that the proteins do not participate in the fundamental properties of natural rubber [5]. The long chain fatty acid groups linked to rubber molecule as phospholipids are the major abnormal groups to form branch-point and gel in natural rubber [6]. Since Natural rubber has a good mechanical and dynamic propertie, it can be used in the manufacture of tire for car, truck and plane. However, it is poor oil, cold and hot resistant and gas permeability. Therefore, the strength, hardness, abrasion resistance and elasticity of natural rubber product are necessarily improved by adding reinforcing fillers such as carbon black (CB) and vulcanizing agent such as sulfur and dicumyl peroxide (DCP) into the rubber.

Moreover, it was reported that 2% of naturally occurring proteins in NR can sensitize atopic persons and cause allergy [7-8]. Therefore, deproteinized natural rubber (DPNR) was produced. Two long chain fatty acid ester group per rubber

Copyright by Mahidol University

chain application in the manufacture of dipped products requiring special electrical properties [2].

In 1910, Perkin produced butadiene which could be polymerized to yield rubber. Then, in 1914, Kondakoff, Butlerow, Ostromislensky and Lebedev who were produced butadiene as early as 1910 and whose works played an important part in the development of the synthetic rubber industry. Most synthetic rubber are produced in two main stages. In 1930, I.G. Farbenindustrie produced styrene butadiene rubber (SBR) which was prepared from butadiene and styrene by using emulsion polymerization. Styrene butadiene rubber is a general purpose rubber which is employed in industries especially in tire. The double bond in the butadiene unit is slightly less active than that in isoprene. It still respond sulfur vulcanization and attack by oxygen. Therefore, the temperature limits placed on the NR products apply similarly to the SBR products, and the same compounding principles apply. SBR has the high hysteresis and greater heat build up in cyclic deformation. It shows a far greater loss of strength than NR at elevated temperature. Thus, SBR is not used for truck tires but it is usually used as an engineering rubber such as tire treads for car, gum, flooring, rubber shoe soles, electrical insulation and hoses.

In 1935, the polymerization of isobutyl to give a rubbery but non vulcanized rubber was produced by Standard Oil Co.. Then, in 1939 Thomas produced IIR (butyl rubber) which could be produced at low price by the cationic low temperature copolymerization of isobutylene in the presence of a small amount of isoprene (10%) [9]. The random copolymer chain contains a low concentration of isolated double bonds which assure a low crosslink density. However, butyl rubber can not be prevulcanized by radical prevulcanization because butyl rubber can generate tertiary free radical which is high stability. Therefore, in this study, sulfur is chosen as vulcanizing agent. Butyl rubber has good chemical inertness, low gas permeability, less sensitive to oxidation aging than most other elastomers, better ozone resistance than natural rubber and good solvent resistance. Therefore, butyl rubber is widely employed for inner tubes and as a sealant [9].

In tyre tread compounding, the tyre rolling loss has long been neglected as an area of scientific concern in favour of other tyre performance characteristics. However, the priorities of tyre manufacturers have changed as a result of increasing

Copyright by Mahidol University

environmental concern. The tyre industry is now aspiring to reduce the rolling loss of a tyre in service. This has been in part already achieved by an increase in the understanding of the general principles governing the energy loss in tyres. It has been shown by Willett [10] that a decrease in the storage modulus (E″) of 30% corresponds to a decrease of 27-50% in the tyre's rolling loss. In general, tyre rolling loss is responsible for 3-7 % of the fuel consumption for a passenger car and 12-15% for a fully loaded heavy truck. While several factors including tyre-road friction are known to contribute to the rolling loss in the tyre, it is generally agreed that hysteresis loss are dominant. Approximately 90 % of the tyre's rolling loss [10] may be attributed to the viscoelastic behaviour of the cord and rubber components of the tyre materials. A reduction in a tyre's rolling loss can be achieved by using a lower hysteresis loss compound such as an oil extended elastomer, however these may lower other aspects of the tyre's performance. An example is given for both rolling loss and cornering stiffness of tyres [11] having top treads with different oil and carbon black levels. If the carbon black content is held at a constant level, an increase in oil content reduces the tyre's rolling loss and reduces cornering stiffness. The reduction in the cornering stiffness is partly due to the softening effect of oils on tread compounds. In practice, this can be increased again by increasing the cross-link density. In general, modification of the temperature dependence of the dynamic visco-elastic properties of a rubber compound provides a means of tailoring a rubber compound for a particular application. In particular there is a need to control the dynamic mechanical loss properties as a function of temperature [12]. The dynamic behaviour of the filled elastomer was studied as a function of temperature [13]. The results indicated that dynamic loss modulus decreased when the temperature was increased. The reduction in the stress due to the breakdown of the interactions affected the viscoelastic behaviour. The failure of the linkage might arise from the poor temperature controlling in the experimental system. The temperature was repeatedly changed in a small range before reaching the design temperature in the temperature environment chamber. The unexpected reduction in creep due to this temperature cycling process was studied by Deeprasertkul [14]. It was apparent that the reduction might result from additional relaxation occurring in the carbon black elastomer interface. The study of the viscoelastic behaviour under the temperature

Copyright by Mahidol University

cycling may reveal the information about elastomer-filler interaction which can be used to improve the properties of the rubber product.

Copyright by Mahidol University

CHAPTER II
LITERATURE REVIEW

Rubber is usually used for application in which it undergoes rapid cyclic deformation at a rang of frequency such as the tread or the sidewall of a rotating tire, a bridge bearing and an automobile part. Therefore, designing products for these applications are important, a theory of rubber like elasticity can be used to explain the relationship between the load and the deformation.

2.1 Theory of rubber like elasticity

A theory of the elastic behaviour of rubber is established by Treloar [15-16], Gee [17], Rivlin [18]. The development of statistical kinetic theory is based on the elastic retraction force which results from the configuration change in the molecular network during the deformation of the elastomer.

2.1.1 Thermodynamics of elastomer deformation

The thermodynamic behaviour of elastomer can be explained by the Gough-Joule effect [16]. The first law of the thermodynamic defines the change in the internal energy. It is written down in the equation 2.1.

$$dU = dQ - dW \qquad (2.1)$$

where, dQ is the heat absorbed by the system

dW is the work done by the external force

dU is the change in the internal energy of the system

Copyright by Mahidol University

This theory assumes that the deformation of the elastomer is a reversible process. The second law of the thermodynamic for reversible process defines the entropy change. It is written down in the equation 2.2.

$$TdS = dQ \tag{2.2}$$

where, T is the temperature

dS is the entropy change of the system

For the deformation at a constant temperature, the total work can be expressed in term of the force and the extension. It is shown in the equation 2.3.

$$dW = F\,dl \tag{2.3}$$

where, F is the force

dl is the extension

In the tension mode, the force can be expressed as the sum of two terms which is written in the equation 2.4.

$$F = \left(\frac{\partial U}{\partial l}\right)_T - T\left(\frac{\partial S}{\partial l}\right)_T \tag{2.4}$$

The first law of the thermodynamic represents the change in internal energy and the second law of the thermodynamic represents the entropy change per unit increase in the length can be rewritten down in the equation 2.5.

$$\left(\frac{\partial S}{\partial l}\right)_T = -\left(\frac{\partial F}{\partial T}\right)_l \tag{2.5}$$

Copyright by Mahidol University

The relation in the equation 2.4 and 2.5 can be rewritten in the equation 2.6.

$$F = \left(\frac{\partial U}{\partial l}\right)_T + T\left(\frac{\partial F}{\partial T}\right)_l \quad (2.6)$$

The thermodynamic theory is a basic theory for statistic development of the kinetic theory of rubber elasticity which is explained in the next topic.

2.1.2 Statistical theory of rubber deformation

The statistical theory is developed from the basic concept of the kinetic theory of rubber elasticity and thermodynamic theory. The chain molecule of the elastomer can be represented by using random coil model. When the extension is increased, the entropy of the rubber system is decreased. Thus, the required force for the deformation of the elastomer relates to the entropy change. The root mean square of the end to end distance for single elastomer molecule, $\left(\bar{r}^2\right)^{1/2}$ is the first specified parameter in order to understand this theory. The second parameter is the probability, P(r) which is the distance between both ends of the molecule equals a specified length, r. This theory assumes that the carbon bonds along the backbone of the molecule are free from rotation. The distribution of molecule end to end lengths can be calculated by Gaussian statistic theory [19]. It is written in the equation 2.7.

$$P(r)\,dr = \left(\frac{b^3}{\pi^{3/2}}\right)\exp\left[-b^2\,r^2\right]4\pi r^2\,dr \quad (2.7)$$

where, b is considered to be characteristic of particular chain.

The square root of the number of links in the chains is proportional to the probable end to end length of the random chain. It can be written in the equation 2.8 [20].

Copyright by Mahidol University

$$r = \left(\frac{2n}{3}\right)^{1/2} l_1 = \left(\frac{1}{b}\right) \quad (2.8)$$

where, l_1 is the length

n is the number of links of length l_1 in the chain

Therefore, from equation 2.8, the square root of the number of links in the chains is proportional to the root mean square length like the most probable length. It is written in the equation 2.9.

$$\left(\bar{r}^2\right)^{1/2} = n^{1/2} l_1 \quad (2.9)$$

Equation 2.7 allows the entropy of a single chain to be calculated by using the Boltzmann relationship from statistical thermodynamics which is written in the equation 2.10.

$$S = k \ln \Omega \quad (2.10)$$

where, k is the Boltzmann's constant

Ω is the number of possible conformations the chain can adopt

It can be assumed that Ω will be proportional to the probability density P(r). Therefore, the entropy can be rewritten in the equation 2.11.

$$S = -k_b b^2 r^2 + c \quad (2.11)$$

where, c is the constant

Copyright by Mahidol University

The entropy decreases with an increase in the end to end separation for the molecular chain. The internal energy term is ignored. Therefore, the force, F, required to separate the two chain ends by amount of r, can be rewritten in the equation 2.12.

$$F = \left(\frac{dW}{dr}\right) = -T\left(\frac{dS}{dr}\right) \quad (2.12)$$

Thus, from Equations 2.11 and 2.12, the extension force of the single chain can be determined by the equation 2.13. It is the Gaussian statistical theory.

$$F = 2k_b T b^2 r = \frac{3k_b T r}{nl^2} \quad (2.13)$$

This Gaussian statistical model of a single chain molecule is used to explain the rubber elasticity at small extensions. However, the rubber elasticity at large extensions can be explained by the Non- Gaussian statistical theory. When the carbon atom along the elastomer chain are aligned, the stretching carbon-carbon bonds and the finite extensibility of the elastomer molecule is reached. Kuhn [21] extended the statistical theory by the distribution of the angles between the individual links of the chain when its ends are fixed by using an inverse Langevin function, L (r/nl). It is written in the equation 2.14.

$$L(r/nl) = 3\left(\frac{r}{nl}\right) + \frac{9}{5}\left(\frac{r}{nl}\right)^3 + \frac{297}{175}\left(\frac{r}{nl}\right)^5 + \frac{1539}{875}\left(\frac{r}{nl}\right)^7 + \ldots, \quad (2.14)$$

Thus, the entropy of the single chain for large extension can be rewritten in the equation 2.15.

$$S = c_2 - kn\left[\frac{r}{nl} L(r/nl) + \ln\left(\frac{L(r/nl)}{\sinh(L(r/nl))}\right)\right] \quad (2.15)$$

Copyright by Mahidol University

In addition, the extension force in the non-Gaussian statistical theory can be expressed by the equation 2.16.

$$F = \frac{kT}{l} L(r/nl) \qquad (2.16)$$

If the fraction chain extension is not greater than one-third, the equation 2.16 corresponds with the Gaussian statistic theory. Therefore, the statistical properties of chain over a wide range of the extensions can be represented by a chain of randomly jointed links. The statistical theory of a single molecule chain can derive the elasticity of the molecular network. It is assumed that the network between two crosslinked points can be modeled as a single chain and is fixed at its mean position. In order to consider the deformation of elastomer, it assumes that the chain is deformed to the same principal extension ratio because it is more convenient to use extension ratios λ_1, λ_2, λ_3 rather than inifinitesimal strains [20]. Therefore, the consideration of the global deformation for the entire network can express the change in the entropy of a single chain by the equation 2.17.

$$\Delta S = -k_b b^2 \left[\left(\lambda_1^2 - 1\right)\bar{x}^2 + \left(\lambda_2^2 - 1\right)\bar{y}^2 + \left(\lambda_3^2 - 1\right)\bar{z}^2 \right] \qquad (2.17)$$

where, $\bar{x}$, $\bar{y}$ and $\bar{z}$ are the axes of the strain co-ordinates.

λ_1, λ_2 and λ_3 are the extension ratio in $\bar{x}$, $\bar{y}$ and $\bar{z}$ co-ordinates, respectively.

The root mean square of the chain length between crosslinks in the unstrained state of the network is the same as the mean square of the single chain. Therefore, the change in the entropy can be expressed by the equation 2.18.

$$\Delta S = -\frac{1}{2} N k_b \left(\lambda_1^2 + \lambda_2^2 + \lambda_3^2 - 3\right) \qquad (2.18)$$

where, N is the number of chain per unit volume

Copyright by Mahidol University

N is assumed that there is no change in the internal energy of the system on deformation, Thus, W = -TΔS which is written in the equation 2.19.

$$W = -\frac{1}{2}Nk_bT\left(\lambda_1^2+\lambda_2^2+\lambda_3^2-3\right) \quad (2.19)$$

This equation can be rewritten in the equation 2.20.

$$W = -\frac{1}{2}G\left(\lambda_1^2+\lambda_2^2+\lambda_3^2-3\right) \quad (2.20)$$

where, G is the elastic constant which can be calculated by the equation 2.21.

$$G = Nk_bT = \frac{\rho RT}{M_c} \quad (2.21)$$

where, ρ is the density of rubber.

R is the gas constant, 8.31 $J.mol^{-1}.K^{-1}$.

M_c is the number average molar mass of the chain length between crosslinks.

The elastomer is usually used as an engineering material which its mechanical properties is the important topic. The stress-strain behaviour can be explained by using statistical theory. The force per unit cross-section area required to deform the network in uniaxial tension which can be calculated by the equation 2.22.

$$F = G\left(\lambda-\frac{1}{\lambda^2}\right) \quad (2.22)$$

The consideration of a non-Gaussian distribution at large deformations can be applied to the model to include a prediction of the finite extensibility effects. It can be

Copyright by Mahidol University

expressed by the equation 2.23 [22]. This equation at small extension corresponds with the Gaussian statistical theory.

$$F = Nk_bT\left(\lambda - \frac{1}{\lambda^2}\right)\left[1 + \frac{3}{25n}\left(3\lambda^2 + \frac{4}{\lambda}\right) + \frac{297}{6125n^2}\left(5\lambda^2 + 8\lambda + \frac{8}{\lambda^2}\right) + ...\right] \quad (2.23)$$

The statistical theory is a basic theory of rubber-like elasticity which can be used to explain most of elasticity theory such as theory of linear viscoelasticity which is reviewed in the next section.

2.2 Theory of linear viscoelasticity [23]

The theory of linear viscoelasticity is the phenomenology. It can be used for predicting behaviour under certain circumstances such as creep behaviour, stress relaxation behaviour and dynamic mechanical properties. The model of this theory can be represented in spring and dashpot. The spring is described by the modulus G_u. It is written in the equation 2.24.

$$\gamma = \frac{\sigma}{G_u} \quad (2.24)$$

where, γ is the strain

σ is the stress

G_u is the modulus

The spring may be described by the compliance J_u. It is written in the equation 2.25.

$$\gamma = \sigma J_u \quad (2.25)$$

When the strain rate in the dashpot is multiplied by the dashpot coefficient η, It equals the instantaneous stress. The stress can be written by the equation 2.26.

Copyright by Mahidol University

$$\sigma = \eta \frac{d\gamma}{dt} \quad (2.26)$$

where, η is the viscosity

$\frac{d\gamma}{dt}$ is the strain rate ($\dot{\gamma}$)

The time-dependent mechanical behaviour of polymer can be explained by Maxwell and Zener model [23].

2.2.1 The Maxwell Model [23]

This model can be used to explain time-dependent mechanical behaviour of viscous material. It consists of a spring and a dashpot in series as shown in Figure 2.1.

Figure 2.1: Maxwell model

The strain γ in the system is described in term of the strain in the spring (γ_1) and the strain in the dashpot (γ_2) which can be calculated by the equation 2.27. The stress in series will be identical in each one which can be calculated by the equation 2.28.

Copyright by Mahidol University

$$\gamma = \gamma_1 + \gamma_2 \tag{2.27}$$

$$\sigma = \sigma_1 = \sigma_2 \tag{2.28}$$

The equation 2.24 and the equation 2.25 can be rewritten by equation 2.29 for the spring and the dashpot, respectively.

$$\frac{d\sigma}{dt} = G_u \frac{d\gamma_1}{dt} \quad \text{and} \quad \sigma = \eta \frac{d\gamma_2}{dt} \tag{2.29}$$

The equation 2.29 can be calculated by the equation 2.30 which is used for Maxwell Model.

$$\frac{d\gamma}{dt} = \frac{1}{G_u}\frac{d\sigma}{dt} + \frac{\sigma}{\eta} \tag{2.30}$$

This model is used to predict the exponential stress relaxation of the elastomer, where the strain is kept constant over a period of time. Therefore, the equation 2.30 can be rewritten as the equation 2.31.

$$\frac{d\sigma}{\sigma} = -\frac{G_u}{\eta} dt \tag{2.31}$$

This can be integrated if at $t = 0$, $\sigma = \sigma_0$ and so

$$\sigma = \sigma_0 \exp\left(-\frac{t}{\tau_0}\right) \tag{2.32}$$

Copyright by Mahidol University

where, σ_0 is the initial stress

τ_0 is the relaxation time , $\frac{\eta}{G_u}$

This model is used to predict the stress relax completely over a long period.

2.2.2 Zener Model [23]

This model can be posed in two ways which is shown in Figure 2.2. The horizontal parallel line in Figure 2.2 indicate elements which have constant strain: e.g. J_d and η.

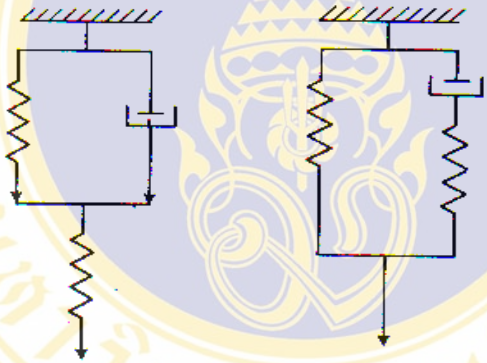

Figure 2.2: Zener model

The Zener Model is used to derive the differential equation describing the relationship between σ, γ, $\dot{\sigma}$ and $\dot{\gamma}$. It is shown in the equation 2.33.

$$\gamma - \sigma J_u = J_d (\sigma - \sigma_1) \qquad (2.33)$$

where, σ_1 is the stress in the dashpot

$$\frac{1}{J_R}\left[\gamma + \tau_\sigma \frac{d\gamma}{dt}\right] = \sigma + \tau_\gamma \frac{d\sigma}{dt} \qquad (2.34)$$

Copyright by Mahidol University

$$J_R = J_u + J_d \tag{2.35}$$

$$\tau_\sigma = J_d + \eta \tag{2.36}$$

$$\tau_\gamma = \tau_\sigma \left(\frac{J_u}{J_R} \right) \tag{2.37}$$

where, τ_σ is the time constant

τ_γ is the time constant

t is the time

The Zener model can be used to describe the creep and the stress relaxation behaviour. However, in this study, the effect of temperature cycling on stress relaxation behaviour is investigated. Thus, the modulus at time G(t) is described in term the stress relaxation. It is shown in the equation 2.38.

$$G(t) = G_u - (G_u - G_R)\left\{1 - \exp\left[-\left(\frac{t}{\tau_\gamma} \right) \right]\right\} \tag{2.38}$$

where, G_u is the modulus in spring

G_R is the modulus at equilibrium stress

The stress relaxation curve at ageing time can be fitted with the Kohlrausch - Williams – Watts stretched exponential function [24-26]. It is written in the equation 2.39. In this equation, β is used for describing shape of relaxation curve which is equal to 0.5 for most of the polymers [26].

$$E(t) = E_0 \exp\left[-\left(\frac{t}{\tau} \right)^{\beta} \right] \tag{2.39}$$

Copyright by Mahidol University

where, E(t) is the modulus at time

E_0 is the modulus at t = 0, the unrelaxed modulus

τ is the characteristic relaxation time

β is the constant

The stress relaxation behaviour of elastomer at long time was investigated by Chasset and Thirion [28]. They recognized a representation of their data which was given by the equation 2.40. The stress was reduced at the equilibrium value. It could be expressed in term the isothermal relaxation modulus E(t). The equation 2.40 is used for temperature which no chemical reaction or degradation occurs during the experiment. In addition, it is sometime used for estimating the equilibrium modulus E_q from stress relaxation experiments. From the equation 2.40, the value of m in most system is approximately 0.1.

$$E(t) = E_q\left[1+\left(\frac{t}{\tau_0}\right)^{-m}\right] \qquad (2.40)$$

where, E(t) is the isothermal relaxation modulus

E_q is the equilibrium modulus

t is the long time

m is the material parameter

τ_0 is the relaxation time

Plazek [28], Dickie and Ferry [29] observed that viscoelastic curve at fixed crosslink density displayed conventional time-temperature superposition behaviour [30]. This implies that E_q and τ_0 in the equation 2.40 depend on temperature. It can be rewritten in the equation 2.41. Plazek [28] observed a power law dependence of a_x on crosslink density. It is rewritten in the equation 2.42.

Copyright by Mahidol University

$$\tau_0(T,\nu) = \tau_0(T_0,\nu_0)\, a_T\, a_x \qquad (2.41)$$

where, T_0 is the reference temperature

ν_0 is the crosslink density at reference temperature

a_T is the shift factor for temperature

a_x is the shift factor for crosslink density

$$a_x = \left(\frac{\nu}{\nu_0}\right)^{-x} \qquad (2.42)$$

where, ν is the crosslink density at temperature

x is the Plazek exponent

Moreover, the effect of crosslink density on stress relaxation behaviour of elastomer at long time was investigated by Curro and Pincus [31]. They predicted that the Plazek exponent (x) in the equation 2.42 is approximately related to the Chasset and Thirion exponent (m) in the equation 2.40 for the relaxation modulus. It is written down in the equation 2.43.

$$x \approx \frac{2}{m} \qquad (2.43)$$

The time dependent phenomenon such as relaxation process and the dynamic mechanical properties of elastomer are described by the viscoelastic behaviour. The major topic of research in this work concerns with the effect of temperature cycling on the dynamic mechanical properties and the stress relaxation behaviour which are reviewed in the next section.

Copyright by Mahidol University

2.3 Dynamic Mechanical Properties

Dynamic mechanical properties refers generally to the responses of material to a periodic variation in the stress or strain. They are usually defined for a small variation in the stress or strain which does not cause permanent change of properties during investigation. The deformation of material confined between two parallel plates is shown in Figure 2.3.

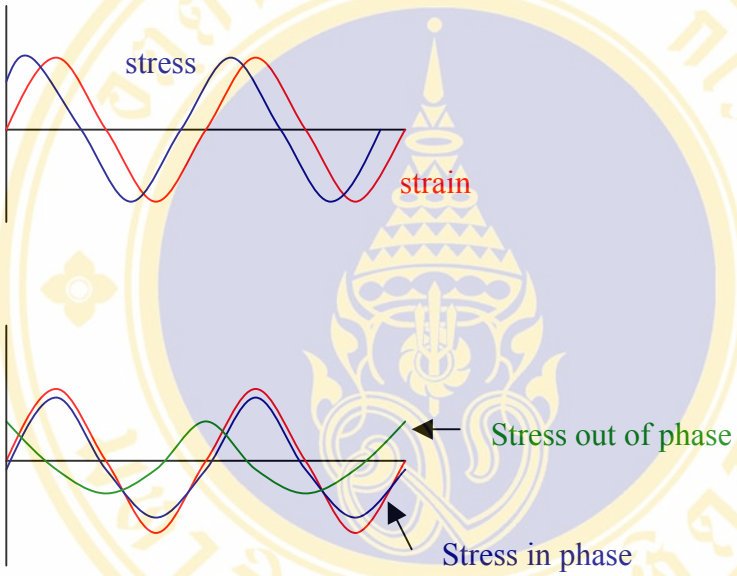

Figure 2.3: Sinusoidally varying simple shear: strain and stress decomposed into in-phase and out-of-phase components [2].

Figure 2.3, the stress can be defined as the tangential force per unit area producing the deformation. The strain is defined as the tangent of the angle which the cubical element is deformed, as displacement of the top surface divided by height of the material. The strain varies sinusoidally with time can be calculated by the following equation 2.44.

$$\gamma(t) = \gamma_0 \sin \omega t \qquad (2.44)$$

where, $\gamma(t)$ is the strain varies sinusoidally with time

Copyright by Mahidol University

γ_0 is the strain amplitude (peak strain)

ω is the angular frequency (2π times the frequency in Hertz)

t is time

Figure 2.3, the stress will lead the strain in time, and the phase shift is given by phase angle δ. The stress which varies sinusoidally with time could be calculated by the following equation 2.45.

$$\sigma(t) = \sigma_0 \sin(\omega t + \delta) \tag{2.45}$$

where, $\sigma(t)$ is the stress that varies sinusoidally with time

σ_0 is the stress amplitude

δ is the phase angle

The stress can be decomposed into a component in phase with the strain proportional to sin ωt, and the other $\pi/2$ out of phase, proportional to cos ωt. They are shown in the equation 2.46-2.47. The total stress can be calculated by the following equation 2.48.

$$G' = \frac{\sigma_0}{\gamma_0} \cos\delta \tag{2.46}$$

$$G'' = \frac{\sigma_0}{\gamma_0} \sin\delta \tag{2.47}$$

$$\sigma(t) = \gamma_0 \left[G'(\omega) \sin\omega t + G''(\omega) \cos\omega t\right] \tag{2.48}$$

where, G' is the storage modulus

G'' is the loss modulus

The storage modulus, G' is a measure of energy (elastic) stored and recovered in cyclic deformation. The loss modulus, G'' is a measure of energy

Copyright by Mahidol University

dissipated as heat. The modulus is usually shown in complex notation. It can be calculated by using equation 2.49. G^* is the complex modulus made up of a real and an imaginary component. The ratio G''/G' is tan δ, the loss tangent.

$$G^* = G' + iG'' \quad (2.49)$$

The factors that affect the dynamic mechanical properties of elastomer such as the effect of strain amplitude, the effect of carbon black and the effect of crosslink density were described in the next section.

2.3.1 Effect of strain amplitude on the dynamic mechanical properties of carbon black filled elastomer

The effect of strain amplitude on the dynamic mechanical properties of the elastromer was initially investigated by Naunton and Waring [32]. They found that the elastic modulus of compound decreased with an increase in the strain amplitude. The testing dynamic of elastomers, the high strain amplitude refer to a double strain amplitude (DSA) above 5%. The medium strain amplitude refer to DSA between 1-5% and the low strain amplitude refer to DSA below 1%. The carbon black network structure at high and medium strain amplitudes is broken down during the strain cycle. Therefore, the contribution of carbon black to the elastic modulus depended on the network structure of carbon black, and was independent of surface area of carbon black [33]. The dynamic storage shear modulus at high and medium strain amplitudes decreased on increasing the strain amplitude. At low strain amplitude, the dynamic modulus was dominated by the surface area of the carbon black at high filler content and at low temperature [34]. Therefore, the dynamic storage shear modulus increased on increasing the strain amplitude [35].

The dynamic loss modulus is related to the internal viscosity of the compound. It is a measure of the magnitude of the hysteresis phenomena [33,36]. This hysteresis may be the break down and the reformation of the interaggregate bond within the carbon black. At high strain amplitude, the tan δ and the elastic modulus decrease and the loss modulus is quite low [37]. At intermediate amplitude, the loss

Copyright by Mahidol University

modulus is high because of the break down and reformation of the elastomer interaggregate. At low strain amplitude is little broken down, the loss modulus is low.

2.3.2 Effect of carbon black on the dynamic mechanical properties of elastomer

The effect of carbon black on the dynamic mechanical properties of the elastomer depends on the degree of dispersion of the carbon black and the interaction of the elastomer and the carbon black. The effect of dispersion of the carbon black has been studied [38-40]. They found that the improvement of the dispersion of the carbon black by increasing the mixing time, the carbon black interaction within the carbon black aggregates decrease. Therefore, the storage and loss dynamic modulus are reduced when the dispersion is increased.

The effect of interaction of the elastomer and the carbon black is changed by heat treating filler such as graphitised black. The effect of heat treatment results in a worse microdispersion as the graphitised black has a higher self-aggregation caused by a decrease of the association linkage between the rubber and the black surface [41]. Therefore a graphitised black can be used to study the effect of the reduction in the interaction between the elastomer and the carbon black. The graphitised black gave higher tan δ than a normal black [42]. This effect has been also studied [43-44]. They observed that an increase in the interaction between the elastomer and the carbon black reduces the hysteresis. When the interaction such as a higher temperature mixing, a chemical modification of carbon black and a surface oxidation of the carbon black increased, the hysteresis procedures adopted. This phenomenon is due to the separation breakdown of the carbon black aggregates and a reduction in the reagglomeration of the carbon black particles.

2.3.3 Effect of oil on the dynamic mechanical properties of elastomer

The effect of oil on the dynamic mechanical properties has been studied [45-46]. They found that the viscoelastic properties decrease with an increase in the amount of liquids incorporated. The dynamic loss modulus decreased with increased

Copyright by Mahidol University

the extent of the swelling [47]. The result can be explained by using the fractional free volume theory.

2.3.4 Effect of crosslink density of elastomer on the dynamic mechanical properties

Crosslink density as the characteristic of rubber can be controlled by the formulation of the rubber compound and by the condition of the vulcanizing process. Crosslink density has been widely used to characterize rubber and rubber blend. The crosslink in vulcanized rubber blend can be estimated by sol-gel analysis, dynamic mechanical thermal analysis, differential scanning calorimetry, stress-strain model, swollen state NMR spectroscopy [48], network visualization microscopy and isopotential swelling [49]. However, in this study, the crosslink density in vulcanized rubber is measured by using either a chemical or a physical technique.

2.3.4.1 Chemical method

Chemical method is suitable for measuring the crosslink density of both unfilled and filled carbon black rubber. The vulcanized rubber specimen is weighed in air using an electronic balance and immersed in a solvent such as toluene and n-decane. The measurement of crosslink density in vulcanized rubber by using a chemical method has been studied [50-58]. The difference between the weight of the swollen and the unswollen rubber sample is recorded as a function of time. The volume fraction of rubber network in the swollen rubber can be calculated by using the equation 2.50.

$$V_{rnet} = \left(\frac{M_0}{\rho_{RH}}\right)\left(\frac{M_{rnet}}{M_{tf}}\right) \qquad (2.50)$$

where, V_{rnet} is the volume fraction of rubber network

M_0 is the mass of the rubber specimen

M_{rnet} is the mass of the rubber hydrocarbon and the sulfur combined

Copyright by Mahidol University

M_{tf} is the total weight of mix formulation

ρ_{RH} is the density of rubber hydrocarbon

The density of natural rubber is 0.92 $g.cm^{-3}$. The volume fraction of the rubber can be calculated by the equation 2.51

$$V_r = \left(\frac{V_{rnet}}{V_{rnet} + V_{solv}} \right) \quad (2.51)$$

where, V_r is the volume fraction of rubber

V_{solv} is the volume fraction of solvent absorbed at equilibrium

The volume fraction of solvent absorbed at equilibrium is investigated from the mass uptake after swelling. The crosslink density [X] is calculated by using the Flory-Rehner equation [59]. It is written as the equation 2.52.

$$\ln(1 - V_r) + V_r + \chi V_r^2 + 2\rho_{RH} V_0 [X] (V_r)^{1/3} = 0 \quad (2.52)$$

where, V_0 is the molar volume of the solvent

χ is the rubber solvent interaction parameter

However, the carbon black filler in compounded rubber itself has been observed to restrict the mobility of the rubber during the swelling process. The measured physical crosslink density in a carbon black filled elastomer is written by the equation 2.53 [60].

$$[X]_{act} = \frac{[X]}{1 + K_f \phi} \quad (2.53)$$

where, K_f is the constant characteristic of filler

ϕ is the volume fraction of the carbon black

Copyright by Mahidol University

$[X]_{act}$ is the actual physical crosslink density

2.3.4.2 Physical method

The determination of crosslink density in a physical method has been studied [61-62]. The crosslink density is usually presented in terms of an average molecular weight between two crosslinking points, $M_{c,phys}$. This parameter can be calculated by using the equation 2.54. The average amount of the molar mass between all crosslinks ($M_{c,phys}$) can be calculated by the following equation 2.55.

$$M_c = \frac{1}{2[X]_{act}} \quad (2.54)$$

$$M_{c,phys} = \frac{\rho_r RT}{2C_1} \quad (2.55)$$

where, ρ_r is the density of rubber

R is the gas constant, 8.31 $J.mol^{-1}.K^{-1}$

C_1 is the coefficient constant

T is the temperature (K)

$M_{c,phys}$ is the average amount of the molar mass between all crosslinks

From the equation 2.55, C_1 is derived from the Mooney-Rivlin equation given in Equation 2.56 [2]. It can be rewritten by the equation 2.57. When the reduced stress (Φ) is plotted against the inverse of extension ratio (λ^{-1}), the y-interception of this curve is the coefficient constant (C_1) which is used to determine the average amount of the molar mass between all crosslinks ($M_{c,phys}$).

Copyright by Mahidol University

$$F = 2A_0\left(\lambda - \frac{1}{\lambda^2}\right)\left(C_1 + C_2\frac{1}{\lambda}\right) \quad (2.56)$$

$$\Phi = \frac{F}{2A_0\left(\lambda - \lambda^{-2}\right)} = C_1 + \frac{C_2}{\lambda} \quad (2.57)$$

where, Φ is the reduced stress term

F is the force per cross-section area of the undeformed specimen,

A_0 is cross-section area of the undeformed specimen

λ is the extension ratio

C_2 is the coefficient constant

In this study, a physical method is chosen to determine the crosslink density due to its free solvent used. The effect of crosslink density on the dynamic mechanical properties of the elastomer was initially observed as the high hysteresis in an undercured elastomer. The storage modulus of unfilled elastomer increased with the level of the crosslinking [48]. Studebaker and Beatty found that the storage modulus of carbon black filled natural rubber was a linear function of the crosslink density [64]. The loss angle decreased with an increase in the degree of crosslinking.

2.4 Stress relaxation behaviour

When the elastomer is held at constant deformation, the stress set up decrease with time as the crosslinked network approaches an equilibrium condition [2]. This phenomenon is stress relaxation which can be of great importance in an automobile part application [64]. Stress relaxation can be used to predict life time of elastomer by considering a decrease in the stress as a function of time.

Copyright by Mahidol University

2.4.1 Measurement of stress relaxation

Stress relaxation is usually defined as the stress loss which is expressed as a percentage of the initial stress and calculated by using the equation 2.58 [64]. The relaxation time, τ is the time required for the stress to be reduced 1/e of its initial value [65].

$$\text{Stress relaxation} = \frac{\sigma_0 - \sigma_t}{\sigma_0} \quad (2.58)$$

where, σ_0 is the stress at the initial time

σ_t is the stress at time

$$\text{Rate of stress relaxation} = \frac{\text{stress relaxation}}{\text{time}} \quad (2.59)$$

The rate of stress relaxation can be calculated by the equation 2.59. For unfilled rubbers having the same type of vulcanizing system, the relaxation rate decreases with increasing hardness [2]. However, the stress relaxation rate of filled rubbers increase with increasing the amount of filler. The relaxation mechanisms can be divided into two categories, namely physical and chemical relaxations.

2.4.1.1 Physical relaxation

Physical relaxation is associated with disengagement and rearrangement of chains, with reorientation of the molecular network under strain, with the breaking bond due to secondary valence forces between chains, between filler particles or between chain and filler particles. Physical relaxation is not very sensitive to temperature at constant operating temperature however it is sensitive to temperature cycling. Physical relaxation can be described by using the equation 2.60 [64].

Copyright by Mahidol University

$$\frac{\sigma_0 - \sigma_t}{\sigma_0} = A \log \frac{t}{t_0} \quad (2.60)$$

where, A is the stress relaxation rate in percent per decade of time (ppd)

t_0 is the initial time

t is the time

Relaxation rates are not strongly dependent on strain or the mode of deformation such as compression, tension or shear [64]. However, type and degree of crosslinking of the elastomer affect the relaxation rate. When crosslink density of elastomer is increased, the relaxation rate of elastomer is decreased [64]. Moreover, the effect of crosslink density on stress relaxation behaviour was investigated at long time [65]. The result shown in Figure 2.4 indicated that the relaxation behaviour was strongly dependent on cross-link density.

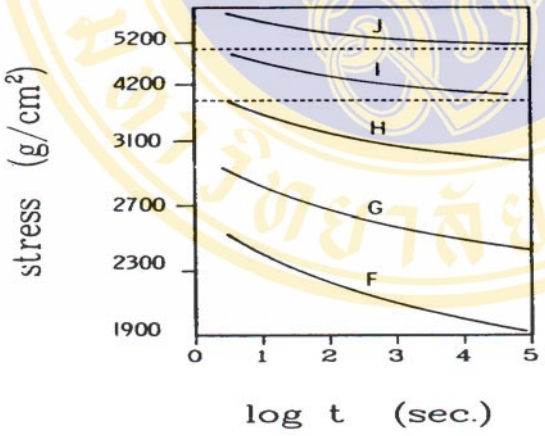

Figure 2.4: Stress relaxation of natural rubber at 30°C and 50% elongation at various cross-link densities. The vulcanizates shown have the following cross-link densities: F, 0.46×10^{-4}; G, 0.62×10^{-4}; H, 0.80×10^{-4}; I, 1.20×10^{-4}; J, 1.69×10^{-4} [65].

Copyright by Mahidol University

Furthermore, fillers as additives of elastomer affect the relaxation rate which cause additional relaxation mechanisms. The filler loading of elastomer was directly proportional to physical relaxation rate of elastomer [64].

2.4.1.2 Chemical relaxation

Chemical relaxation usually predominates over physical relaxation at high temperature. It is very sensitive to temperature associated with chemical reaction. Chemical relaxation is associated with a scission of chemical bonds, either in the polymer chains or in the crosslinks. A specimen thickness strongly influences on the chemical relaxation. This causes the chemical degradation process by fluid such as oxygen. In addition, this effect becomes the most important at higher temperature. A total relaxation rate can be determined by combining physical and chemical relaxation rates, using the equation 2.61 [23].

$$\text{Total relaxation} = A \log \frac{t}{t_0} + B(t-t_0) \qquad (2.61)$$

where, A is the physical relaxation rate

B is the chemical relaxation rate

Moreover, the stress relaxation behaviour can be investigated by using pulse NMR technique which the spin-lattice relaxation time, T_1 and the spin-spin relaxation time, T_2 were determined [65,67-68].

2.4.2 Effect of temperature on the stress relaxation behaviour

The effect of temperature cycling on the stress relaxation behaviour is the major topic of research in this work. The stress relaxation behaviour is strongly affected by temperature [66]. It can be predicted by using William-Landel- Ferry (WLF) theory, depends primarily on the viscosity at which small segment of a

Copyright by Mahidol University

molecule move to new positions as a result of random Brownian motion [64]. The internal viscosity and the energy dissipation are much reduced with increasing temperature. The viscosity can be expressed in term of shift factor (a_T) which is calculated by using the equation 2.62 [67].

$$a_T = \frac{\eta_T}{\eta_{T_r}} = \frac{\tau_T}{\tau_{T_r}} \quad (2.62)$$

where, η_T is the viscosity at temperature

η_{T_r} is the viscosity at reference temperature

τ_T is the characteristic segmental relaxation time at temperature

τ_{T_r} is the characteristic segmental relaxation time at reference temperature

Equation 2.62, a_T can be expressed in general term as log a_T which is calculated by WLF equation as shown in the equation 2.63 [67-70].

$$\log a_T = \frac{-C_1^r\left(T - T_r\right)}{C_2^r + T - T_r} \quad (2.63)$$

where, T is the temperature

T_r is the reference temperature

C_1^r is the coefficient constant at reference temperature

C_2^r is the coefficient constant at reference temperature

The constant of C_1^r and C_2^r depend on the type of material and changing temperature. It is written down in Table 2.1.

Copyright by Mahidol University

Table 2.1: Parameters characterizing temperature dependence of a_T for various polymer systems [30,67,69,71-72].

Polymer	T_r(K)	T_g(K)	C_1^r	C_2^r (deg)
Rubbers				
Hevea rubber	200	200	16.80	53.6
	248	200	8.86	101.6
	298	200	5.94	151.6
Butyl rubber	205	205	16.80	108.6
	298	205	9.03	201.6
Styrene-butadiene rubber	210	210	20.30	25.6
	298	210	4.57	113.6
Polybutadiene, cis-trans	298	172	3.64	186.5
Polybutadiene, high cis	298	161	3.44	196.6
Polybutadiene, cis-trans-vinyl	298	205	5.97	123.2
Polybutadiene, high vinyl	298	261	6.23	72.5

When $(T - T_r)/\log a_T$ was plotted against $T - T_r$, the slope, s and intercept, i of the resulting straight line the two empirical constants, C_1^r and C_2^r were calculated by the equation 2.64-2.65 [67].

$$C_1^r = \frac{-1}{s} \tag{2.64}$$

$$C_2^r = \frac{i}{s} \tag{2.65}$$

Equation 2.63 is independent of the choice of T_r. The determination of C_1^r and C_2^r is frequently useful to choose a second reference temperature T_1 and repeat the graphical evaluation which provides the coefficient constant at a second reference

Copyright by Mahidol University

temperature, C_1^1 and C_2^1 corresponding to T_1. The relationship between the coefficient constant at reference temperature, C_1^r and C_2^r and the coefficient constant at a second reference temperature, C_1^1 and C_2^1 can be written down in the equation 2.66-2.67 [67].

$$C_1^r = \frac{C_1^1 C_2^1}{C_2^1 + T_r - T_1} \quad (2.66)$$

$$C_2^r = C_2^1 + T_r - T_1 \quad (2.67)$$

The relationship between the reference temperature, T_r and the second reference temperature, T_1 is written down in the equation 2.68 [67].

$$T_r - C_1^r = T_1 - C_2^1 \equiv T_\infty \quad (2.68)$$

Where T_∞ is a fixed temperature at which, regardless of the arbitrary choice of T_r, $\log a_T$ becomes infinite in accordance with the equation 2.63. The temperature, T_∞ is usually called the Vogel temperature because the characteristic temperature is the same as the characteristic temperature which is employed in an empirical equation for temperature dependence of viscosity by Vogel [73]. Therefore, the equation 2.63 can be rewritten down in the equation 2.69.

$$\log a_T = \frac{C_1^r (T - T_r)}{T - T_\infty} \quad (2.69)$$

2.4.3 Effect of temperature cycling on the stress relaxation behaviour

The temperature cycling and the difference in temperature which goes up and down during the day affect the relaxation behaviour and life time of rubber. Therefore, the viscoelastic behaviour is chosen for this investigation. It can be divided into two categories, namely creep and stress relaxation behaviour. The elastomer is

Copyright by Mahidol University

used to absorb dynamic forces at constant forces such as a bridge bearing. The initial length of rubber increases with time. This phenomenon is called the creep behaviour. The effect of the temperature cycling on the creep behaviour of the elastomer was investigated [14]. This result shown in Figure 2.5 indicated that the creep bahaviour under temperature cycling, from 40°C to 60°C and back to 40°C, was accelerated by 4 times compared to the percentage of creep obtained only at 40°C. This was investigated in an environment chamber which air was used as the medium but the control of temperature by using air as the medium was poor due to the low heat conductivity.

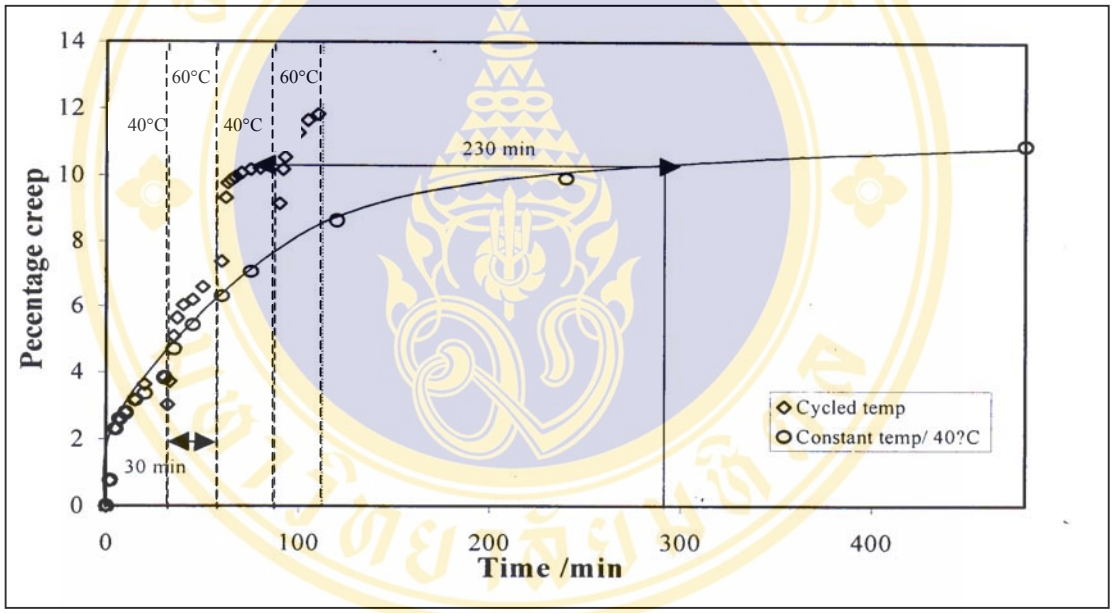

Figure 2.5: Comparison between creep behaviour of rubber when the temperature is cycled between 40°C and 60°C and the long term creep of rubber at 40°C at a fix stress that results in an approximate initial 50% pre-strain [14].

Furthermore, the effect of temperature cycling on the stress relaxation behaviour was investigated [74-75]. The results indicated that the stress relaxation bahaviour under temperature cycling, from 80°C to 83°C and back to 80°C, depended on the relaxation mode acting when compared to the stress relaxation obtained only at 80°C. This result is shown in Figure 2.6, which the physical processes in the initial regime and after the temperature-step are the same when the point B is rejoined with

Copyright by Mahidol University

the point A. The result indicated that the relaxation mode acting at one temperature completely stops when temperature is changed and re-continues when temperature is returned to initial value.

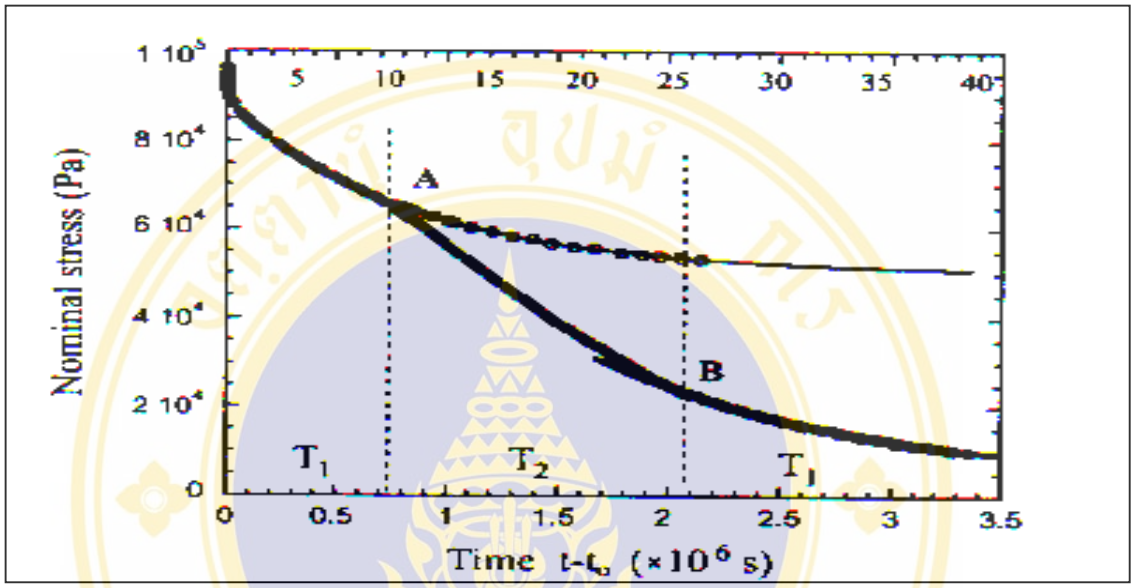

Figure 2.6: The stress relaxation of NR after 5% extension with an intermediate temperature change. Form T_1 = 80°C to T_2 = 83°C and then returned back to T_1 [74].

These results indicated that the temperature cycling strongly affects the viscoelastic behaviour. Therefore, in this work, the time-temperature superposition principle was investigated. It could be predicted by using WLF theory. The results of the effect of temperature cycling on the dynamic mechanical properties and stress relaxation behaviour in this work are reviewed in CHAPTER V.

2.5 Mechanism of carbon black reinforcement.

Generally, carbon black reinforced elastomers show an increase in the strength and wear properties, resulting from the rubber-carbon black network. Although the actual mechanisms of reinforcement are not clear, the fundamentals of this reinforcement are related to the interaction between carbon black and the elastomer chain. Using an electron microscope, Hess et al. [76] developed a technique to evaluate

Copyright by Mahidol University

the adhesion between filler particles and the elastomer. Their results showed that the adhesion increased with a smaller particle size and a higher structure for the carbon black. Many studies have been undertaken to explain the definitive rubber-carbon black network model. The models so far developed are explained below.

2.5.1 Bound rubber model

Bound rubber is a measure of the degree of adsorption of the elastomer chain onto the filler surface. It is assumed to be a measurement of the reinforcing property of the carbon black. Bound rubber is formed during both the mixing and the pressurized vulcanization stage of manufacture. The interaction between the filler and elastomer is both physical and chemical in nature. The bound rubber is formed by the mechanical breakdown of both the elastomer and carbon black aggregates. The new surfaces of the elastomer and the carbon black are highly reactive and can form Van der Waals force and covalent bond due to free-radical interactions. The bound rubber has a reduced mobility of the elastomer chains. This results in an increase in the stiffness of the rubber-carbon black network system [77-78]. As the glass transition temperature (T_g) reflects the mobility of the elastomer molecules, it is expected to change a little by the incorporation of the carbon black. This result was confirmed by Funt [79] who observed a higher T_g in the immobilized layer of the chain segment absorbed on the filler surface. Dannenberg [80] used NMR techniques to measure the thickness of the bound rubber and found that it varied between 0.5-5 nm. The amount of bound rubber is proportional to the surface area of the filler [81-82], which is increased by an increase in the structure of the carbon black.

2.5.2 Mechanical interaction model

The mechanism for this mechanical interaction model is explained by considering the relation between the occluded rubber and the void volume in the carbon black aggregate [83]. The occluded rubber refers to the elastomer which has been shielded within the irregular contours of the aggregate from the deformation experienced in the rest of the rubber network when the system is subjected to the applied stress. The

Copyright by Mahidol University

occluded rubber has no segmental motion between the elastomer and the filler aggregates. A high internal porosity in the carbon black would result in an increase in the amount of occluded rubber. Kraus [84] assumed that the internal void volume in carbon black aggregates was proportional to the Dibutyl Phthalate Absorption (DBPA). The DBPA test is a technique used to investigate the structure of carbon black. Some experiments have been undertaken to measure the amount of the occluded rubber [1,85] by using Nuclear Magnetic Resonance, NMR. The amount of occluded rubber can then be included when the relationships are derived to calculate the effect of the carbon black on the mechanical properties of the base elastomer.

2.5.3 Physical interaction model

The Van Der Waals force between the carbon black surface and elastomer matrix is another source of reinforcement. The reaction occurs only at the interface and it reduces the mobility of the elastomer segment and may form a chain orientation. Both phenomena influence the viscoelastic properties of the elastomer. The evidence for the chain orientation due to the physical interaction can be obtained by the observation of the properties of the carbon black filled non-crystallized elastomers. Normally, non-strain crystallized elastomers have poorer properties. However, they show good vulcanization capability and good mechanical properties when carbon black is incorporated. This indicates that chain orientation due to the physical interaction between carbon black and the elastomer occurs in carbon black filled elastomer that can not strain crystallise.

2.5.4 Chemical interaction model

The chemical interaction model assumes that elastomer chains are grafted onto the carbon black surface by covalent bonds. The interaction is caused by a reaction between the functional group at the carbon black particle surface and free radicals. Pike and Watson [86] suggested that these free radicals were formed during the chain scission processes that occur during rubber mixing. Free radicals are also formed when the carbon black filled elastomer is strained. The carbon black particle surface is active due

Copyright by Mahidol University

to the presence of functional groups such as phenolic, hydroxyl or carboxyl groups. This effect has been investigated by Donnet et al. [85] using graphitised carbon black where the structure of the carbon aggregates is altered by a heat treatment. These experiments indicated that the mechanical properties were reduced when compared to the properties of an elastomer reinforced with a normal carbon black. It was also reported by Gessler [87] that the removal of the oxygen groups at the surface of the carbon black reduced the mechanical properties and hence the reinforcing behaviour when carbon black was incorporated into a butyl rubber.

It is apparent that several mechanisms have been proposed to explain the reinforcing phenomena when carbon black is incorporated into the elastomer. It is also clear that no simple model in isolation can satisfactorily be used to predict the behaviour. A first step in understanding the stiffness and viscosity of a carbon black filled elastomer can be made by using a hydrodynamic theory, which is discussed in the next section. This theory is normally used to describe the stress-strain relationship of a carbon black filled elastomer at low strain. At higher strain, several models have been proposed to explain in detail the real deformation behaviour of a carbon black filled elastomer.

2.6 Mechanism of elastomer deformation

A model was proposed by Mullins and Tobin [88] to describe the stress-strain behaviour of a filled elastomer. The modulus of the carbon black filled elastomer was studied at small deformations. After a single condition loading cycle, the Young's modulus of a filled elastomer can be calculated from the modulus of an unfilled elastomer. They suggested that the difference between the stress-strain behaviour of unfilled elastomer and carbon black filled elastomer could be explained by a strain amplification factor. The strain amplification effect produces local strains in the elastomer that are larger than the global strains applied to the filler-elastomer network. This strain amplification factor has been used in the past to analyse the stress-strain data obtained at a large deformation.

Copyright by Mahidol University

It has been known for a long time that cyclic deformations result in a progressive stress softening of the elastomer. It is also known that if an elastomer is initially cycled at low strains and then loaded to a single higher strain, at the point when the elastomer exceeds the maximum strain experienced in the cyclic loading, there is an initial increase in the tangent modulus just below the maximum strain experienced in the previous cyclic deformation. As the strain is further increased, the stress strain relationship approaches which the material would have experienced if it had been deformed to the large strain in its initial loading cycle. In an unfilled elastomer, the softening is attributed to the disentanglement and a further orientation of long chain molecules during the deformation [89-90] or the breakdown of the molecular network chains. In a carbon black filled elastomer, the softening has also been attributed to the breakdown of the carbon black structure or the slippage of linkages between the carbon black and the elastomer.

2.6.1 Chain breakage

This mechanism is sometimes used to explain softening at high strain deformations [91]. The network chains between filler particles and the filler and the rubber network have a distribution of the chain lengths. When a stress is applied, the shortest chains will break during the deformation. Since the stress on a chain before rupture is large, they make a significant contribution to the overall stiffness of the rubber-carbon black system. After breakage the chains no longer support the load and stress softening can be observed.

2.6.2 Molecular slippage

Dannenberg [80] and Boonstra [92] used the concept of slippage during the deformation to explain stress softening. They assumed that a major portion of the molecular segments of the rubber adsorbed on the filler surface can undergo surface slippage under the applied stress. This movement inhibits the rupture of the network chain by redistributing the stress to neighbouring chains. The resulting molecular alignment will help increase the strength. The rearrangement due to the applied stress

Copyright by Mahidol University

would appear to absorb energy and increase the hysteresis in the loading cycle. On the removal of the stress, the elastomer-carbon black system will regain a more random orientation, however, this is a time dependent process that results only in a slow molecular rearrangement at the filler surface.

2.6.3 Filler-filler linkage breakdown

By considering the stress softening and the strain amplification effects together, Harwood, Payne and Mullins [93] found that the degree of softening was similar in magnitude in unfilled and filled rubbers. This suggested that a model incorporating the breakdown of the filler structure was not required to explain the stress softening effects in filled elastomers. However, Payne [37] reported that, at a small strain, the dynamic modulus of filled vulcanised elastomer decreased with an increase in the strain. This change was attributed to a breakdown of weak aggregates of filler particles within the elastomer matrix. The significance of the breakdown of the filler aggregates under load is therefore unclear and it will be tackled as part of this programme of work.

2.6.4 Sulphur linkage breakdown

Furthermore, when subjected to cyclic deformation, Harwood [94] found that the polysulphide crosslinks, commonly encountered in conventionally cured elastomers, were broken down during the cyclic process and reformed in an extended condition. This explains the greater cyclic stress softening and lower level and rate of recovery in polysulphide crosslinked elastomers when compared with mono and di-sulphide system.

Copyright by Mahidol University

CHAPTER III
OBJECTIVES OF THIS STUDY

In the introduction, it was stated that the dynamic behaviour of the filled elastomer decreased when the services temperature was raised [13]. The reduction in the stress due to the breakdown of the interactions affected the viscoelastic behaviour. The failure of the linkage might arise from the poor temperature controlling in the experimental system. The temperature was repeatedly changed in a small range before reaching the design temperature in the temperature environment chamber. In many applications, the rubber product was also employed under the temperature cycling condition. Therefore, the main objective of this study was to study the relaxation behaviour of the rubber under the temperature cycling condition. A few work has been done on the temperature cycling effect which some limited works was already reviewed in Chapter 2.

The micro-tension apparatus had to be built in this investigation. This apparatus could be used to determine the force while the rubber specimen was controlled in the water environment. Water was chosen as a media because of its high heat conductivity compared to air. Therefore, calibration of the apparatus and also the effect of water on the relaxation behaviour were also investigated. Important factors such as crosslink density, initial strain, types of rubber were controlled in order to simplify the study of the stress relaxation behaviour under temperature cycling. The effects of these factors on the relaxation behaviour were also studied.

Unfilled elastomer was initially employed to study of the relaxation behaviour under the temperature cycling. The changing in viscoelastic behaviour of elastomer should follow the WLF approach. This point should also be verified. Not only, the unfilled elastomer, carbon black filled was also employed in order to study the effect of temperature cycling on the filler-elastomer interaction which could be help to define the interaction between the filler-elastomer of the carbon black filled NR prepared by a innovative technique reported by Tangboriboonrat et. al [95-96].

Copyright by Mahidol University

CHAPTER 4
MATERIALS AND METHODS

4.1 Apparatus

The apparatus employed in this present study are listed in Table 4.1.

Table 4.1: Trade mark of the instrument are used throughout this study.

Apparatus	Supplier
Brabender (Plasti-Corder Lab-Station)	-
Dynamic Mechanical Analyser	GABO
Electronic Densimeter	MD-200S Mirage
Hydraulic Hot Press	Wabash
Internal Mixer	Chaichareon Karnchang
Micro-tension	-
Mooney Shearing Disk Viscometer	Tech. Pro.
Oscillating Disc Rheometer	Monsanto 100S
Rubber Process Analyser	Alpha Technologies
Shaker	Burrell
Extensometer	Instron

Copyright by Mahidol University

Table 4.1: Trade mark of the instrument are used throughout this study (Continued).

Apparatus	Trade mark
Two-roll Mill	Labtech KRM 150, Nishimura NS 76
Ultrasonic bath	Sonorex RK 100H, Bandelin Electronic
Vacuum oven	Sheldon,1430-D

4.2 Materials and chemical additives

The materials and chemical additives employed in this present study are listed in Table 4.2 and 4.3.

Table 4.2: The chemical reagents are used throughout this study.

Reagent	Supplier	Grade
Acetone	Fluka	Commercial
Methanol	Fluka	Commercial
Nonidet P40	Fluka	GR
Toluene	Fluka	Commercial

Copyright by Mahidol University

Table 4.3: The materials and chemical additives are used throughout this study.

Material	Supplier
Carbon black (N220)	Thai Carbon Product
Carbon black (N330)	Thai Carbon Product
Carbon black (N550)	Thai Carbon Product
Carbon black (N774)	Thai Carbon Product
Dicumyl peroxide (DCP)	Siam Chemicals Public Co., Ltd.
Glacial acetic acid	Lab scan
High ammonia natural rubber latex	Thai Rubber Latex
2-mercaptobenzothiazole disulfide (MBTS)	China National Chemical Construction Jiangsu Company
Natural rubber (NR)	Chanel Chemical
Stearic acid	Petch Thai Chemical Co., Ltd.
Sulphur	Siam Chemicals Public Co., Ltd.
Tetramethylthiouram disulfide (TMTD)	China National Chemical Construction Jiangsu Company
Zinc oxide (ZnO)	Muti- Chemical & Engineering Co., Ltd.
N-1,3-dimethylbutyl-N’-phenyl p-phenylenediamine (6PPD)	Siam Chemicals Public Co., Ltd.

Copyright by Mahidol University

4.3 Preparation of rubber sheet from high ammonia Natural rubber Latex (NR)

4.3.1 Preparation of rubber sheet from natural rubber latex

Concentration Natural rubber Latex (HA, dry rubber content DRC = 60% w/w) was cast on the glass plate (140x140x1mm^3).

4.3.2 Preparation of CB/NR masterbatch [96-97]

Carbon black was mixed with natural rubber latex (NR-mast). Carbon Black powder grade N550 (6g) was dispersed in an aqueous solution of 2.0 % w/w$_{CB}$ non-ionic surfactant (Nonidet P40) (25ml). A flask containing the mixture was immersed in an ultrasonic bath (Sonorex RK 100H) for 15 minutes to obtain a good dispersion. Then, it was shaken for 16 h at room temperature by using a shaker (Burrell) for attaining an equilibrium adsorption of surfactant molecules on carbon black surface. Dicumyl peroxide (DCP) is mixed into concentrated high ammonia preserved natural rubber latex (HA, dry rubber content DRC = 60% w/w). The latex is stirred until DCP was dissolved. Then carbon black powder grade N550 (30 phr) dispersed in aqueous solution of 2% w/w$_{CB}$ Nonidet P40 was added into latex system while stirring. The CB/NR Masterbatch was pressed in to thin sheets (140x140x1mm^3) and dried in an oven at 40°C for 1 day. The rubber formulation of NR in CB/NR Masterbatch method (NR/mast) is written down in Table 4.4.

Table 4.4: The rubber formulations of different type of interaction between CB and NR

Rubber ingredients	NR-Conv	NR-Mast
NR latex (phr)	100.0	100.0
Carbon Black/N550 (phr)	30.0	30.0
DCP (phr)	2.0	2.0

Copyright by Mahidol University

4.4 Preparation of rubber compound

Rubber mixing process was performed in the internal mixer for 12 minutes in the following condition: rotor speed 50 rpm, temperature 50°C and the fill factor 0.7. At first, rubber was charged into the internal mixer and masticated for 2 minutes before adding ZnO and Stearic acid. Then 6PPD and carbon black were incorporated into the rubber compound after 4 and 5 min of rubber charging, respectively.

Figure 4.1: Internal mixer 0.5L

Finally, Sulphur, MBTS and TMTD were incorporated into the rubber compound for 2 min. The thickness of compounded rubber was controlled between 1-2 mm by using two roll mill at 50°C. The picture of internal mixer and two roll mills is shown in Figure 4.1 and 4.2. The rubber formulations are written down in Table 4.5-4.7.

Figure 4.2: Two rolls mill

Copyright by Mahidol University

Table 4.5: The rubber formulations with different amount of carbon black.

Ingredient	NR-0CB	NR-10CB	NR-30CB	NR-60CB
NR (phr)	100.0	100.0	100.0	100.0
Carbon black/N550 (phr)	-	10.0	30.0	60.0
Anti-oxidant (phr)	3.0	3.0	3.0	3.0
Accelerator (phr)	2.5	2.5	2.5	2.5
Sulphur (phr)	2.0	2.0	2.0	2.0

Table 4.6: The rubber formulations with different amount of sulfur.

Ingredient	NR-1S	NR-1.5S	NR-2.5S
NR (phr)	100.0	100.0	100.0
Carbon black/N550 (phr)	10.0	10.0	10.0
Anti-oxidant (phr)	3.0	3.0	3.0
Accelerator (phr)	2.5	2.5	2.5
Sulphur (phr)	1.0	1.5	2.5

Table 4.7: The rubber formulations with different type of carbon black.

Ingredient	NR-N2	NR-N3	NR-N5	NR-N7
NR (phr)	100.0	100.0	100.0	100.0
Carbon black/N220 (phr)	10.0	-	-	-
Carbon black/N330 (phr)	-	10.0	-	-
Carbon black/N550 (phr)	-	-	10.0	-
Carbon black/N774 (phr)	-	-	-	10.0
Anti-oxidant (phr)	3.0	3.0	3.0	3.0
Accelerator (phr)	2.5	2.5	2.5	2.5
Sulphur (phr)	2.0	2.0	2.0	2.0

Copyright by Mahidol University

• Preparation of the carbon black filled NR compound

The preparation of the carbon black filled NR compound for this study could be divided into two methods. Conventional mixing using internal mixer was the first method to be selected. Another method, the carbon black was mixed into the latex natural rubber which was described in 4.3.3. In order to mix according to the conventional method, natural rubber prepared from latex was dried under the hot oven which the temperature was controlled at 50°C. The rubber sheet was mixed with carbon black and curative in the internal mixer (Brabender). The picture of the Brabender is shown in Figure 4.3. The mixing condition is listed in Table 4.8. The rubber formulations are written down in Table 4.4.

Table 4.8: The mixing condition of different type of interaction between CB and NR used in this study

Testing Conditions	
Rotor speed	50 rpm
Temperature	50°C
Fill factor	0.7

Figure 4.3: Brabender

Copyright by Mahidol University

4.5 Cure characteristic measurement [2]

The vulcanization characteristic of compounded rubber was measured by using Oscillating Disc Rheometer (ODR). Approximately 8-10 g of the compounded rubber was enclosed in a heated cavity which the schematic design of the oscillating disk rheometer is shown in Figure 4.4. Vulcanization characteristic was measured by the increase in the torque required to maintain a given amplitude of oscillation at a given temperature. The torque was proportional to a low-strain modulus of elasticity which measured at the elevated temperature of vulcanization. Therefore, it had been assumed that the increase in torque during vulcanization was proportional to the number of crosslinks formed per unit volume of rubber. The torque was automatically plotted against time to give a so-called rheometer chart, rheograph or cure curve which is shown in Figure 4.5. The curve could be analyzed to get the important parameter such as cure time (τ_{90}), scorch time (τ_2), maximum torque (τ_{max}) and minimum torque (τ_{min}). The cure time was measured at 90% of maximum torque as τ_{90}. Furthermore, this curve could be used to determine the scorch time (τ_2) which represented the time that rubber could flow and filled up the cavity of mould. In this study, the vulcanization characteristics of the compounding rubber was measured at 160 °C. The vulcanization times determined in this study are shown in Appendix A.

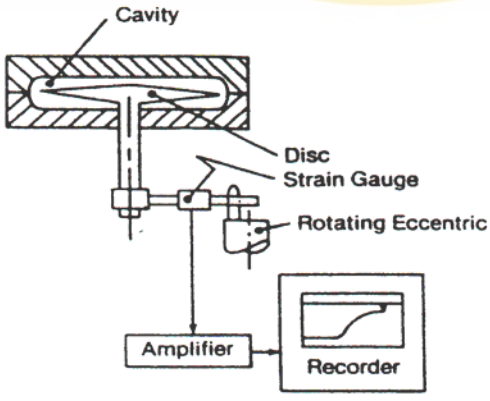

Figure 4.4: Schematic design of the oscillating disk rheometer [2]

Copyright by Mahidol University

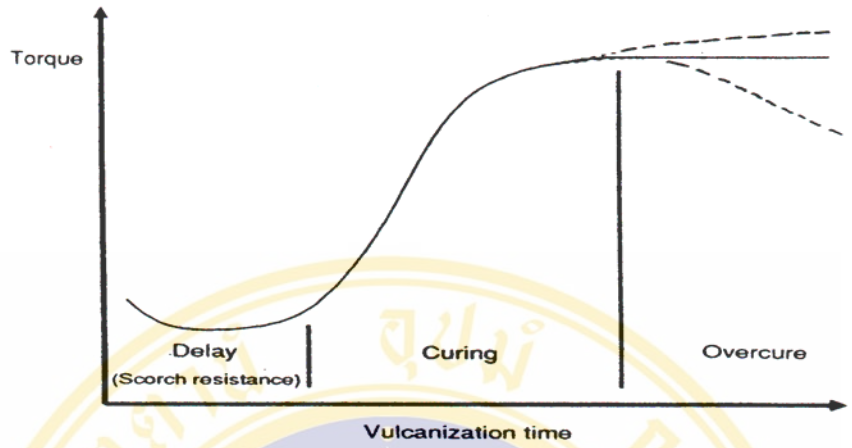

Figure 4.5: Rheometer cure curve [2]

4.6 Compression moulding

A sheet of vulcanized rubber was prepared by using compression moulding. The compounded rubber had been put in the metal mould which was later compressed in Wabash Genesis Series Hydraulic Press, G30H at 160 °C under air pressure of 15 atm. The picture of Hydraulic Hot Press is shown in Figure 4.6.

Figure 4.6: Wabash Genesis Series Hydraulic Press, G30H

Copyright by Mahidol University

4.7 Physical properties measurement

4.7.1 Total solid content (%TSC)

Total solid content (%TSC) of natural rubber latex is expressed as a percentage by weight of the concentrated latex which is non-volatile at a definite temperature in a vented air oven. The %TSC of concentrated natural rubber latex was calculated by the equation 4.1, according to ASTM D1076-97 [98].

$$\%TSC = \left(\frac{W_2}{W_1}\right) \times 100 \quad (4.1)$$

where, W_1 is The weight of NR latex sample (g)

W_2 is The weight of dry NR sample (g)

4.7.2 Dry rubber content (%DRC)

Dry rubber content, %DRC, of natural rubber latex is expressed as a percentage by weight of the concentrated latex which is precipitated by adding of 5% acetic acid. The %DRC of concentrated natural rubber latex was calculated by the equation 4.2, according to ASTM D1076-97 [98].

$$\%DRC = \left(\frac{W_3}{W_1}\right) \times 100 \quad (4.2)$$

where, W_3 is The weight of dry coagulum (g)

Copyright by Mahidol University

4.7.3 Density measurement

The density of compounded rubbers were measured in order to control the quality of mixing. The density of approximately 0.6 – 0.8 g of vulcanized rubber was measured by using Electronic Densimeter (MD-200S Mirage) at room temperature. The picture of Electronic Densimeter is shown in Figure 4.7. Both weight in the air medium and in the distilled water medium of vulcanized rubber was determined. Then the density was calculated by using Electronic Densimeter (MD-200S Mirage).

Figure 4.7: Electronic Densimeter (MD-200S Mirage)

4.7.4 Crosslink Density Measurement

In this study, a physical method was chosen to determine the crosslink density of vulcanized rubber. It was measured by using INSTRON extensometer apparatus as shown in Figure 4.8. The vulcanization sheets were cut into the dumbell shape before measuring the stress-strain behaviour at 10 mm/min of crosshead speed. The dimensions of the tensile specimen and the stress strain curve are shown in Figures 4.9 and 4.10, respectively. Crosslink density could be calculated by using Equation 2.54-2.57. From Equation 2.57, the reduced stress (Φ) was plotted against the inverse of extension ratio (λ^{-1}). This curve was shown in Figure 4.11. The y-

Copyright by Mahidol University

interception of this curve was the constant (C_1) which was used to determine the average amount of the molar mass between all crosslinks ($M_{c,phys}$). The crosslink density of rubber specimen used in this study are shown in Appendix B.

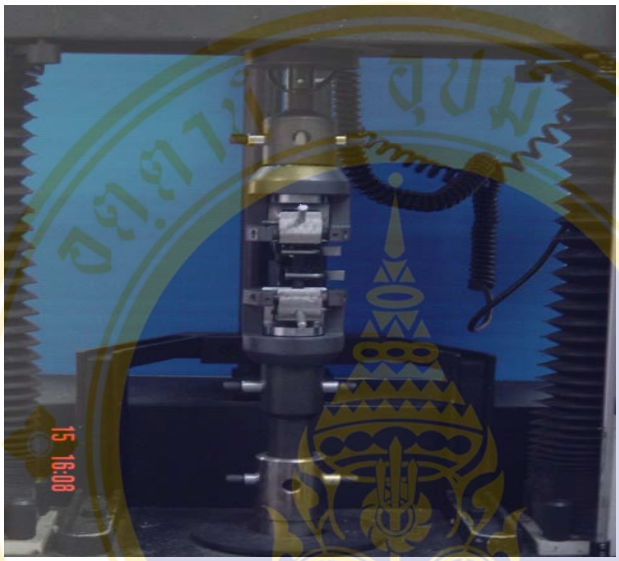

Figure 4.8: INSTRON extensometer

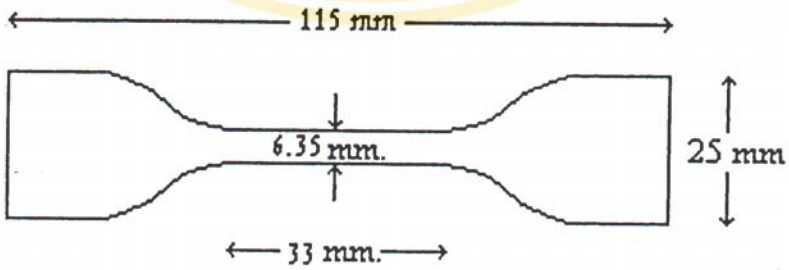

Figure 4.9: Dimensions of the tensile specimen

Copyright by Mahidol University

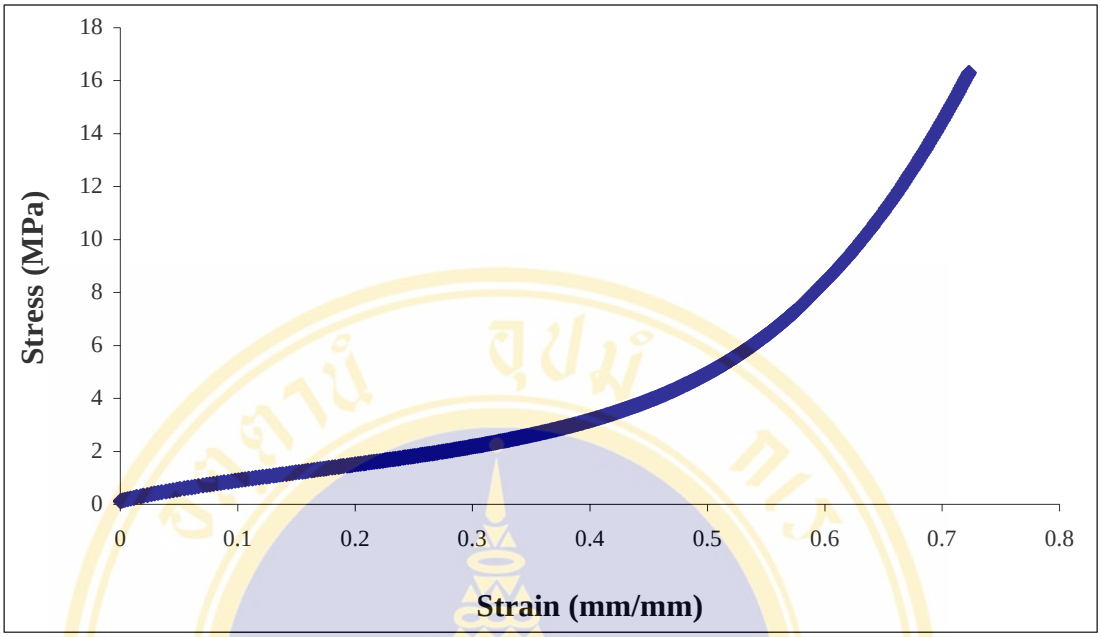

Figure 4.10: Stress-strain behaviour of unfilled NR

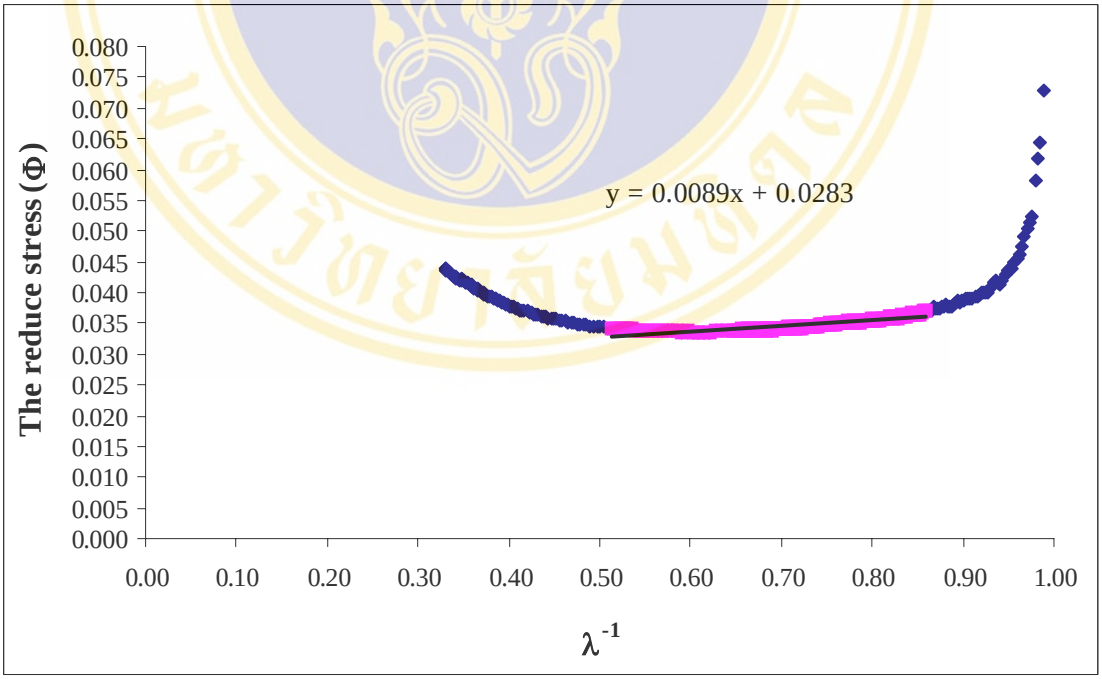

Figure 4.11: the reduced stress (Φ) against the inverse of extension ratio (λ^{-1}) of NR-2.5S.

Copyright by Mahidol University

4.8 Rheological properties measurement

Mooney viscosity measurement

The viscosity of compounded rubber was measured by Mooney Shearing Disk Viscometer at 100°C for 7 min. The picture of Mooney Shearing Disk Viscometer is shown in Figure 4.12. Approximately 20 g of compounded rubber was contained in the heat cavity and embedded on the rotating disk [2]. Viscosity was continuously measured at a constant rate as a function of time. In this study, the S rotor was used to measure the viscosity of compounded rubber because some compounded rubber in this work had a very high viscosity. The compounded rubber was preheated for 1 min before starting the test. Then the viscosity of compounded rubber was measured for 4 min (MS1+4). The Money viscosity of rubber compound was employed as another criteria to control the amount of carbon black incorporated into the rubber system.

Figure 4.12: Mooney Shearing Disk Viscometer

Copyright by Mahidol University

4.9 Mechanical properties measurement

4.9.1 Dynamic mechanical analyser (DMA)

Dynamic Mechanical Analyser (DMA) is an apparatus which could be employed to investigate the glass transition temperature and the characteristic dynamic mechanical properties. In this study, the DMA was used to study the characteristic of dynamic mechanical properties in tension mode at room temperature for the investigation of the temperature cycling effect on dynamic mechanical properties. The DMA apparatus is shown in Figure 4.13. The storage modulus (E′), the loss modulus (E″) and Tan delta (δ) of vulcanized rubber were measured by varying frequency between 1-50 Hz at sinus wave pulse 1 amplitude, 10% strain of the static load and 1 % strain of dynamic load.

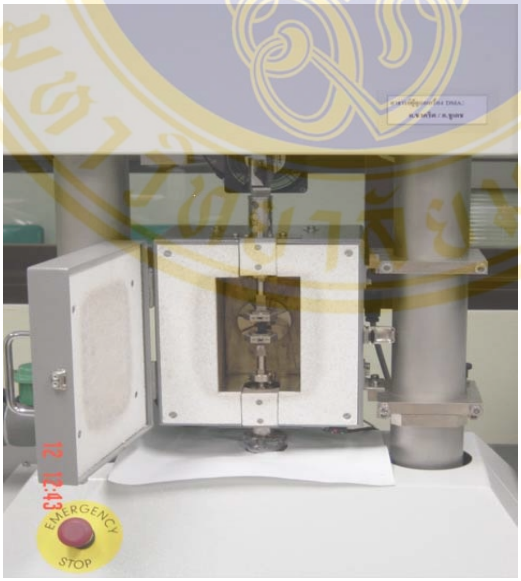

Figure 4.13: Dynamic Mechanical Analyser (DMA)

Copyright by Mahidol University

4.9.2 Micro-tension apparatus

In order to investigate the temperature cycling effect on the viscoelastic behaviour of rubber, the micro–tension apparatus was built. The picture of the micro-tension apparatus is shown in Figure 4.14. Steel springs having difference in spring constant were employed for the calibration of the micro-tension apparatus. In this investigation, the stress relaxation was studied in 1-dimensional tension due to the low complicated mode. The vulcanized rubber was cut as the rectangular shape ($5x30x1mm^3$).

Figure 4.14: Micro-tension

Copyright by Mahidol University

CHAPTER 5
RELAXATION BEHAVIOUR OF ELASTOMER

The mechanical properties, dynamic mechanical properties and failure properties of the elastomer represented the viscoelastic behaviour of the elastomer chains. Many theories, reviewed in Chapter 2, have been developed in order to explain and predict the elastomer properties. The viscoelastic behaviour under the dynamic force at high temperature was a topic focused by many researchers [74,99-104]. Both dynamic storage modulus and the dynamic loss modulus of the elastomer decreased when the temperature was raised up [103]. This might be due to the reduction of the internal viscosity and the interactions break down. Another explanation might be due to the poor temperature controlling in the experimental system. The temperature was repeatedly changed in a small range before reaching the design temperature in the temperature environment chamber. The failure of the linkage might arise from this temperature cycling process In order to verify this, the dynamic behaviour of elastomer which already relaxed under the temperature cycling condition was investigated. Natural rubber (NR) vulcanized with 0-60 phr of carbon black was employed for this study. The compound formulation is shown in Table 4.5. The specimens were divided into two groups. One group was the controlled group. The rubber specimen was extended to 50% static strain and was allowed to relax at 25°C. Another group, the rubber specimen was allowed to relax under the temperature cycling between 25°C and 50°C. The rubber specimen was first extended to 50% static strain in a tension mode using micro-tension apparatus. It was allowed to relax in the water environment at 25°C for 5 min. The system was then transferred into the water chamber controlled temperature at 50°C. The rubber system again was allowed to relax in the water environment for 5 min before transferring back to 25°C water chamber and was left for another 5 min. The rubber specimen was then dried and the dynamic behaviour was suddenly measured by using Dynamic Mechanical Analyzer

Copyright by Mahidol University

(DMA). The dynamic storage modulus was investigated as a function of frequency. The testing conditions are shown in Table 5.1

Table 5.1: DMA testing condition for study of the effect of temperature cycling on dynamic mechanical behaviour of elastomer

Testing Conditions	
Mode of Testing	Tension
Temperature	25 ^{o}C
Static strain	10%
Dynamic strain	1%
Frequency	1-50 Hz

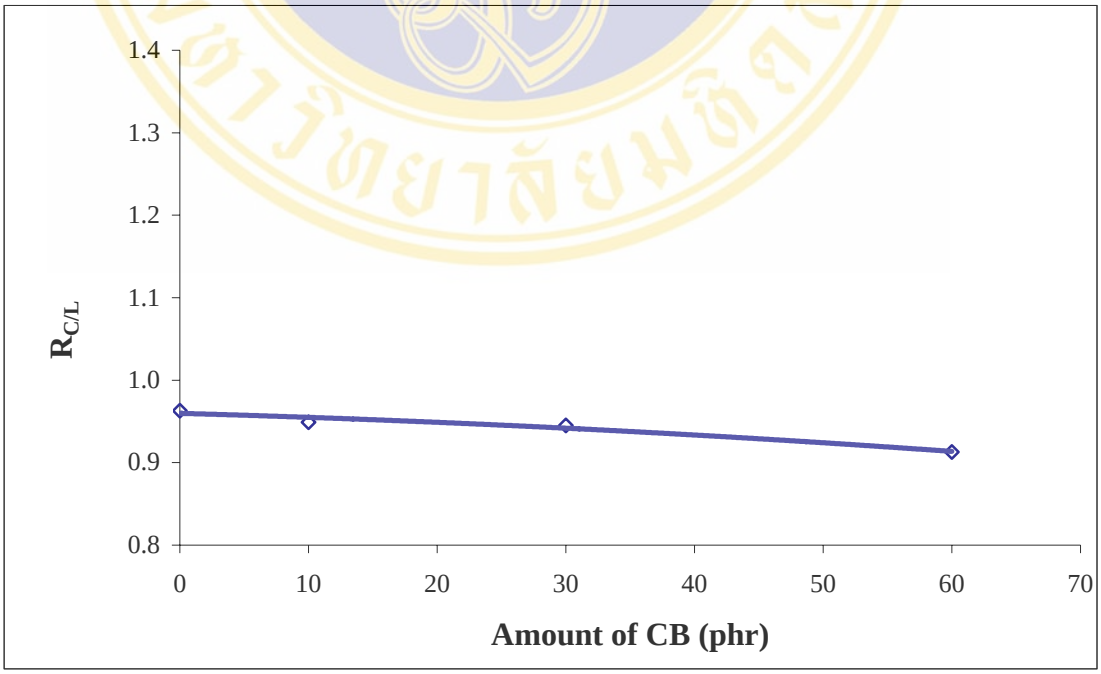

Figure 5.1: The effect of CB loading in the effect of temperature cycling on dynamic mechanical properties

Copyright by Mahidol University

The dynamic storage modulus of the carbon black filled NR did not significantly change over the range of frequency in this investigation. The dynamic behaviour at 6 Hz was selected to study the effect of temperature cycling on the dynamic behaviour [13, 104-105]. The ratio ($R_{C/L}$) between the dynamic storage modulus determined from the rubber specimen relaxed under the temperature cycling condition and the dynamic storage modulus determined from the rubber specimen relaxed under constant temperature was calculated. $R_{C/L}$ was plotted as a function of carbon black as shown in Figure 5.1

From Figure 5.1, it can be noticed that the dynamic storage modulus of the rubber relaxed under temperature cycling was lower than that of the rubber relaxed under constant temperature. This indicated that the temperature cycling process took part in the reduction of the viscoelastic of the elastomeric molecular chains. Therefore, the systematic work should be performed in order to explore the temperature cycling effect on the viscoelastic behaviour. Although the viscoelastic behaviour can normally be measured in term of creep and stress relaxation, the stress relaxation was selected because most of the rubber products for the engineering applications are employed at a constant strain.

The elastomer which should be used as a model in this investigation had to present the high relaxation rate in order to simplify the experiment. The relaxation behaviour depends on the chemical structure of the elastomer. Therefore, various types of elastomer were employed in order to select one as a model to study the effect of the temperature cycling. Furthermore, the effect of the important factors such as crosslink density, initial strain, water environment, carbon black on the relaxation behaviour were also investigated

5.1 Effect of crosslink density on the relaxation behaviour

NR with different amount of sulphur (1-2.5 phr) was employed in order to investigate the effect of crosslink density on the relaxation behaviour. The mixing formulations for NR compound are listed in Table 4.6. The method of determining crosslink density was reviewed in Chapter 4. In order to determine the relaxation

Copyright by Mahidol University

behaviour, the rubber specimen (5x30x1mm^3) was extended in a tension mode to 50% static strain at 25°C. The relationships between stress relaxation and time for rubber with different amount of crosslinking were observed. The relationship between calculated long term relaxation rate and crosslink density is illustrated in Figure 5.2. The stress relaxation increased with increasing the crosslink density in the rubber system. Therefore, crosslink density of the rubber specimen should be controlled throughout the temperature cycling experiment.

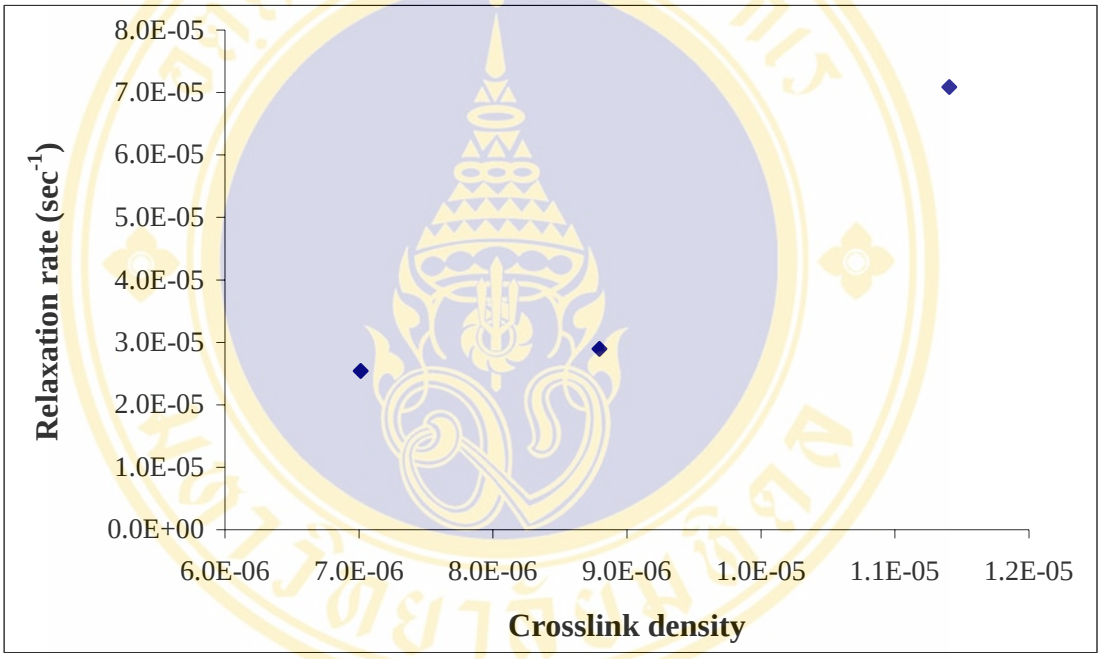

Figure 5.2: The relationship between the relaxation rate (sec^{-1}) and the crosslink density of unfilled NR.

5.2 Effect of initial strain on the relaxation behaviour

The unfilled NR (NR-0CB) specimen which was prepared according to the formulation in Table 4.5. The rubber specimen (5x30x1mm^3) was extended to specific static strain between 50 and 150% . The relationships between stress relaxation and time at 25°C were measured. The relationship between calculated long term relaxation rate and initial strain is illustrated in Figure 5.3. NR showed a higher relaxation rate at

Copyright by Mahidol University

the high level of strain for a long term relaxation. However, due to the limitation of the micro-tension apparatus, the highly filled NR could not be extended over the 50% static strain. Therefore, 50% static strain was chosen as the initial strain for study the relaxation behaviour of elastomer under the temperature cycling.

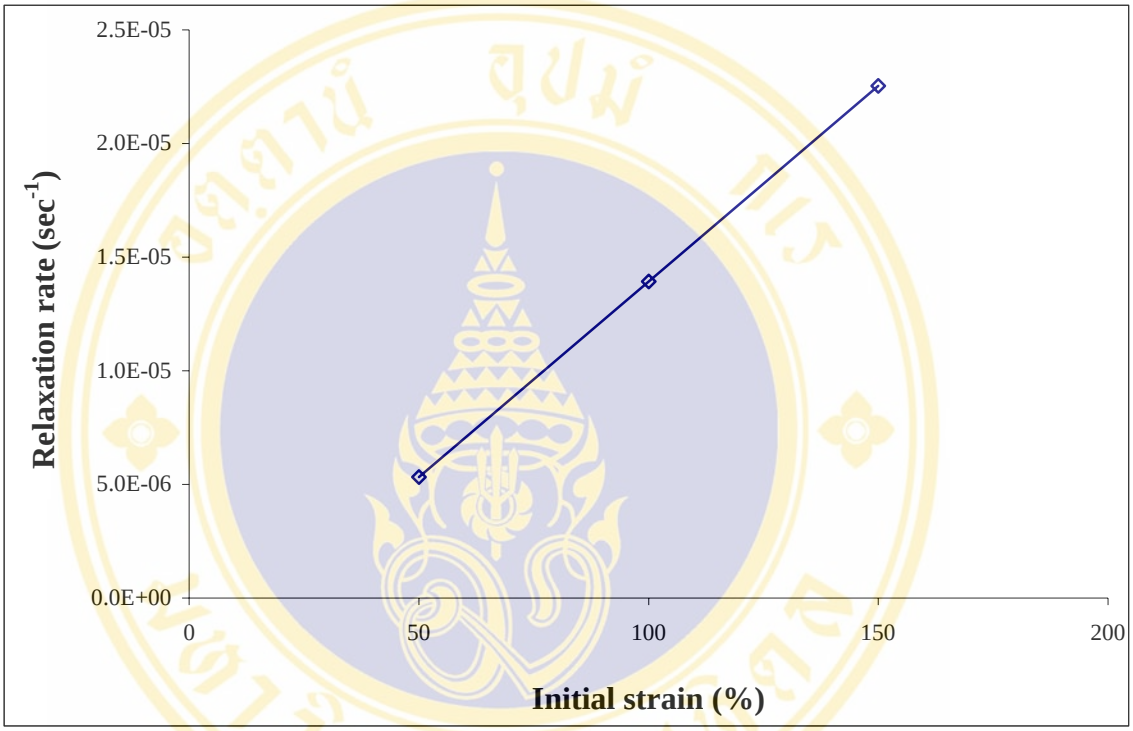

Figure 5.3: The relationship between calculated long term relaxation rate and initial strain (%) of unfilled NR.

5.3 Effect of water on the stress relaxation behaviour

It was reported by Deeprasertkul [14] that the slow rate of temperature changes in the specimen as its temperature was controlled by the air in an oven impedes the accuracy of the creep under temperature cycling. Therefore, water which has a high level of heat conductivity was selected as a media in order to study the effect of the temperature cycling. The rubber specimen with 0 phr of carbon black was extended in the tension mode to 50% static strain by micro-tension apparatus. The specimen was allowed to relax at 25°C in both air and water environment. The

Copyright by Mahidol University

relationships between stress relaxation and time were measured as illustrated in Figure 5.4. The relaxation rate at specific time for both determined in water and in air was nearly identical as shown in Figure 5.5. Therefore, water could be used as a medium in the temperature cycling experiment.

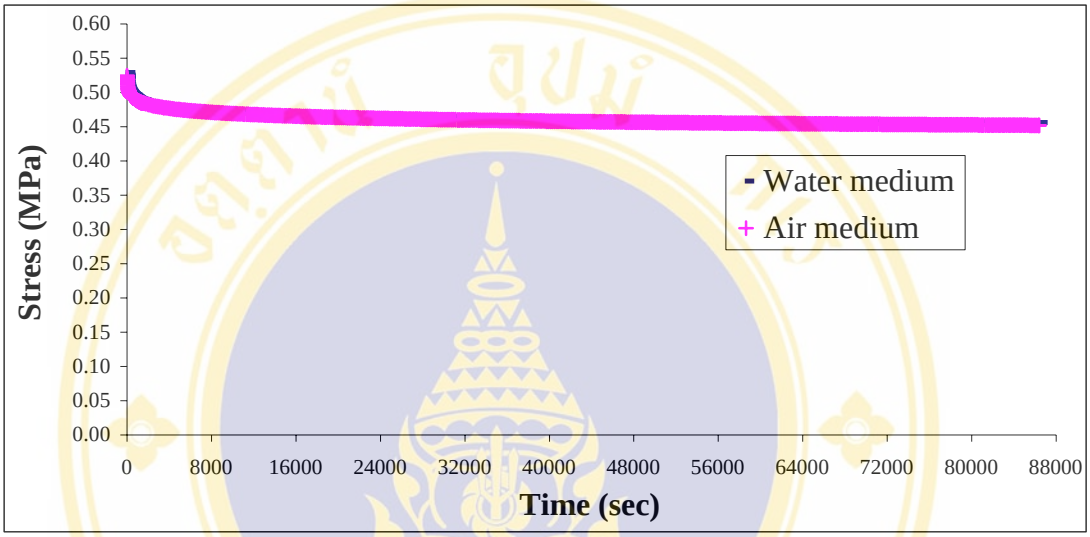

Figure 5.4: The relationships between stress relaxation and time of unfilled NR determined in water medium and in air medium.

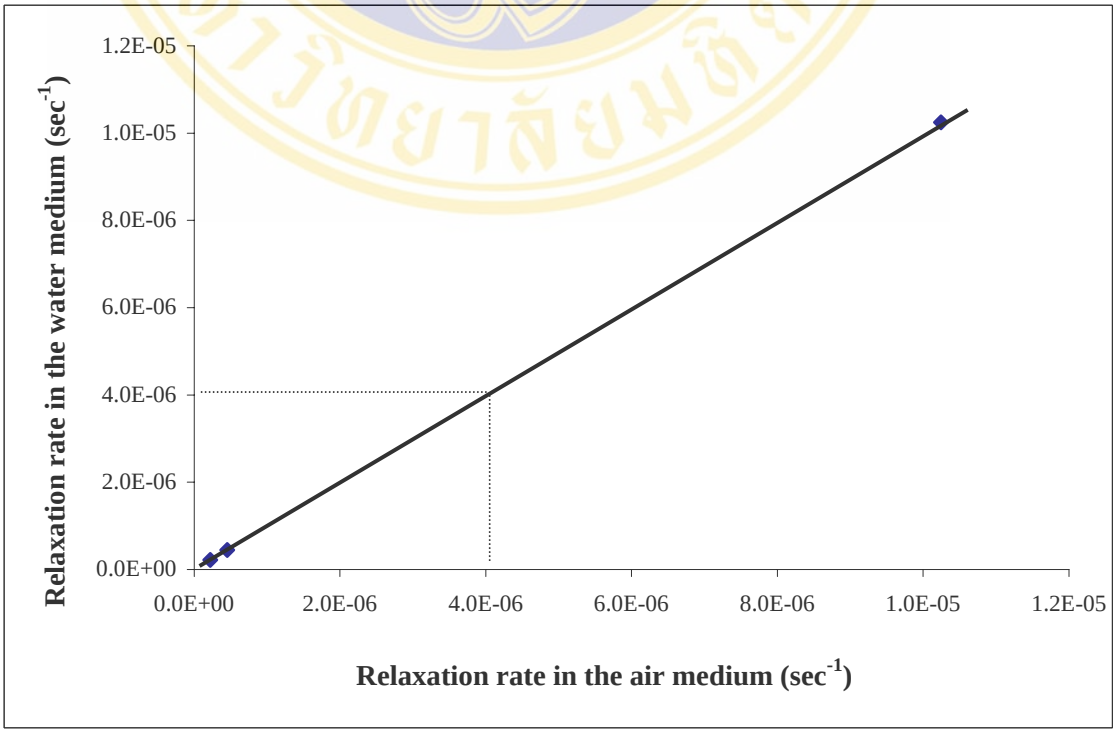

Figure 5.5: The relationships between relaxation rate at specific time of unfilled NR for both determined in water medium and in air medium.

Copyright by Mahidol University

5.4 Effect of carbon black on the relaxation behaviour

Carbon black is usually employed as a reinforcing filler of the elastomer. The amount and the characteristics of carbon black such as its surface area affect the viscoelastic behaviour of the elastomer. Therefore, the effect of carbon black on the stress relaxation was also studied.

5.4.1 Amount of carbon black

NR with different amounts of carbon black (0-60 phr) was employed in order to investigate the effect of carbon black on the relaxation behaviour. The mixing formulations for NR compound are listed in Table 4.5. In order to determine the relaxation behaviour, the rubber specimen (5x30x1mm^3) was extended in a tension mode to 50% static strain at 25°C. The relationships between stress relaxation and time of rubber with different amounts of carbon black were observed. The relationship between calculated long term relaxation rate and crosslink density is illustrated in Figure 5.6.

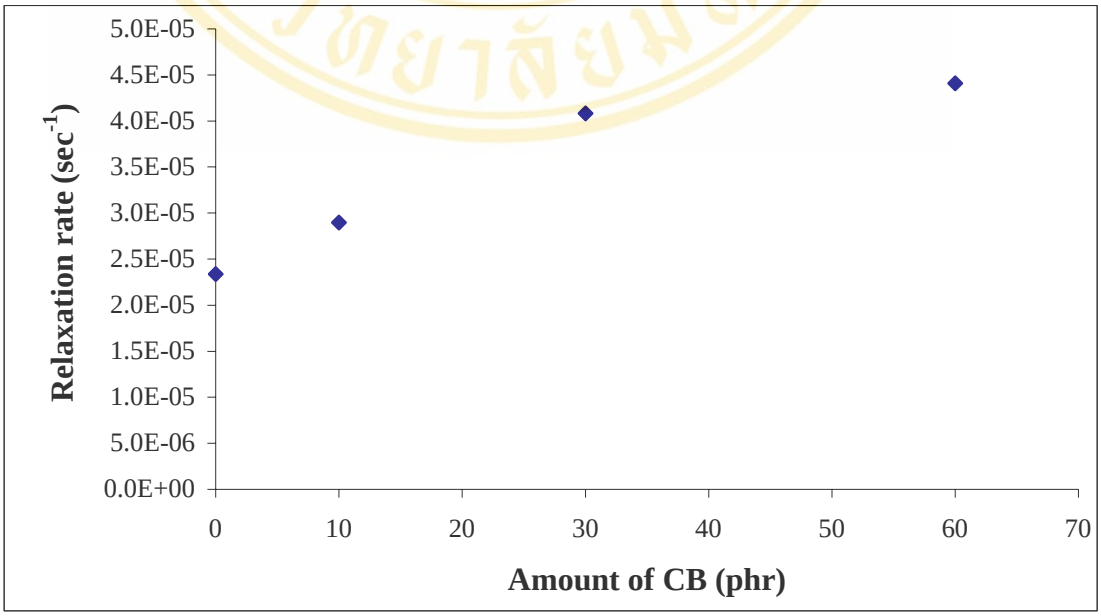

Figure 5.6: The relationships between stress relaxation rate (sec^{-1}) and different amounts of carbon black (phr).

Copyright by Mahidol University

The result indicated that the long term stress relaxation rate increased with increasing amount of incorporated carbon black. It could be explained by considering the increasing in the carbon black network and the interaction between carbon black and elastomer.

5.4.2 Surface area of carbon black

The carbon black whose the surface area is determined by Nitrogen absorption between 25-122.5 [106] was employed in order to investigate the effect of surface area on the relaxation behaviour. The mixing formulations for NR compound are listed in Table 4.7. The values of surface area of the different type of carbon black [106] are listed in Table 5.2.

Table 5.2: The surface area of the different type of CB

Type of CB	Surface area of CB (m^2/g)
N220	122.5
N330	80.0
N550	43.5
N774	25.0

In order to determine the relaxation behaviour, the rubber specimen ($5x30x1mm^3$) was extended in a tension mode to 50% static strain at 25°C. The relationships between stress relaxation and time were observed. The relationship between calculated long term relaxation rate and surface area of carbon black is illustrated in Figure 5.7. The result indicated that the surface area of the carbon black did not affect on the stress relaxation behaviour of natural rubber.

Copyright by Mahidol University

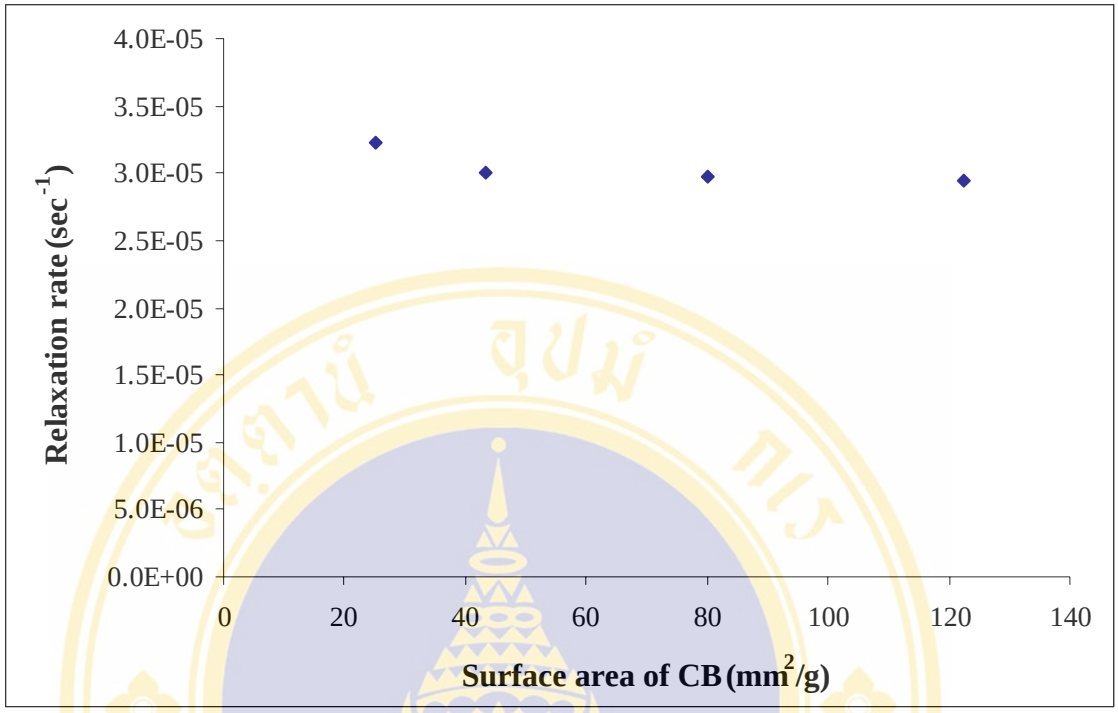

Figure 5.7: The relationship between calculated long term relaxation rate and surface area of carbon black

It could be concluded from the results presented in this chapter that natural rubber was a model which would be employed to study the stress relaxation under the temperature cycling condition in the water environment. For each rubber compound prepared, the crosslink density had to be controlled. The characteristic of carbon black should be concerned when the relaxation behaviour of carbon black filled NR was investigated. The density measurement should be performed in order to control the level of carbon black incorporated into the rubber matrix.

Copyright by Mahidol University

CHAPTER 6
EFFECT OF THE TEMPERATURE CYCLING ON STRESS RELAXATION BEHAVIOUR OF ELASTOMER

Currently, the elastomer has been employed as an engineering material which practically tolerated under the severe environment such as under the sunlight for the dynamic absorption application. The difference in temperature which goes up during the day and lowers in the night affects the dynamic absorbing ability of the elastomer. Instead of dynamic condition, the viscoelastic behaviour of the elastomer under the static force was studied in order to simplify the temperature cycling investigation. Although the viscoelastic behaviour could normally be measured in term of creep and stress relaxation, the latter was selected. Because most of the rubber products for the engineering applications are employed at a constant strain. The stress relaxation of the elastomer was measured under the cyclic temperature conditions. The rectangular elastomer specimen (5x30x1 mm^3) was initially extended in a horizontally geometry. The stress relaxation was considered as a function of time by using micro-tension apparatus in the water medium whereas the temperature was cycled repeatedly between two specific temperatures.

6.1 Effect of temperature cycling on the stress relaxation behaviour of unfilled natural rubber

From the previous chapter, the dynamic behaviour of the unfilled NR reduced when the elastomer had been placed under the temperature cycling process. This must be concerned with changing in viscoelastic behaviour. Therefore, the stress relaxation behaviour under temperature cycling was investigated. The unfilled NR specimen was extended in a tension mode to 50 % static strain in the water environment

Copyright by Mahidol University

at 25°C. The rubber was maintained at this temperature for 20 min. Then, the rubber was transferred into another water reservoir which the temperature was controlled at 50°C. The rubber specimen was controlled at this temperature for 30 minutes before transferring back to the water reservoir which the temperature was controlled at 25°C. The step of temperature cycling process is written down in Table 6.1. The relationship between stress and time under the temperature cycling conditions is illustrated in Figure 6.1.

Table 6.1 The temperature cycling steps for unfilled NR.

Step	Temperature (^{o}C)	Time (min)	Total time (min)
1	25	20	20
2	50	30	50
3	25	20	70
4	50	30	100
5	25	20	120
6	50	30	150
7	25	20	170

As shown in Figure 6.1, the viscoelastic behaviour of the natural rubber was presented in term of stress relaxation when the rubber specimen was maintained at 25°C. The stress in the first region immediately increased from point A to point B when the temperature was increased from 25°C to 50°C. This phenomenon could be explained by considering the thermodynamic of the elastomer deformation. A rubber is expected to be under the thermodynamic equilibrium when the rubber is aged at the temperature above it T_g. When the temperature is raised, the entropy of the rubber system is increased spontaneously and remains towards the thermodynamic equilibrium and the rubber is possible build up a local stress which can be explained by the immediate increase in the stress [99]. The phenomenon is later called “the thermodynamic effect”. This effect could be observed only at the first few min after the

Copyright by Mahidol University

change in temperature. Furthermore, the stress decreased with time from point B to point C as shown in Figure 6.1. The stress relaxation rate calculated using Equation 2.59 at 50°C was higher than the stress relaxation rate at 25°C confirmed by Figure 6.2. The more reduction in stress at higher temperature could possible be explained by considering the elastomer chain slippage [104]. The slippage of the chains increases when the temperature is raised caused a reduction in the internal viscosity. This phenomenon is later called "the temperature effect".

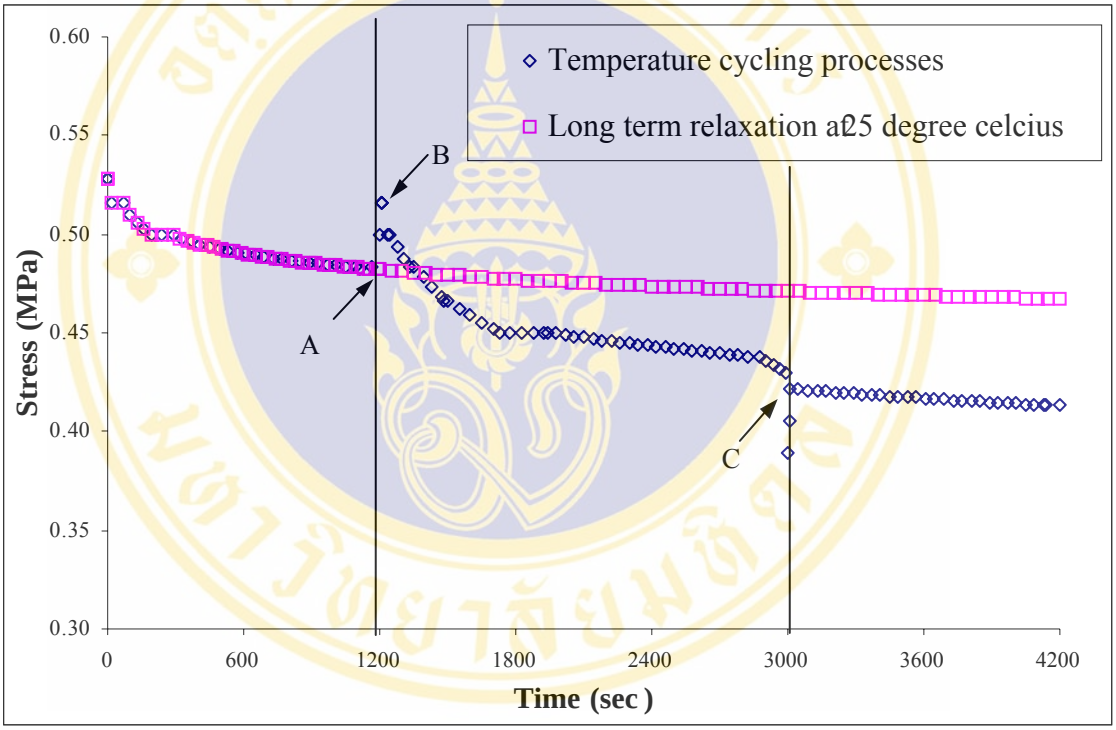

Figure 6.1: The stress relaxation of unfilled NR as a function of time under the temperature cycling condition.

In this investigation, the WLF theory [67,68] was employed in order to verify that the reduction in stress of the elastomer could be explained by using linear viscoelasticity when the temperature was raised. The stress relaxation of unfilled NR at different temperature according to the WLF theory could be calculated by determining the shift factor stated in the Equation 2.63 [67-70]. From Equation 2.63, C_1^r and C_2^r are the coefficient constant at the reference temperature which was 25°C in this investigation. These two coefficients were determined by plotting $(T-T_r)/\log a_T$ against

Copyright by Mahidol University

$T-T_r$. The result is shown in Figure 6.3. The tangent (s), intercept (i) and the two empirical constants (C_1^r, C_2^r) were calculated by using the Equationds 2.64 and 2.65 [67].

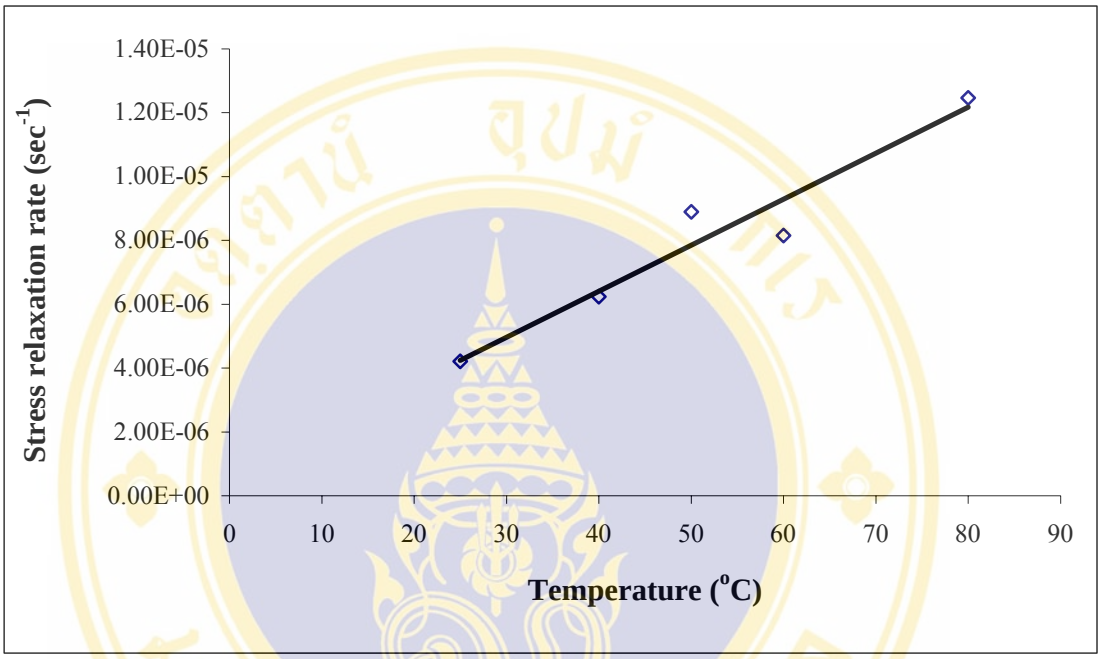

Figure 6.2: Stress relaxation rate of unfilled NR at different temperature

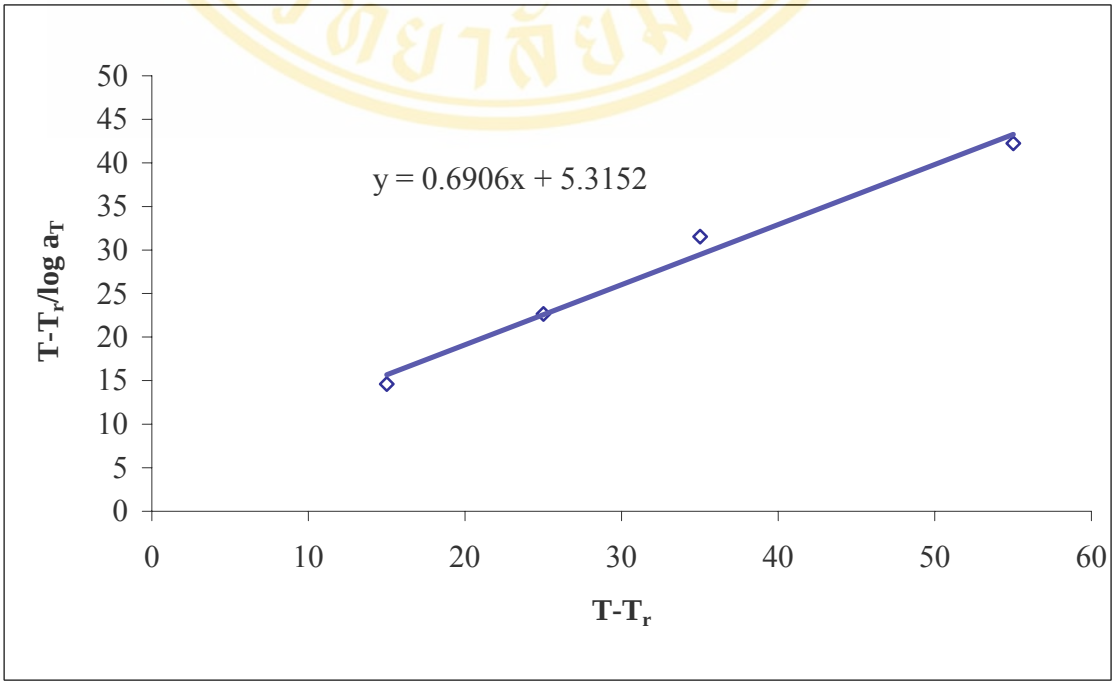

Figure 6.3: The relationship between $(T - T_r) / \log a_T$ and $T - T_r$ of unfilled NR.

Copyright by Mahidol University

Table 6.2: Log a_T of unfilled natural rubber at a specific temperature.

T(^{o}C)	T(K)	T-T_r	Calculated (log a_T)
25	298	0	-
40	313	15	0.96
50	323	25	1.11
60	333	35	1.19
80	353	55	1.27

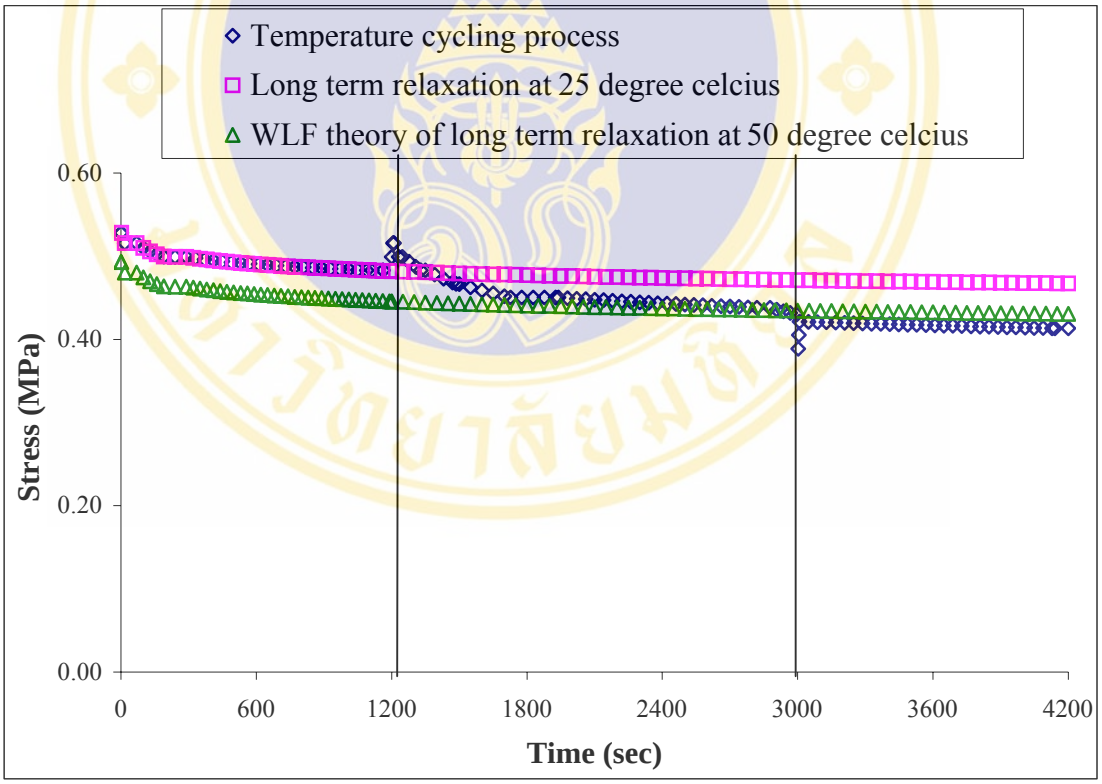

Figure 6.4: The stress relaxation of unfilled NR at 50 % elongation under the temperature cycling condition from 25 °C to 50 °C and then back to 25 °C in the water environment.

The calculated logarithmic shift factor at a specific temperature is shown in Table 6.2. C_1^r and C_2^r are equal to -1.448 and 7.697, respectively. The ratio between the

Copyright by Mahidol University

calculated stress from WLF theory at 50°C and the stress at 50°C under the temperature cycling process was approximately 1. The results are shown in Figures 6.4 and 6.5. This indicated that stress relaxation of unfilled natural rubber under the second step of the temperature cycling (increased the temperature) followed the WLF theory. This allowed both "The thermodynamic effect" and "The temperature effect" to be the explanations for the stress relaxation behaviour under the second step of the temperature cycling.

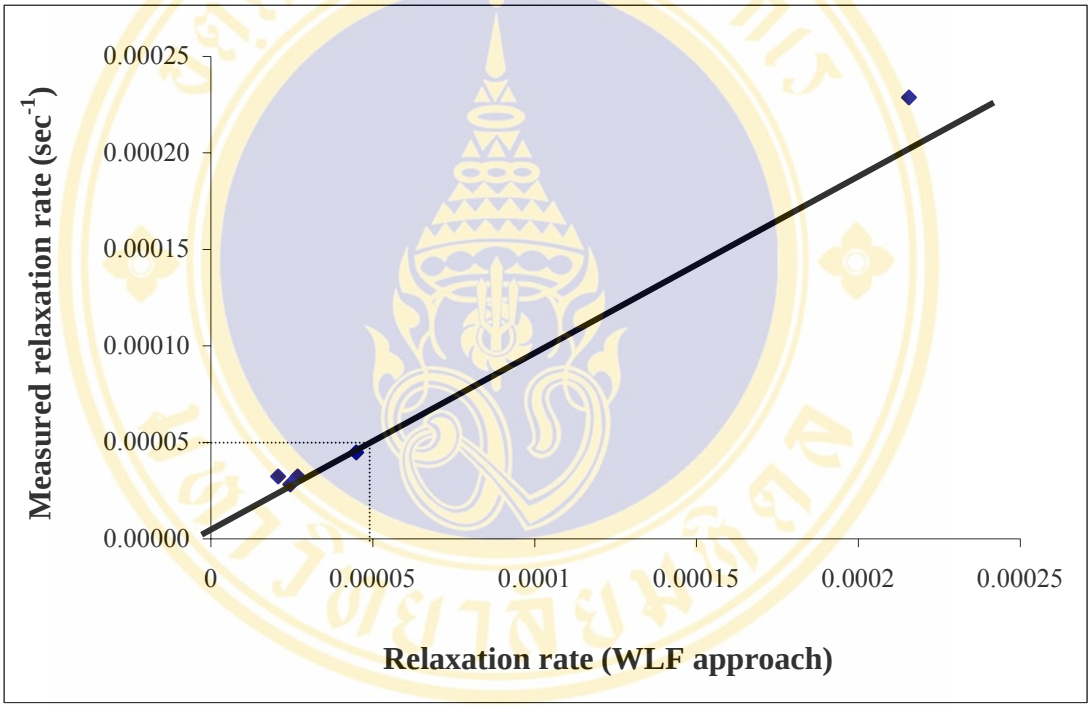

Figure 6.5: The relationship between calculated relaxation rate at 50°C from temperature cycling condition and calculated relaxation rate at 50°C using WLF approach.

However, when the temperature was reduced from 50°C to 25°C in the third step of the temperature cycling, the stress of the unfilled NR was lower than the stress measured from the long term stress relaxation at the 25°C and even lower than stress measured from the stress relaxation at 50°C as shown in Figure 6.1. The abrupt change in temperature might increase the tendency of the chain to move which increased the slippage process resulting in the reduction of the internal viscosity [104]. This could be

Copyright by Mahidol University

considered as an explanation for the decrease in stress when the temperature was reduced under the temperature cycling condition. The ratio between the relaxation rate of unfilled NR at 25°C after temperature cycling and the long term relaxation rate of unfilled NR as shown in Figure 6.6 was much more than 1. The relaxation rate at 25°C after temperature cycling condition had a new equilibrium. This verified the breakdown of the physical interaction between elastomer and elastomer during the temperature cycling process.

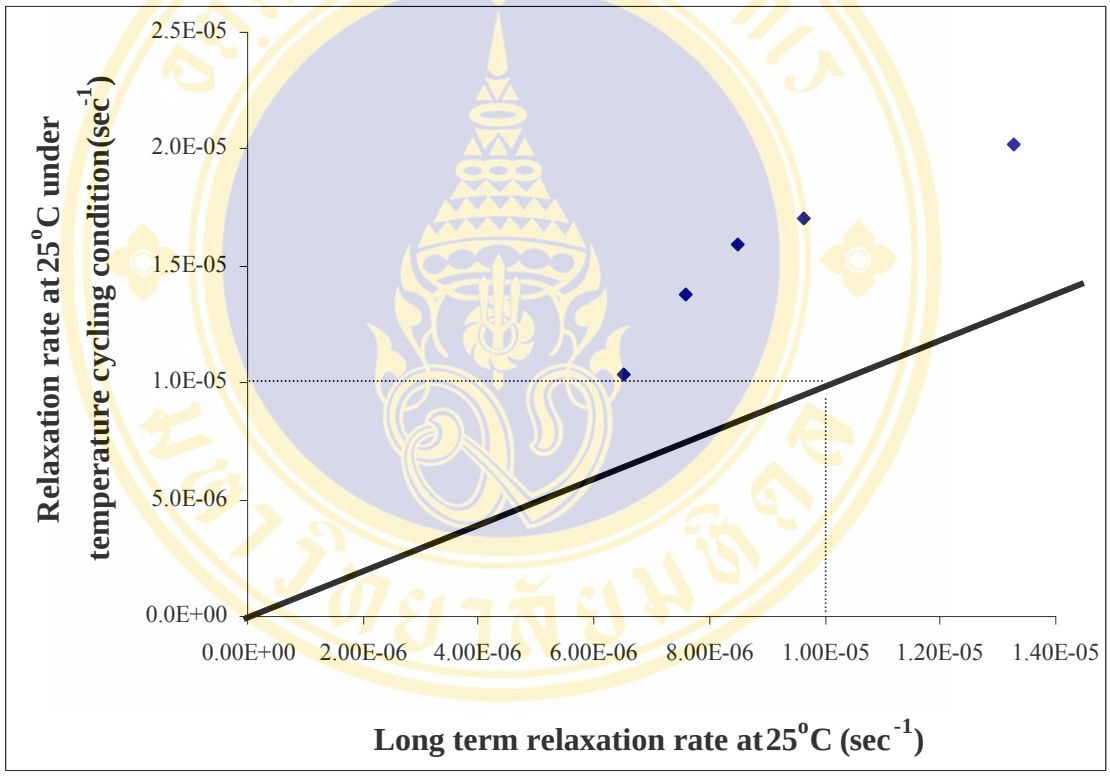

Figure 6.6: The relationship between calculated relaxation rate at 25°C from temperature cycling condition and calculated relaxation rate at long term 25°C.

Moreover, The ratio between the time to reach the same stress of the long term relaxation at the constant temperature of 25°C with the time to reach the same stress of the elastomer relaxation at 50°C under the temperature cycling process ($R_{25L/50C}$) was calculated. The logarithmic decade of ($R_{25L/50C}$) was approximately 1.2 as shown in Figure 6.7. When the calculated shifted valued from 25°C to 50°C considered using WLF approach was predicted to be 1.107 as shown in Table 6.2. The results were

Copyright by Mahidol University

nearly the same. This indicated that the stress of the rubber was relaxed under the raising temperature due to the reduction in the internal viscosity.

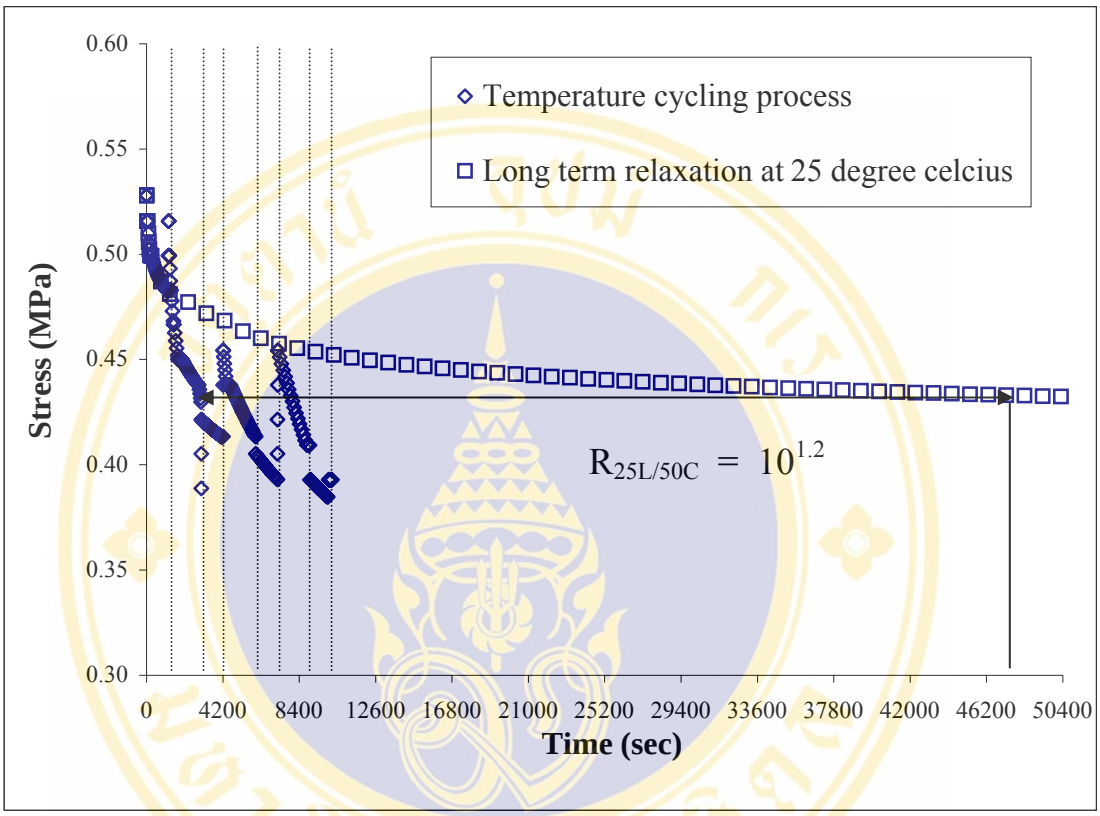

Figure 6.7: Comparison between the stress relaxation behaviour at 50°C from temperature cycling condition and the stress relaxation behaviour at long term 25°C.

When the temperature was reduced to 25°C during the temperature cycling process, the logarithmic decade of the ratio between the time to reach the same stress of the long term relaxation at the constant temperature of 25°C and the time to reach the same stress of the elastomer relaxation at 25°C after the temperature cycling process ($R_{25L/25C}$) was calculated. According to the Figure 6.8, the logarithmic decade of ($R_{25L/25C}$) was approximately 2. This also indicated that the physical interaction between elastomer and elastomer might be broken down by the difference in chain mobility due to the abrupt reduction in temperature.

Copyright by Mahidol University

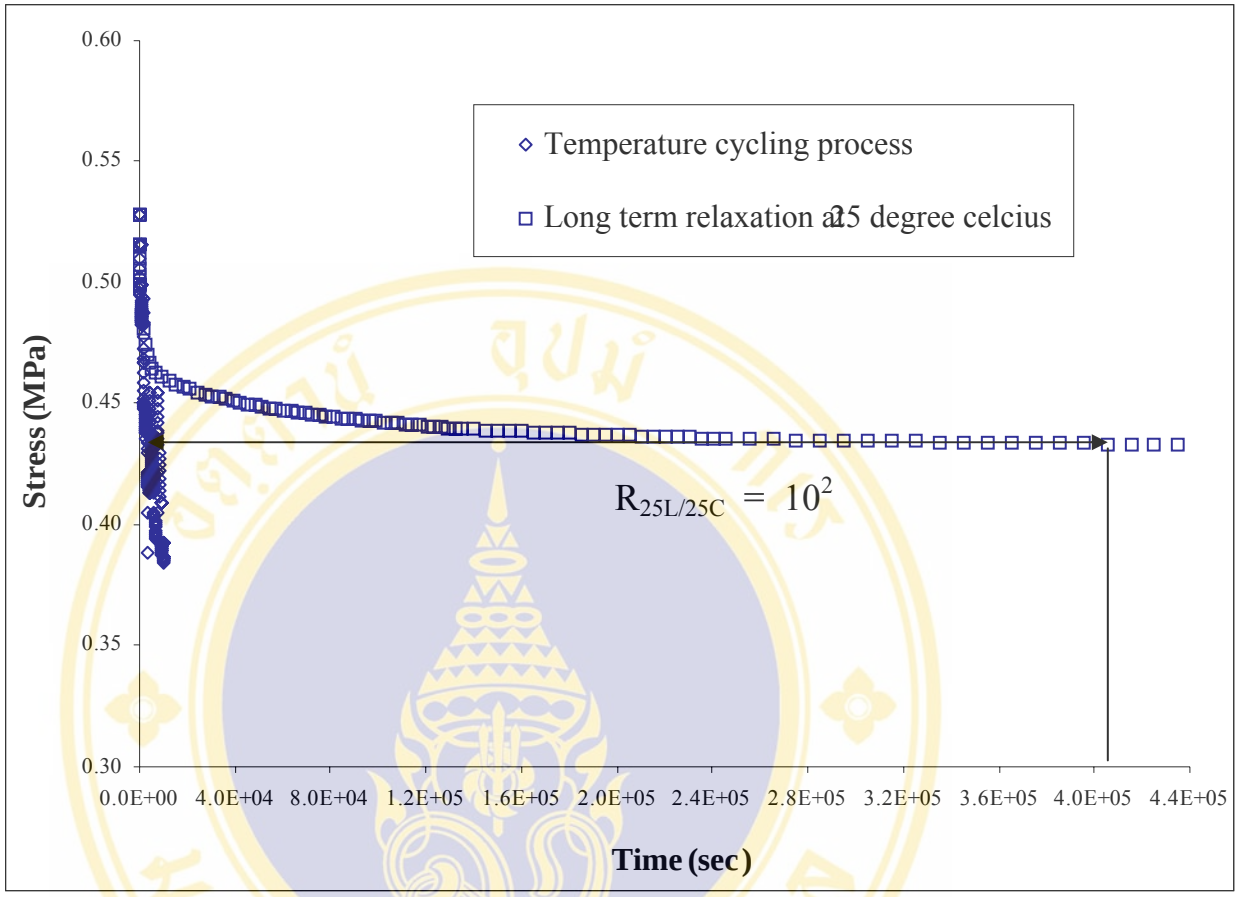

Figure 6.8: Comparison between the stress relaxation behaviour at 25°C from temperature cycling condition and the stress relaxation behaviour at long term 25°C.

In engineering applications, the environment temperature is altered more than once. The effect of cycles of temperature cycling on the stress relaxation was therefore investigated. As shown in Figure 6.9, the stress of the NR increased dramatically when the temperature was immediately raised up to 50°C in the second round of temperature cycling process. "The thermodynamic effect" concerned with the reduction in entropy term was considered as an explanation. "The temperature effect" concerning with the internal viscosity also governed the relaxation process. It also showed that the elastomer molecule relaxed to a new equilibrium at 25°C created by the first step of temperature cycling process. It was also noticed that the relaxation rate at 50°C increased with the cycle of temperature cycling process as shown in Figure 6.10. This indicated the more breakdowns in the physical interaction or might be some chemical interaction with each cycle of temperature cycling process. The logarithmic

Copyright by Mahidol University

decade of ratio ($R_{25L/25C}$) was calculated for each number of cycles. From the relationship illustrated in Figure 6.11, the ($R_{25L/25C}$) dramatically increased with each cycle of temperature cycling process. It indicated that the reduction of stress strongly depended on the number of cycle of the temperature cycling process.

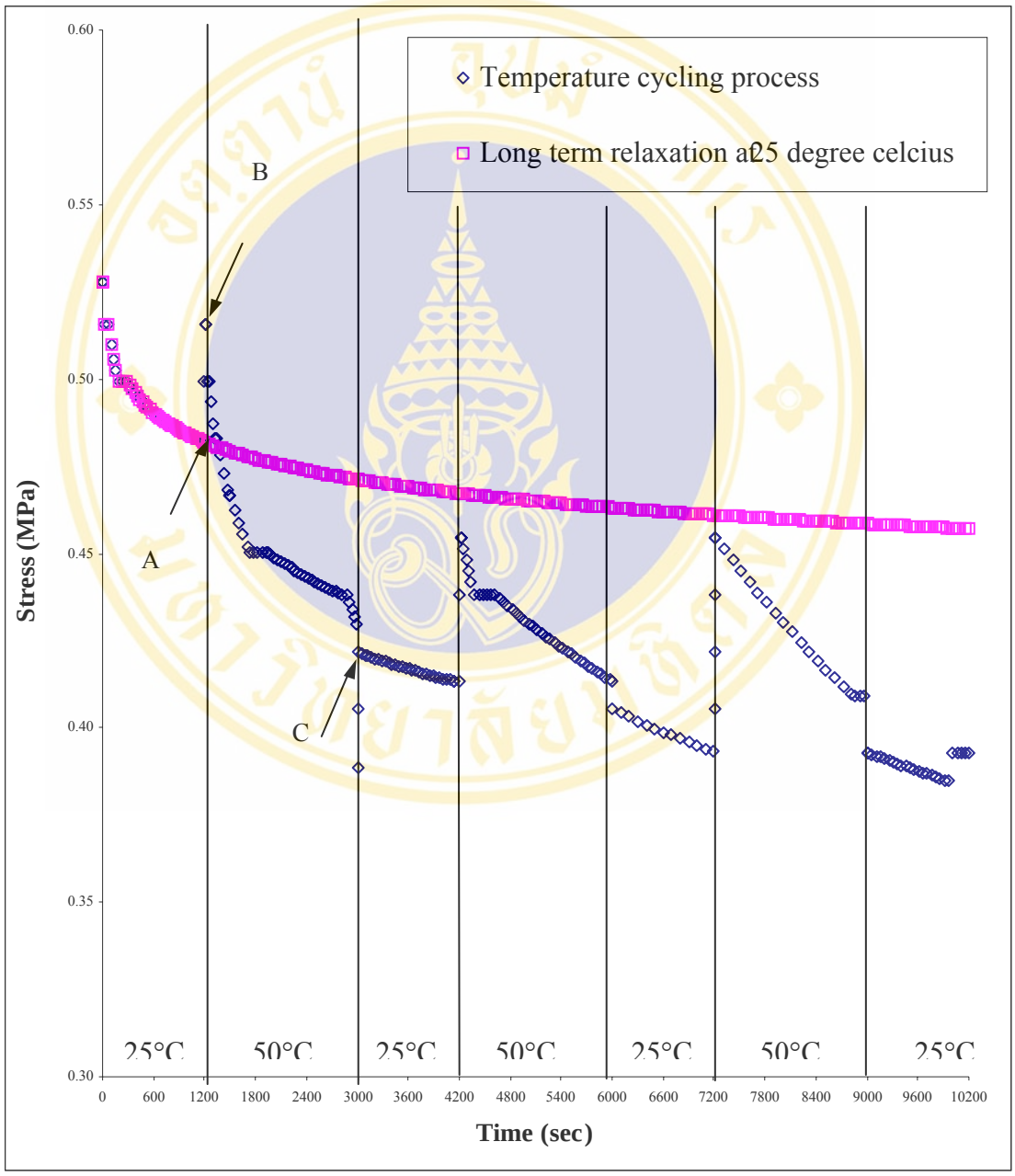

Figure 6.9: The stress relaxation of unfilled NR as a function of time under the temperature cycling condition.

Copyright by Mahidol University

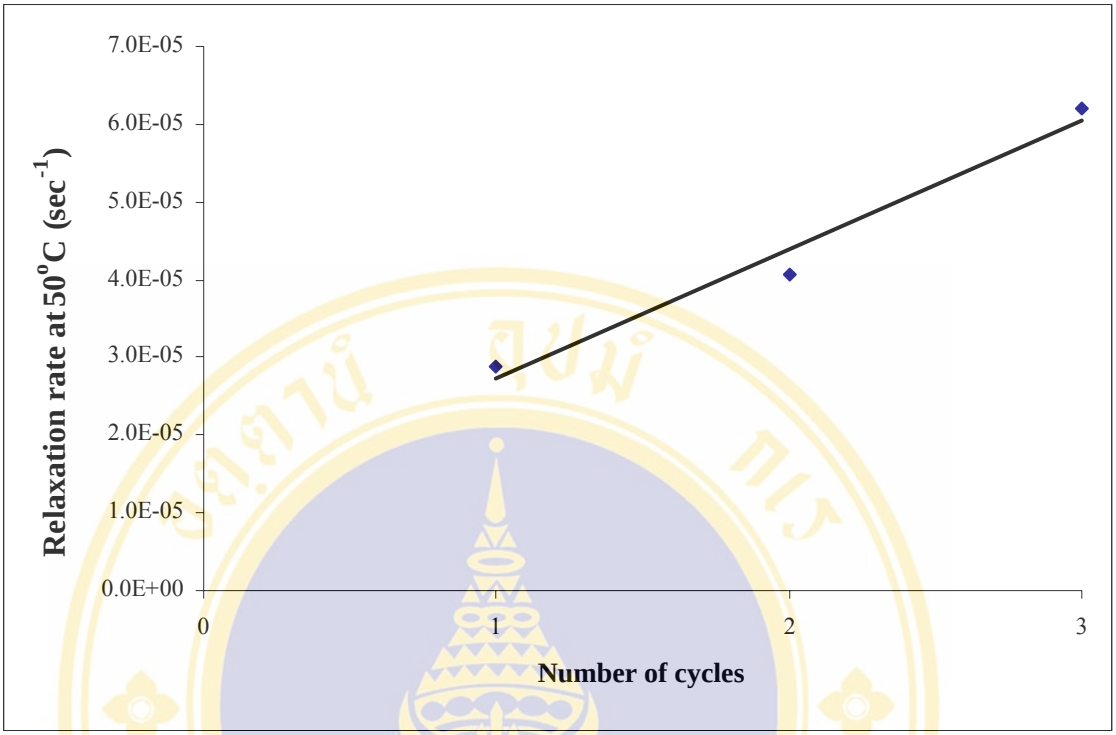

Figure 6.10: The relationship between calculated relaxation rate at 50°C from temperature cycling condition and number of cycles.

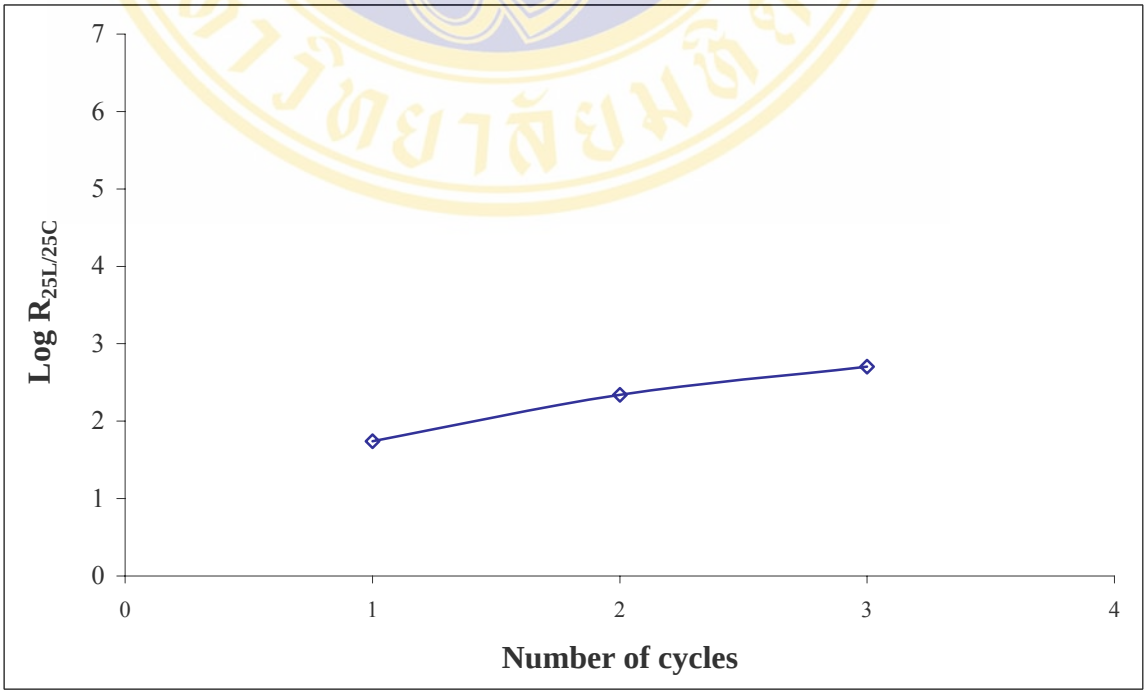

Figure 6.11: The relationship between calculated $R_{25L/25C}$ from temperature cycling condition and number of cycles.

Copyright by Mahidol University

It can be concluded up until now that the elastomer-elastomer interaction is dramatically reduced due to the abruptly change in temperature during the temperature cycling condition. This reduces the rubber product lifetime, especially when the service temperature is cyclically changed. As stated before that the internal viscosity of rubber molecule depends on the service temperature, the temperature gradient (ΔT) during the cycling process may affect the service life of the rubber product. Therefore, the effect of temperature gradient in temperature cycling condition on the stress relaxation was studied and the results are reported in the next section.

6.2 Effect of temperature gradient in temperature cycling condition on the stress relaxation behaviour of unfilled natural rubber

The unfilled NR was again employed in this investigation. The rubber specimen was extended in a tension mode to 50% static strain by micro-tension. The system was later controlled at 25°C in the water environment for 5 min. Then the rubber specimen was transferred into the water reservoir which the temperature was controlled at 40,50,60,70 or 80°C. The specimen was kept in those temperatures for 5 minutes before transferring back to the 25°C water reservoir. The rubber specimen was also kept at this condition for 5 min. The step of the temperature cycling process is written down in Table 6.3. The relationships between stress and time at different temperature gradient for the temperature cycling process are shown in Figures 6.12-6.15.

The ratio R_{600} between stress using WLF approach and the stress measured at time equal to 600 s in Figures 6.12-6.15 was calculated. The stress at 600 s was selected because the internal viscosity of the rubber should be in the equilibrium of the raising up temperature. The results are shown in Figure 6.16. The R_{600} was nearly 1 over the range of experimental temperature. This indicated that the stress relaxation behaviour at different temperature gradient was governed by both “The thermodynamic effect” and “The temperature effect”. However, the stress relaxation of unfilled NR in a tested cycle from 25 to 80°C and 80 to 25°C could not be predicted

Copyright by Mahidol University

correctly by the WLF theory. This might be due to this high temperature, i.e., near the water boiling point, which caused an error in the controlled temperature process.

Table 6.3: The temperature cycling steps for unfilled NR.

The time interval (minutes)		
5	5	5
The step of temperature(^{o}C)		
25	40	25
25	50	25
25	60	25
25	80	25

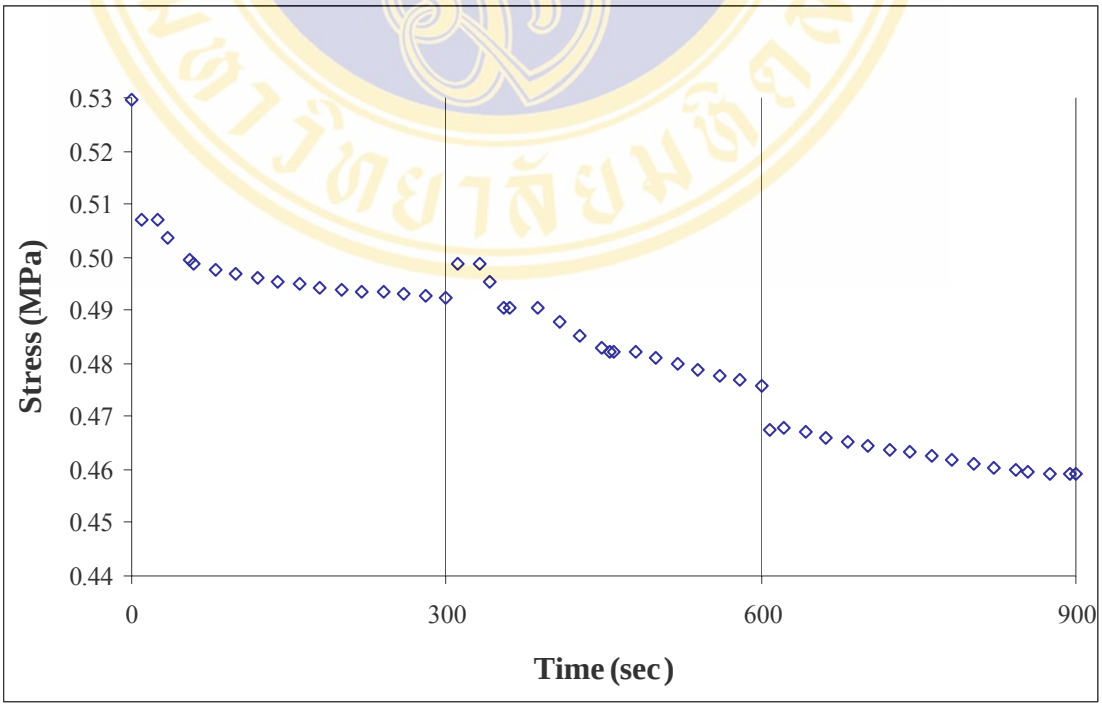

Figure 6.12: The stress relaxation of unfilled NR at 50% elongation under the temperature cycling from 25°C to 40°C and then back to 25°C in the water environment.

Copyright by Mahidol University

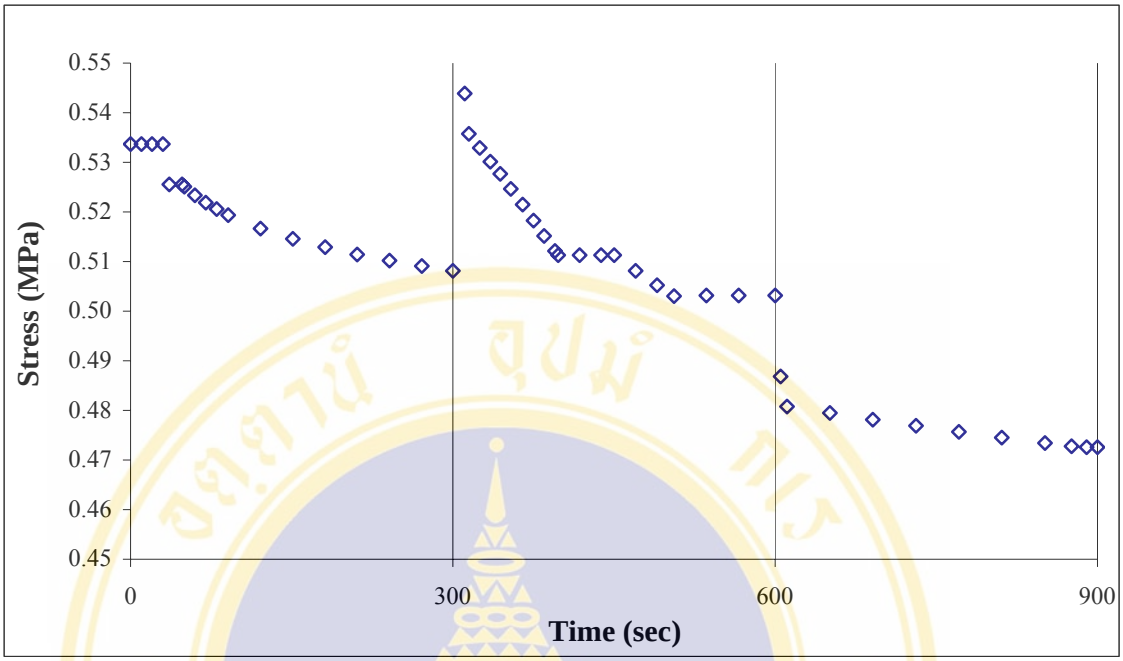

Figure 6.13: The stress relaxation of unfilled NR at 50% elongation under the temperature cycling from 25°C to 50°C and then back to 25°C in the water environment.

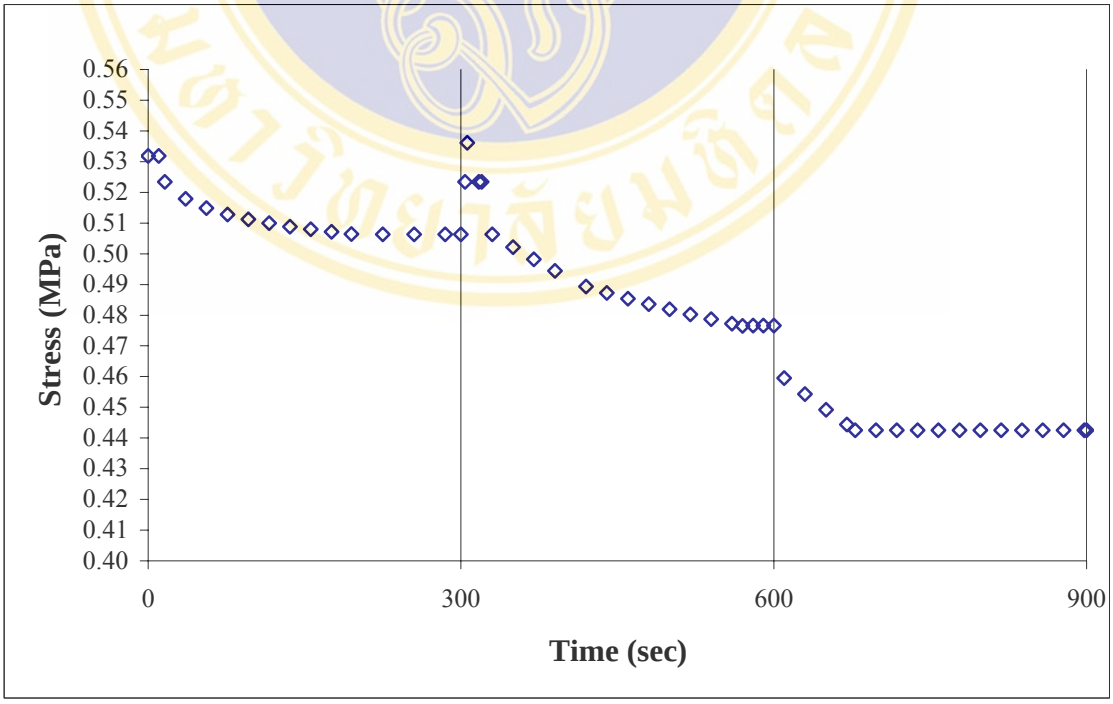

Figure 6.14 The stress relaxation of unfilled NR at 50% elongation under the temperature cycling from 25°C to 60°C and then back to 25°C in the water environment.

Copyright by Mahidol University

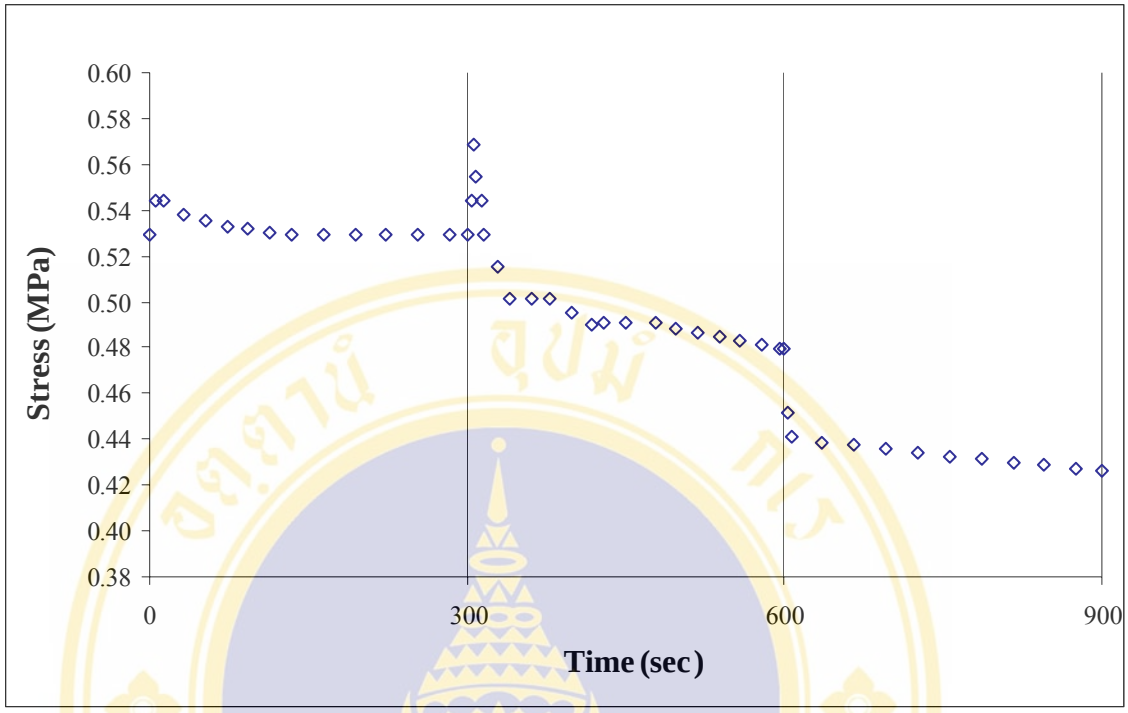

Figure 6.15: The stress relaxation of unfilled NR at 50% elongation under the temperature cycling from 25°C to 80°C and then back to 25°C in the water environment.

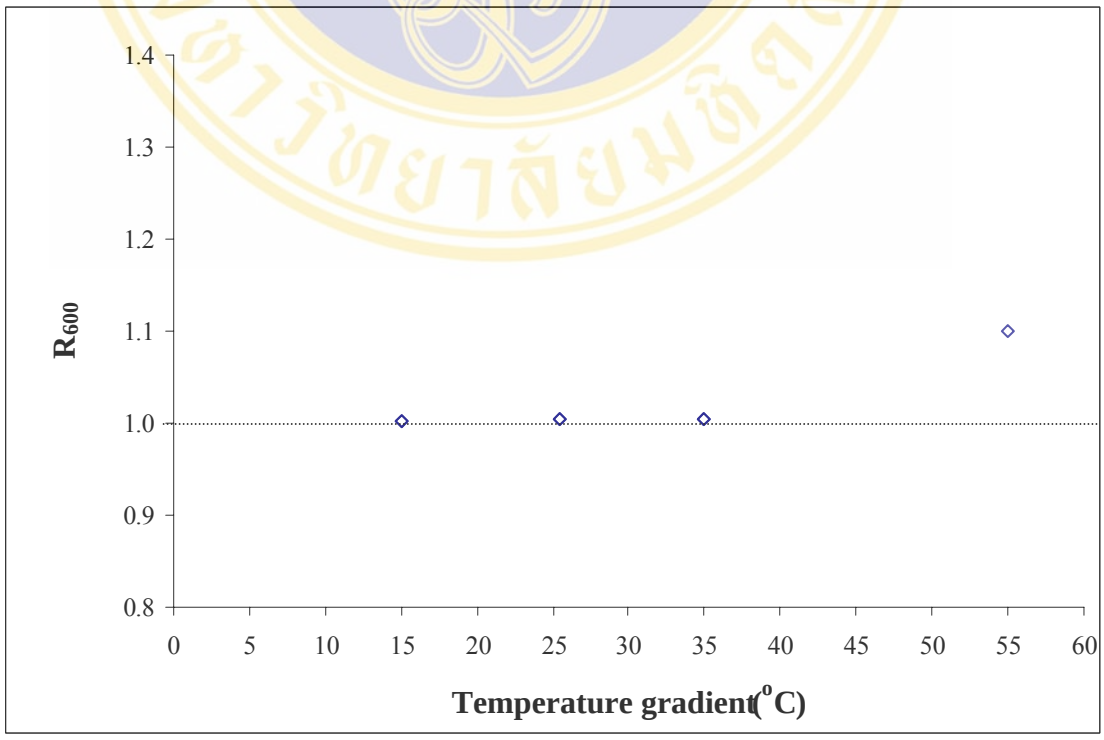

Figure 6.16: The relationship between R_{600} and the temperature gradient (°C).

Copyright by Mahidol University

As stated before that “the thermodynamic effect” and “the temperature effect” was the two phenomena governed the relaxation behaviour under the temperature cycling measurement, therefore, the effect of temperature gradient on each phenomenon was also investigated.

“The thermodynamic effect”

“The thermodynamic effect” represented the change in entropy of the system when the temperature is raised. The rubber system builds up the local residue stresses particularly hydrostatic stress [99]. The ratio $R_{\Delta s}$ between the stress in the temperature cycling process at point A in Figure 6.17 and long term stress relaxation at point B was calculated in order to study “the thermodynamic effect” as a function of temperature gradient. The result is shown in Figure 6.18. It could be noticed that “the thermodynamic effect” increased when the temperature gradient was increased from 15°C to 25°C. However, the increasing rate of “the thermodynamic effect” reduced and nearly zero when the temperature gradient was raised from 35°C to 55°C. This indicated that “the thermodynamic effect” had less important role in governing the stress relaxation behaviour at high temperature.

“The temperature effect”

“The temperature effect” represented the reduction in the internal viscosity (elastomer-elastomer interaction) with an increasing in temperature. The relaxation rate was plotted as a function of temperature gradient as shown in Figure 6.19. It could be noticed that the relaxation rate increased when the temperature was raised. It indicated that the dramatically reduction in the internal viscosity of the rubber system played more important role to govern the relaxation behaviour of the rubber at high temperature than the change in entropy.

Copyright by Mahidol University

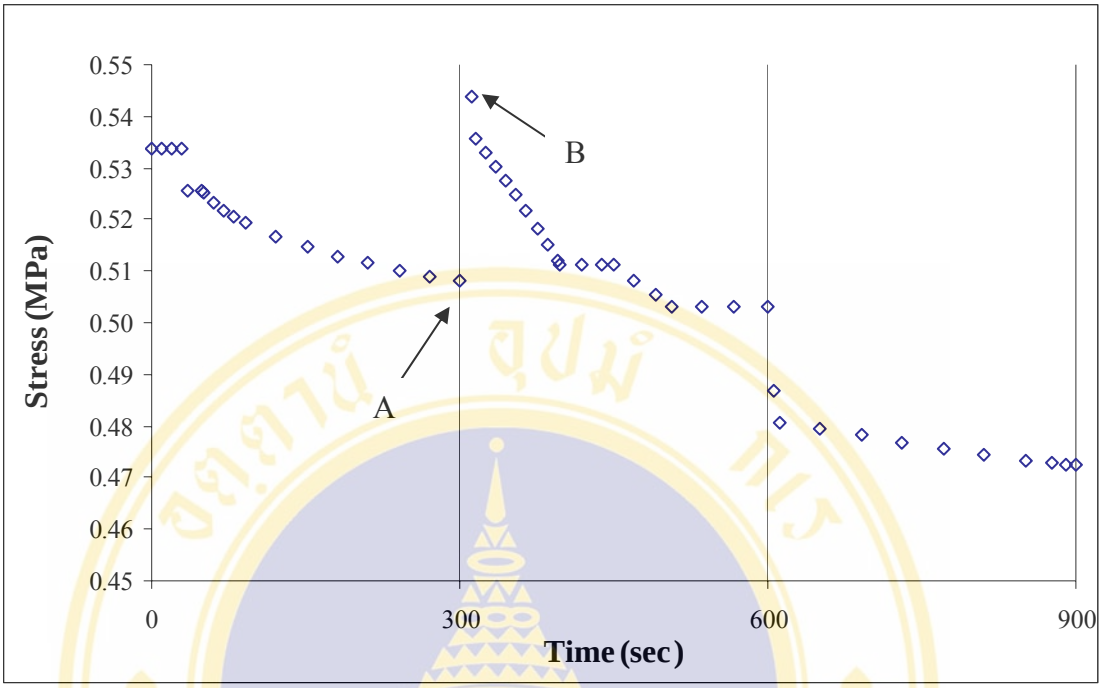

Figure 6.17: The stress relaxation of unfilled NR as a function of time under the temperature cycling condition.

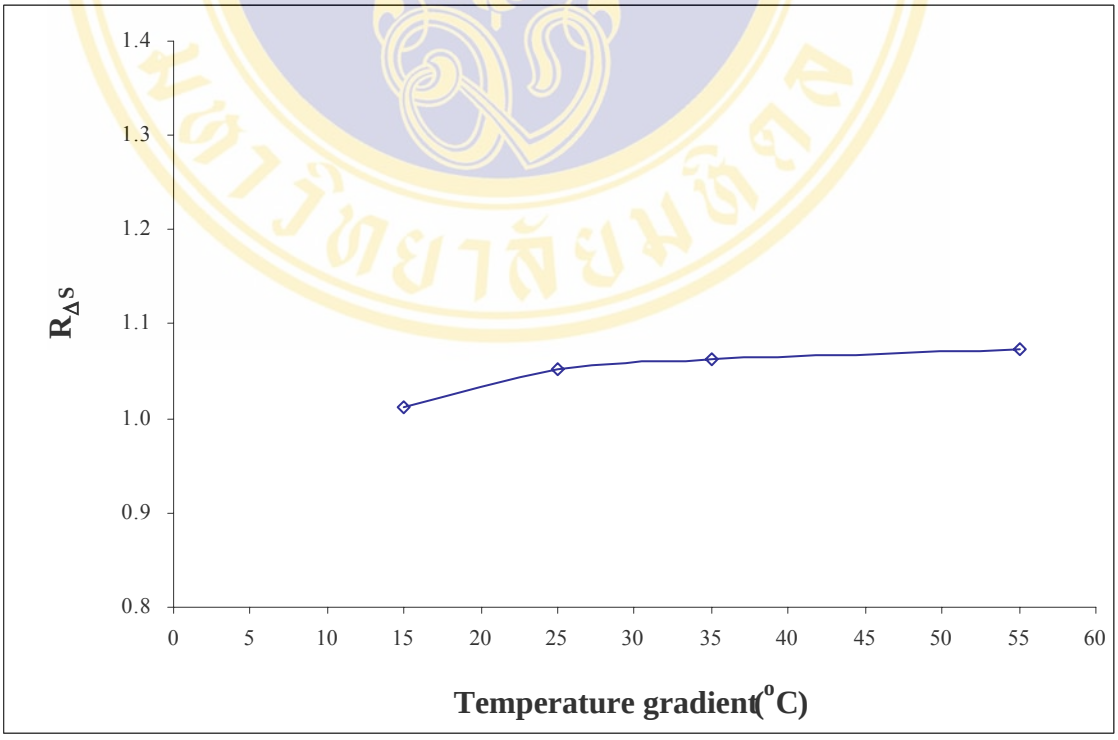

Figure 6.18: The relationship between $R_{\Delta s}$ and the temperature gradient (°C).

Copyright by Mahidol University

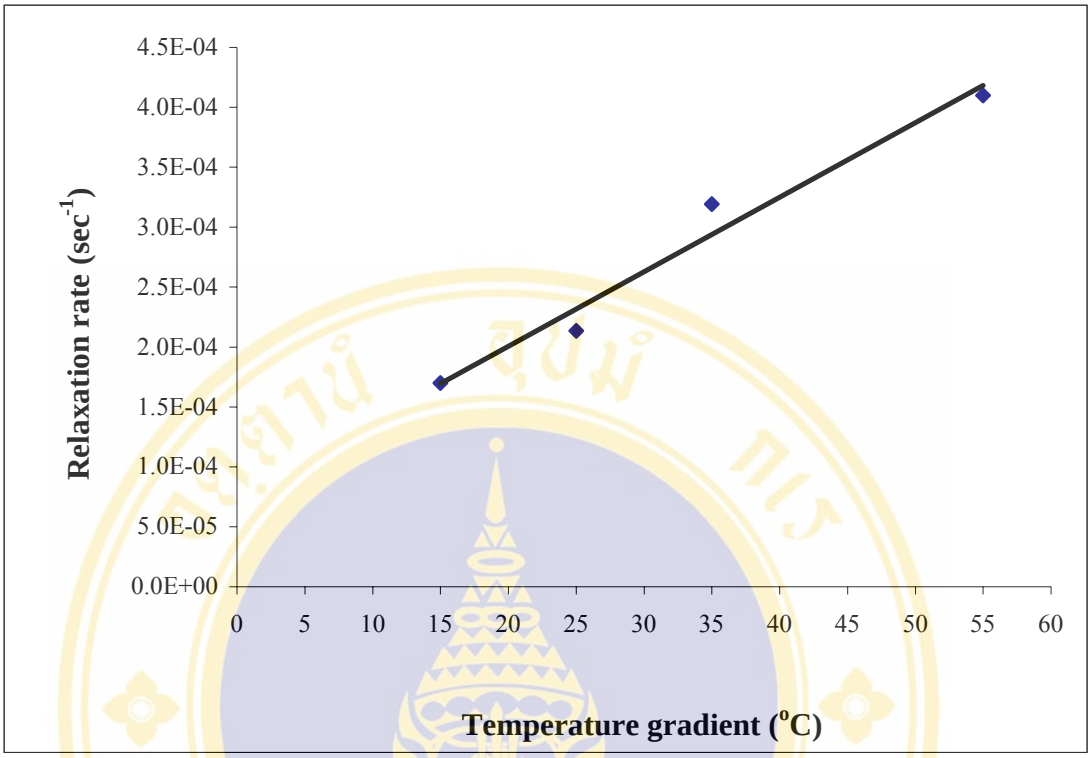

Figure 6.19: The relationship between relaxation rate (sec^{-1}) and the temperature gradient (°C).

In order to investigate the effect of temperature gradient on the stress at 25°C after the temperature cycling process, the logarithmic decade of the ratio between the time to reach the same stress of the long term relaxation at the constant temperature of 25°C and the time to reach the same stress of the elastomer relaxation at 25°C after the temperature cycling process ($R_{25L/25C}$) was calculated. The ratio ($R_{25L/25C}$) was calculated for each temperature gradient. From the relationship illustrated in Figure 6.20, the ($R_{25L/25C}$) dramatically increased at high temperature. It indicated that the reduction of stress strongly depended on the temperature gradient. The dramatically reduction in internal viscosity at high temperature might occur during the immediately change in temperature from high temperature to 25°C. This might relate with the breakdown in both physical and chemical elastomer-elastomer interactions as normally reported in rubber aging mechanism [67,100-106].

In this section, it can be concluded that the temperature gradient in the temperature cycling process affects the physical interaction between elastomer-elastomer. The chemical interaction may be reduced when the temperature is high

Copyright by Mahidol University

enough due to the relocated of the crosslinked chain and the degradation process [100-106]. In the next section, the results concerned with the time interval in the temperature cycling are presented.

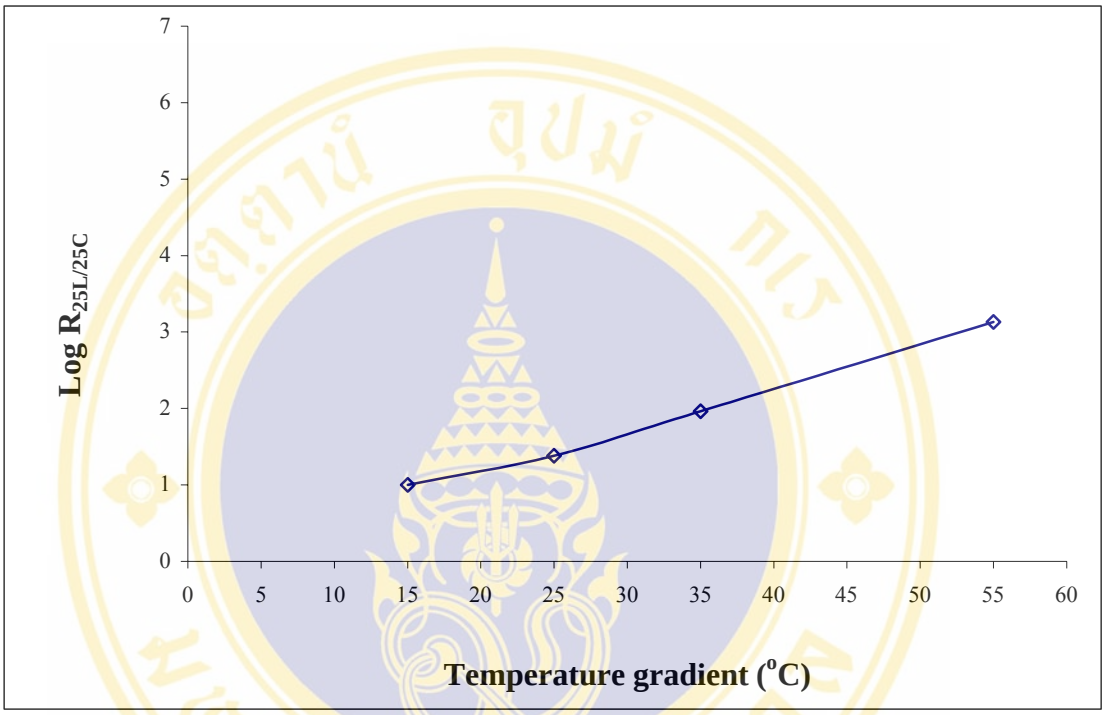

Figure 6.20: The relationship between $R_{25L/25C}$ and the temperature gradient (°C).

6.3 Effect of time interval in temperature cycling condition on the stress relaxation behaviour of unfilled natural rubber.

6.3.1 Time interval in the first step of temperature cycling

The unfilled NR was again employed in this investigation. The rubber specimen was extended in a tension mode to 50% static strain by micro-extensometer. The range of the time interval which the system was controlled at 25°C in the water environment was listed in Table 6.4. Then, the rubber specimen was transferred into the water reservoir which the temperature was controlled at 50°C for thirty min before

Copyright by Mahidol University

transferring back to the 25°C water reservoir. The step of the temperature cycling process is also written down in Table 6.4.

Table 6.4: The temperature cycling steps for unfilled NR of the changing time in the region at 25 °C

The step of temperature (^{o}C)		
25	50	25
The time interval (min)		
5	30	5
10	30	10
20	30	20

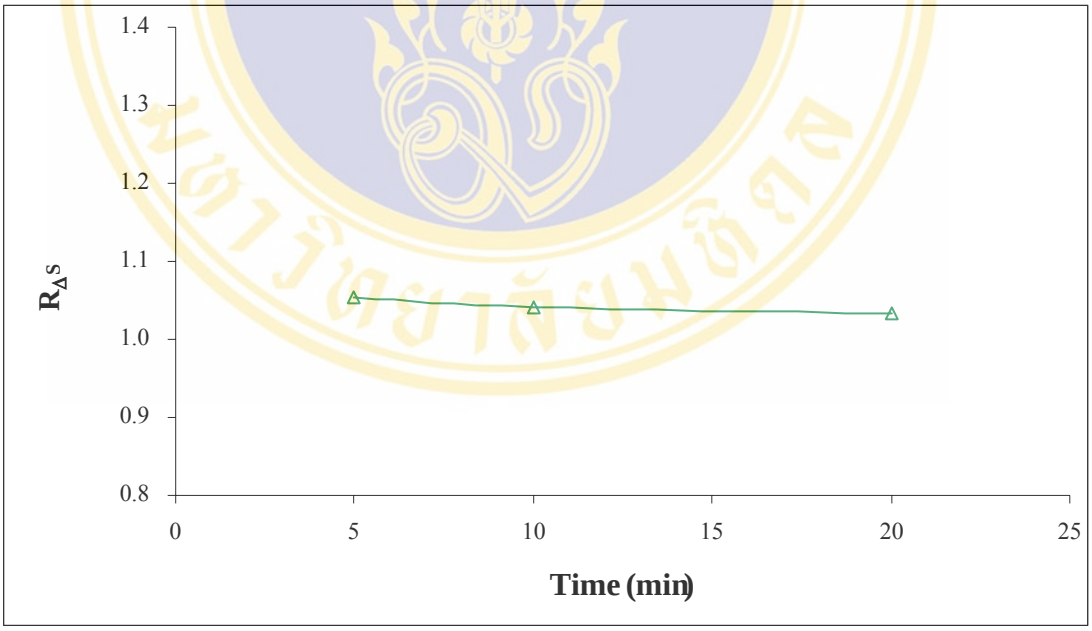

Figure 6.21: The relationship between calculated $R_{\Delta S}$ and time (min)

The effect of the time interval at 25°C on "The thermodynamic effect" was investigated, and the results are shown in Figure 6.21. The thermodynamic effect was nearly constant over the range of the investigated time interval. This indicated that entropy constantly changed at the specific temperature if the rubber system was in the

Copyright by Mahidol University

equilibrium state. The relation between internal viscosity represented by relaxation rate and time interval in temperature cycling was also studied. The results are shown in Figure 6.22. The relaxation rate did not change with the time interval. This also indicated that the time interval in the first step of the temperature cycling, at 25°C had no effect on both entropy and internal viscosity of the rubber chain. Therefore, the time to reach the same stress for the long term relaxation condition and temperature cycling condition should not be differed. This was confirmed by the result shown in Figure 6.23.

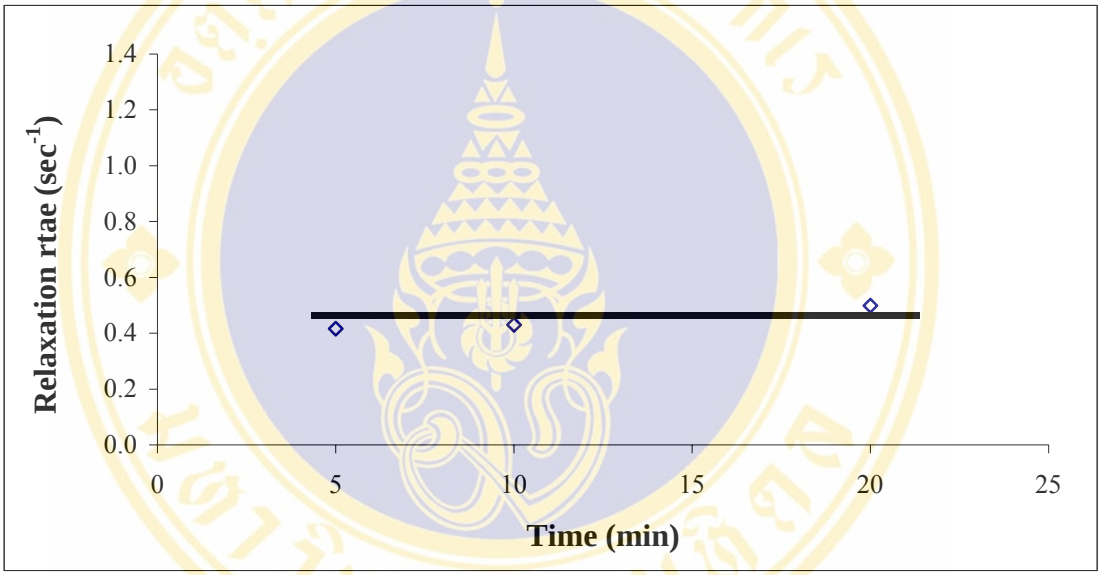

Figure 6.22: The relationship between calculated relaxation rate (sec^{-1}) and time (min)

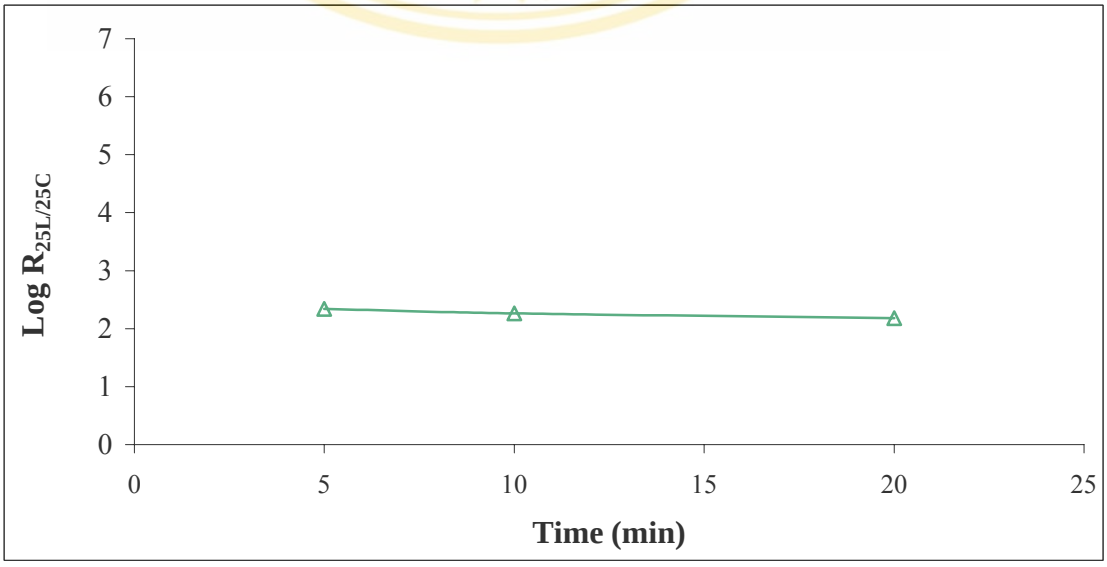

Figure 6.23: The relationship between calculated log $R_{25L/25C}$ and time (min)

Copyright by Mahidol University

6.3.2 Time interval in the second step of temperature cycling

The unfilled NR was again employed in this investigation. The rubber specimen was extended in a tension mode to 50% static strain by micro-extensometer. The system was controlled at 25°C in the water environment for 20 min. Then, the rubber specimen was transferred into the water reservoir which the temperature was controlled at 50°C. The range of the time interval which the rubber was controlled at this temperature is listed in Table 6.5. Then, the rubber was transferred back to the 25°C in water reservoir. The step of the temperature cycling process is also written down in Table 6.5.

Table 6.5: The temperature cycling steps for unfilled NR of the changing time in the region at 50 °C

The step of temperature (^{o}C)		
25	50	25
The time interval (min)		
20	10	20
20	20	20
20	30	20

The time to reach the same stress for the long term relaxation condition and temperature cycling condition was investigated as a function of time interval. The result is shown in Figure 6.24. The log $R_{25L/25C}$ increased with increasing the time interval in the second step of the temperature cycling. This indicated that the time interval at high temperature in the temperature cycling process affected the internal viscosity of the rubber. The physical interaction between elastomer-elastomer was dramatically reduced by the temperature cycling process. Temperature gradient, especially at the high temperature and time interval for the second step of the temperature cycling has a significant effect on the internal viscosity.

Copyright by Mahidol University

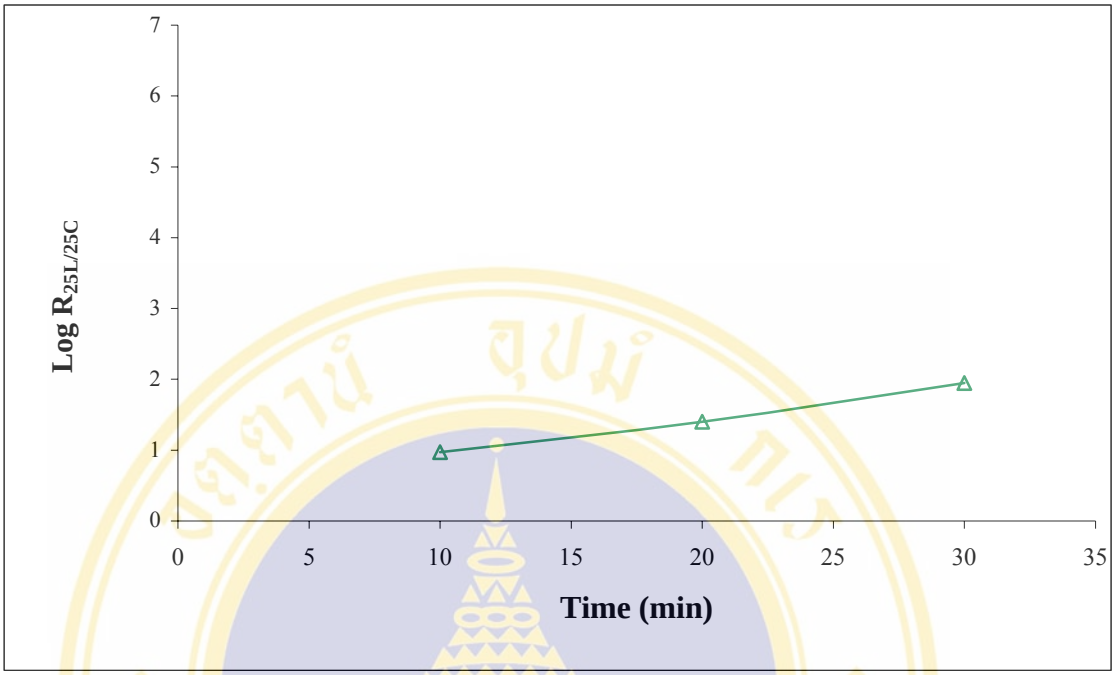

Figure 6.24: The relationship between calculated log $R_{25L/25C}$ and time (min)

However, the elastomer-elastomer interaction alone can not meet the requirement for the engineering applications. Reinforcing filler is needed to be added. Carbon black is a reinforcing filler of the elastomer. The filler-elastomer interaction which depends on the characteristic of the carbon black, its dispersion and distribution in the elastomer matrix governs the mechanical properties and dynamic mechanical properties of carbon black filled elastomer. Therefore, the effect of temperature cycling on stress relaxation of carbon black filled natural rubber was studied and the results are presented in the next section.

6.4 Effect of the temperature cycling process on the stress relaxation behaviour of carbon black filled natural rubber

The carbon black (0-60phr) filled natural rubber was employed for this investigation. The rubber formulations and mixing method was already presented in Chapter IV. The rubber specimen was extended in a tension mode to 50% static strain by micro-extensometer. The system was controlled at 25°C in the water environment.

Copyright by Mahidol University

The rubber specimen was kept at this temperature for 5 min before transferring into the 50°C in water reservoir. The rubber specimen was maintained at this temperature for 5 min. The step of this temperature cycling process is written down in Table 6.6. The relationships between stress and time under the temperature cycling conditions are illustrated in Figures 6.25-6.28.

Table 6.6: The step of the temperature cycling process for the investigation the effect of amount of CB in temperature cycling processes on the stress relaxation behaviour.

Step	Temperature (^{o}C)	Time (min)	Total time (min)
1	25	5	5
2	50	5	10
3	25	5	15

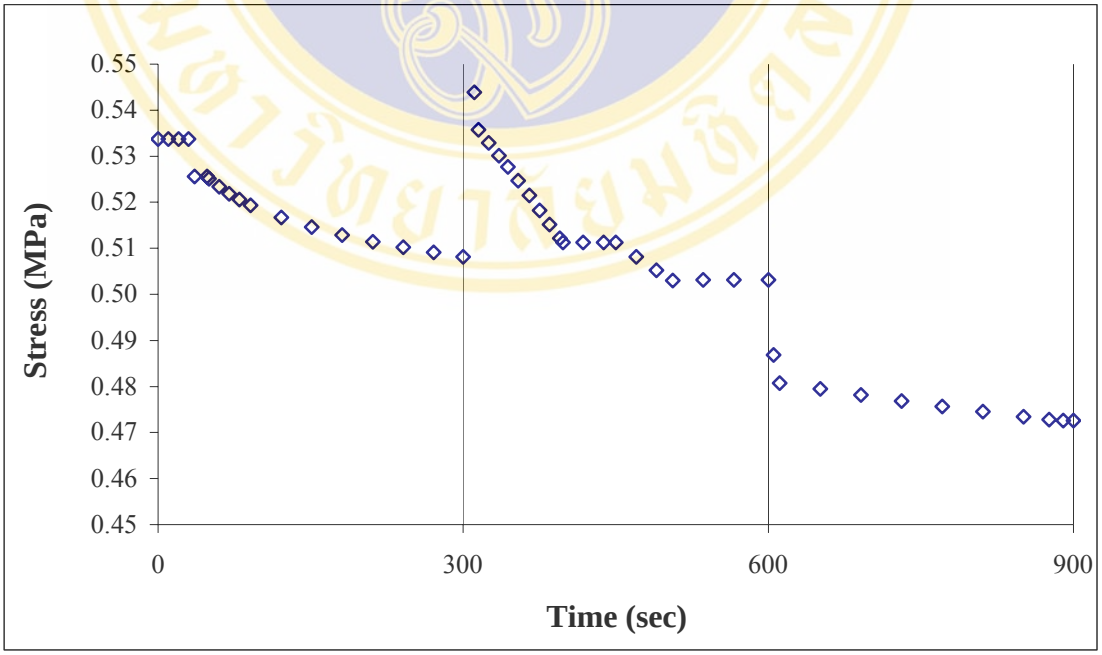

Figure 6.25: The stress relaxation of unfilled NR as a function of time under the temperature cycling condition.

Copyright by Mahidol University

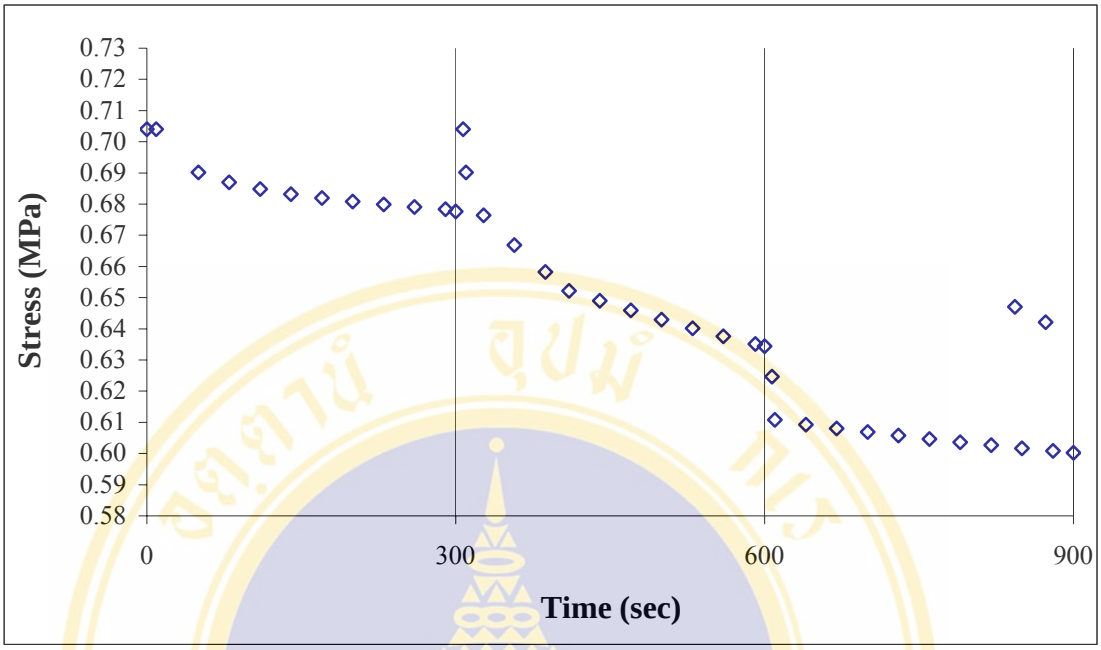

Figure 6.26: The stress relaxation of NR-10CB as a function of time under the temperature cycling condition.

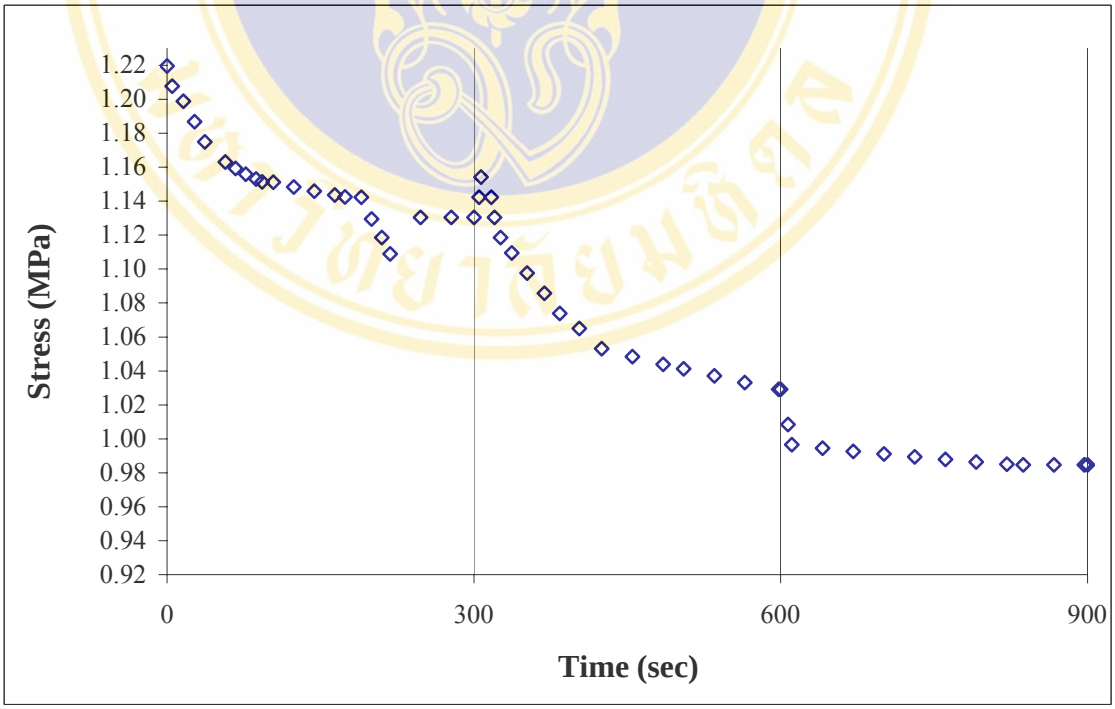

Figure 6.27: The stress relaxation of NR-30CB as a function of time under the temperature cycling condition.

Copyright by Mahidol University

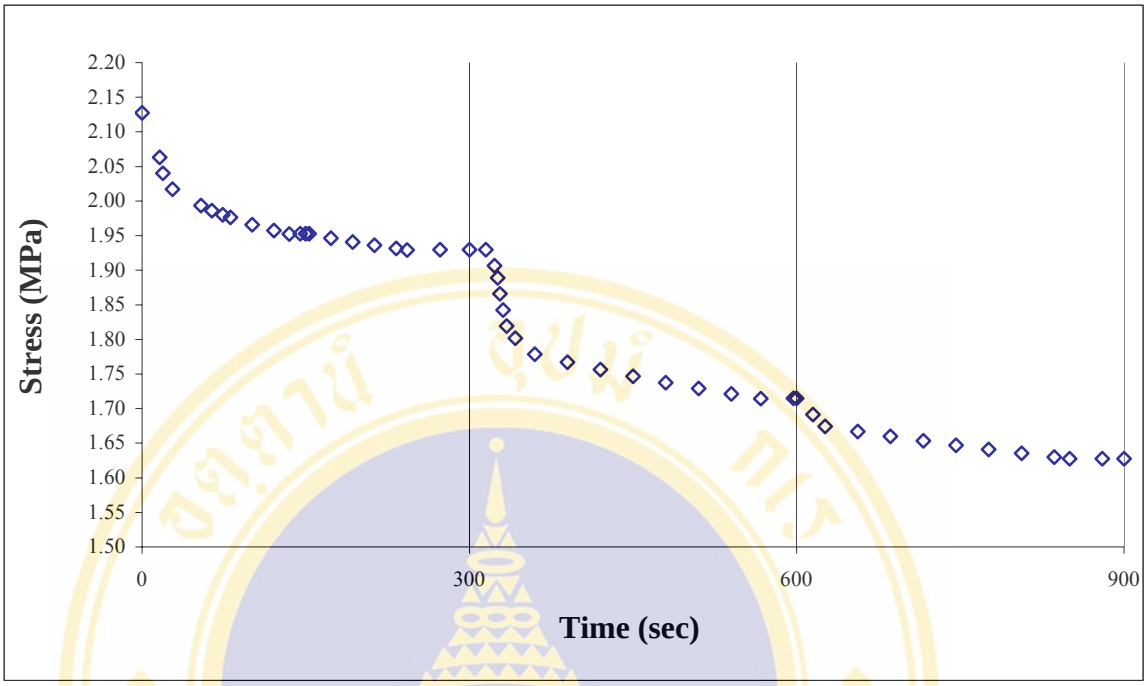

Figure 6.28: The stress relaxation of NR-60CB as a function of time under the temperature cycling condition.

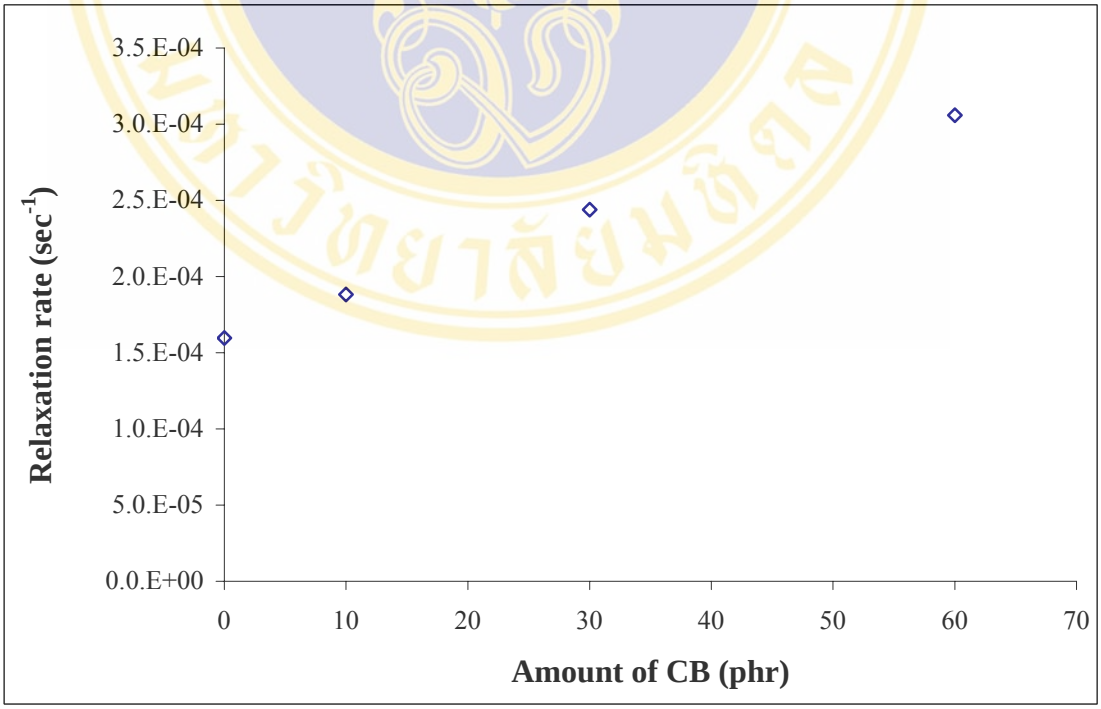

Figure 6.29: The relationship between calculated relaxation rate (sec^{-1}) at 25°C in the first step of the temperature cycling process and the amount of CB (phr).

Copyright by Mahidol University

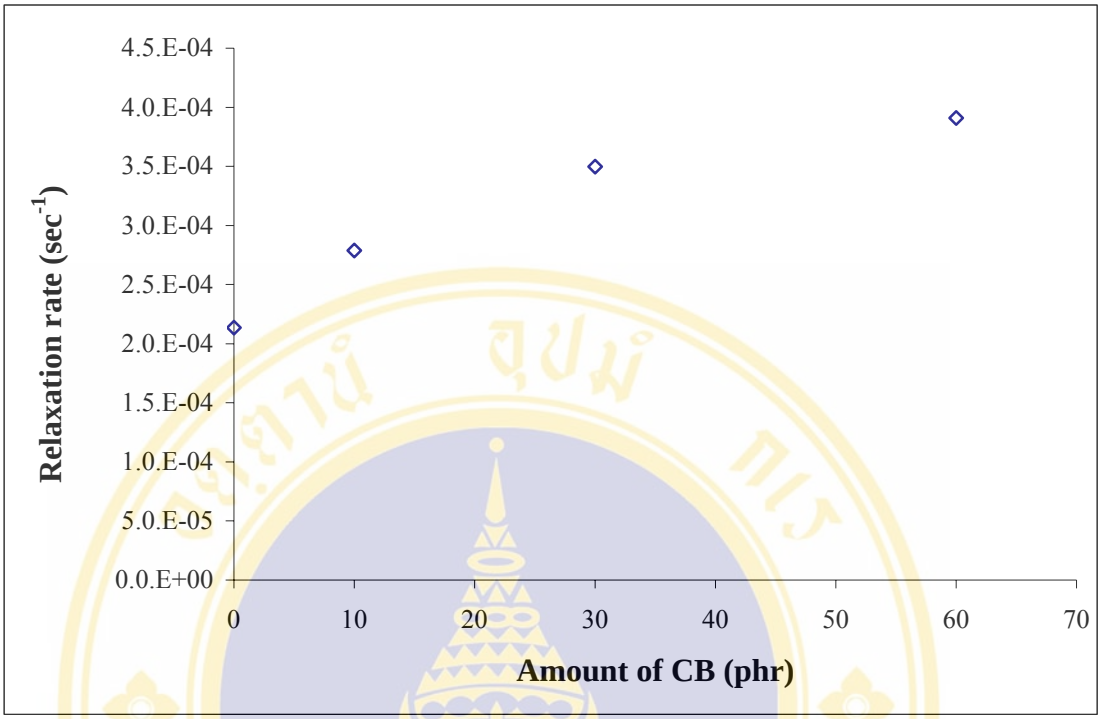

Figure 6.30: The relationship between calculated relaxation rate (sec^{-1}) at 50°C in the second step of the temperature cycling process and the amount of CB (phr).

The relaxation rate of carbon black filled natural rubber at both 25°C and 50°C under temperature cycling process was calculated. It could be noticed from Figure 6.29 and Figure 6.30 that increasing amount of incorporated carbon black, the stress of the carbon black filled relaxed more rapidly. The filler-filler interaction and also filler-elastomer interaction had to be accounted [95-98,105-106].

In order to focus on the point of view of the interaction, the WLF approached was again employed in order to calculate the stress which relaxed under the reduction in the elastomer-elastomer interaction. The ratio $R_{(C/T)}$ between the calculated stress from WLF theory and the stress relaxed under the temperature cycling of carbon black filled NR was considered. The result is presented in Figure 6.31 and Figure 6.32. The calculated ratios were deviated from 1 which verified the interaction between rubber-carbon black and carbon black-carbon black. Both interactions had more affected on the viscoelastic behaviour when the amount of incorporated carbon black was increased. The interaction between the elastomer and carbon black can be separated into two categories, physical and chemical interaction

Copyright by Mahidol University

[95-98]. The investigation concerned with the elastomer-carbon black interaction was focused. The report is later presented.

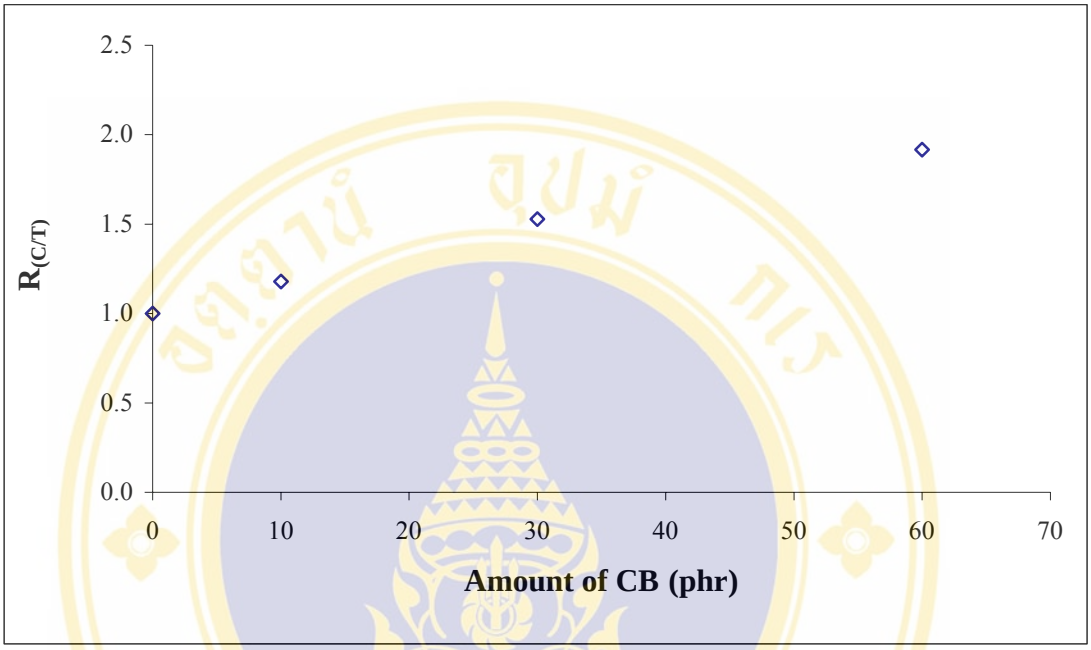

Figure 6.31: The relationship between calculated $R_{(C/T)}$ in the first step of the temperature cycling process and the amount of CB (phr).

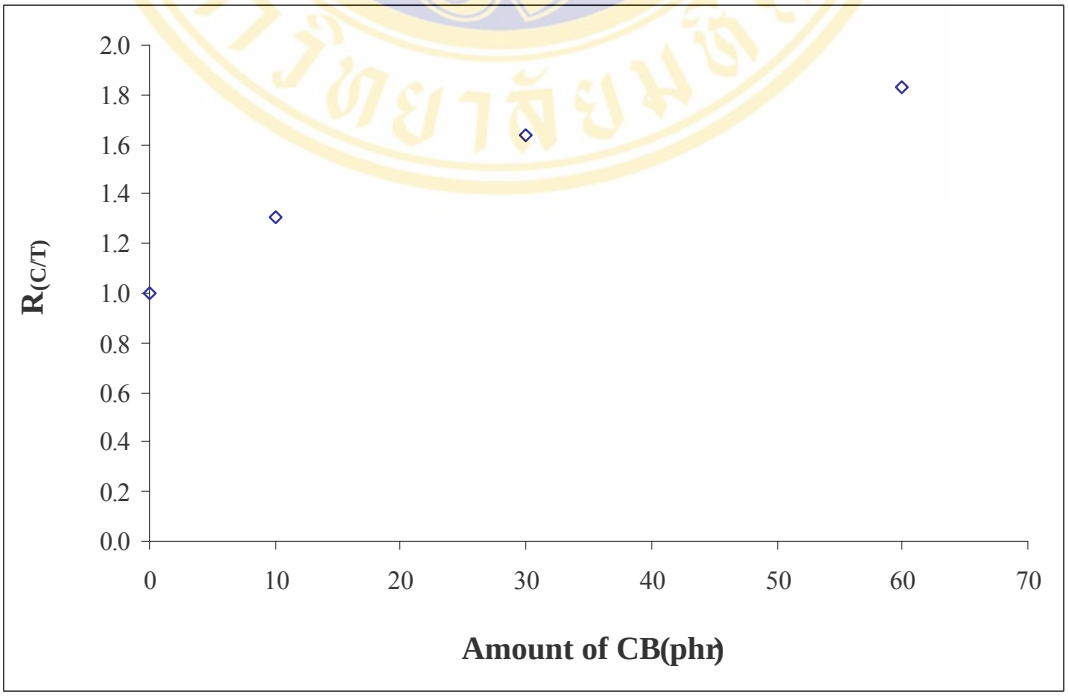

Figure 6.32: The relationship between calculated $R_{(C/T)}$ in the second step of the temperature cycling process and the amount of CB (phr).

Copyright by Mahidol University

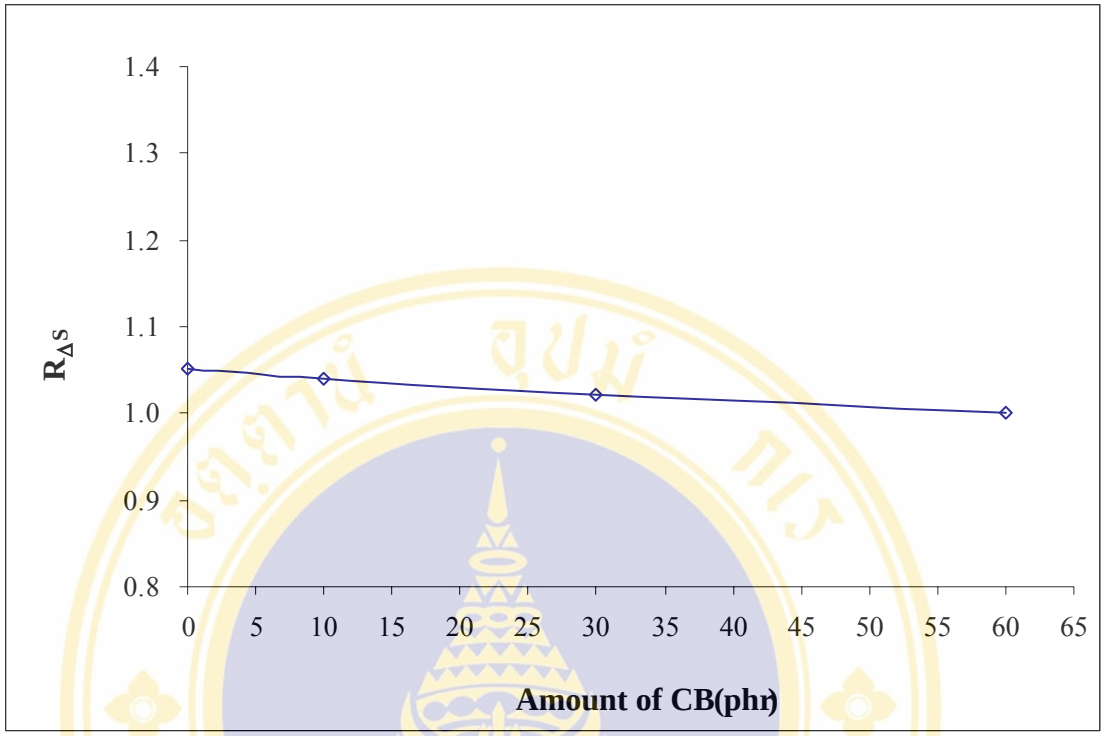

Figure 6.33: The relationship between calculated $R_{\Delta S}$ under the temperature cycling process and the amount of CB (phr).

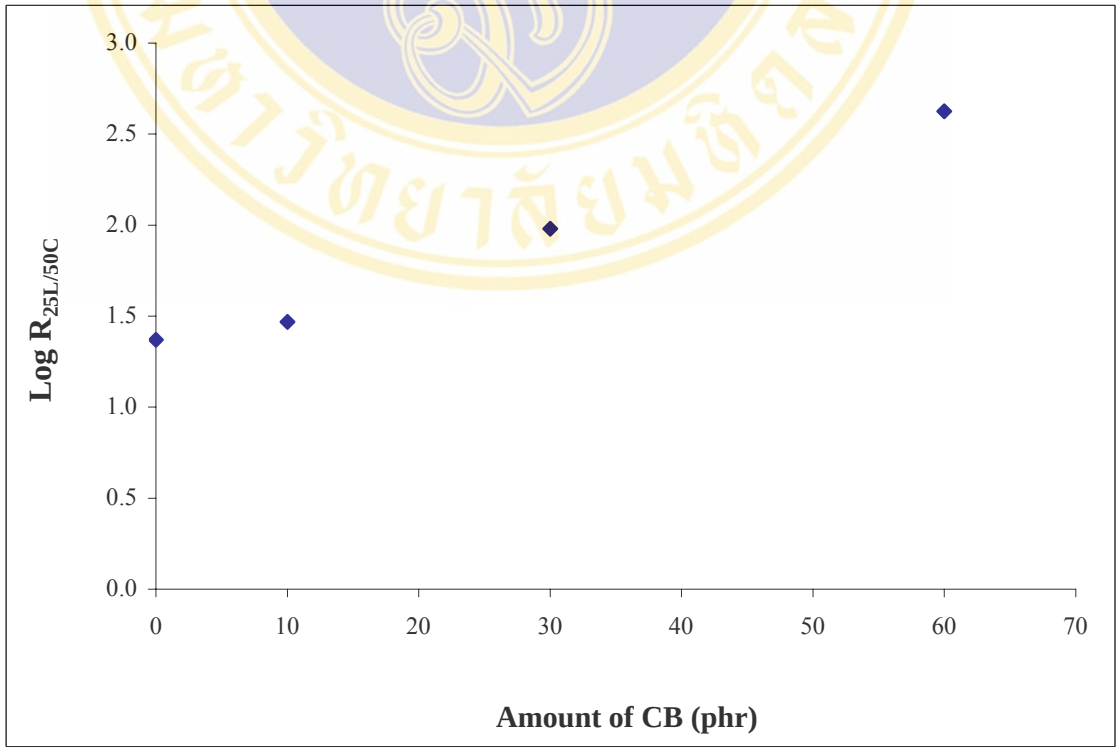

Figure 6.34: The relationship between calculated $R_{25L/50C}$ under the temperature cycling process and the amount of CB (phr).

Copyright by Mahidol University

For the carbon black filled NR, the internal viscosity of the rubber system was higher than that of unfilled NR due to the filler-elastomer and filler-filler interactions because the elastomer molecular chain could not easily rotate. This could be verified by the relation between "The thermodynamic effect" and the amount of carbon black. The result is showed in Figure 6.33. The reduction in stress due to the change of entropy decreased with increasing carbon black [105-106]. This confirmed the difficult mobility of the elastomer chains in the presence of carbon black.

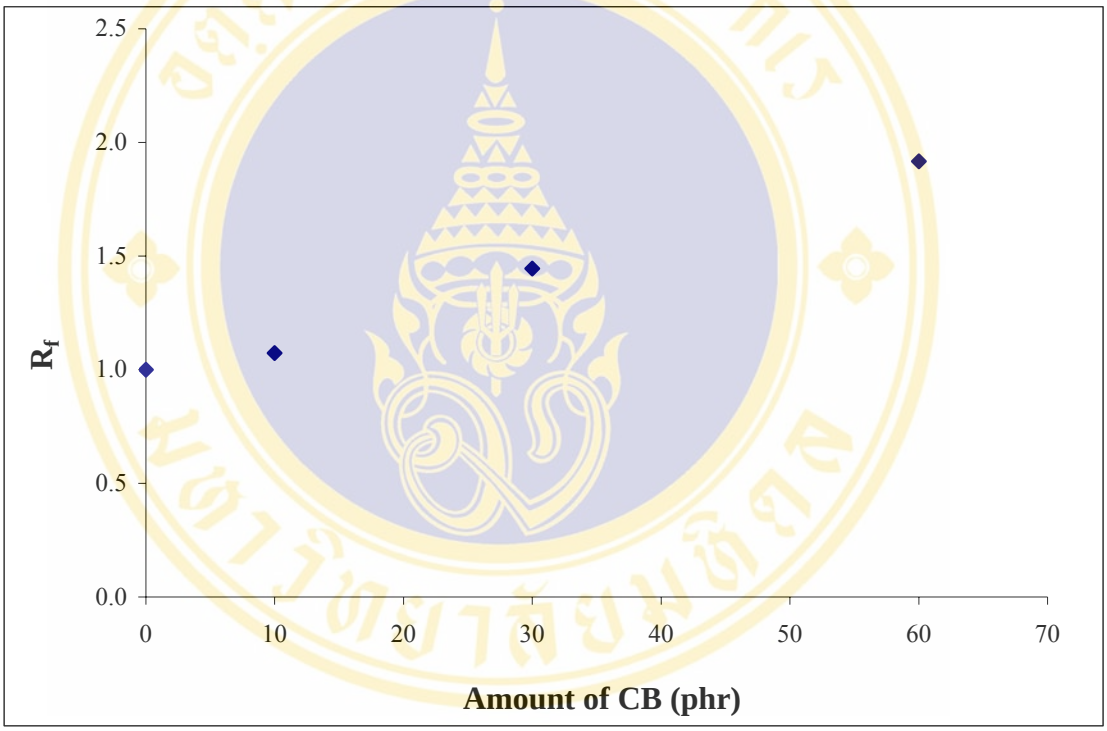

Figure 6.35: The relationship between calculated R_f under the temperature cycling process and the amount of CB (phr).

Moreover, The ratio between the time to reach the same stress of the long term relaxation at the constant temperature of 25°C with the time to reach the same stress of the elastomer relaxation at 50°C under the temperature cycling process ($R_{25L/50C}$) was calculated over the range of incorporated carbon black. The relationship between logarithmic decade of ($R_{25L/50C}$) and the amount of carbon black is illustrated in Figure 6.34. It could be noticed that the long term relaxation time of highly carbon black filled NR could be dramatically reduced by operating under the temperature

Copyright by Mahidol University

cycling condition. However, the reduction in stress due to the temperature cycling did not affect only the elastomer-elastomer interaction. It also equally reduced the filler-elastomer and filler-filler interaction. The ratio (R_f) between logarithmic decade of ($R_{25L/25C}$) at different amount of carbon black and logarithmic decade of ($R_{25L/25C}$) for unfilled NR was calculated and plotted as a function of carbon black. This plot is shown in Figure 6.35. The result was quite similar to the plot shown in Figures 6.31 and 6.32 confirmed that the temperature cycling process equally reduced the elastomer-elastomer interaction and filler-elastomer, filler-filler interaction.

- **Interaction between Carbon black and natural rubber determined by relaxation behaviour under the temperature cycling.**

The innovative technique of mixing carbon black into the natural rubber latex has been developed and published by Tangboriboonrat et. al [96-97]. According to this technique, the carbon black filled natural rubber can be prepared without using the common mixing technique such as internal mixer. Therefore, the interaction between elastomer and filler should be mostly in the physical state instead of combination of chemical and physical interaction found in carbon black filled elastomer prepared by conventional method [86-87]. The temperature cycling technique was applied to verify the physical interaction between elastomer and filler.

The relaxation behaviour of (NR-Conv) and (NR-Mast) under the temperature cycling condition is illustrated in Figure 6.36-6.37. The testing condition was listed in Table 6.7.

Table 6.7: The temperature cycling step for the investigation the effect of interaction between CB and rubber under temperature cycling processes.

Step	Temperature (^oC)	Time (min)	Total time (min)
1	25	5	5
2	50	5	10
3	25	5	15

Copyright by Mahidol University

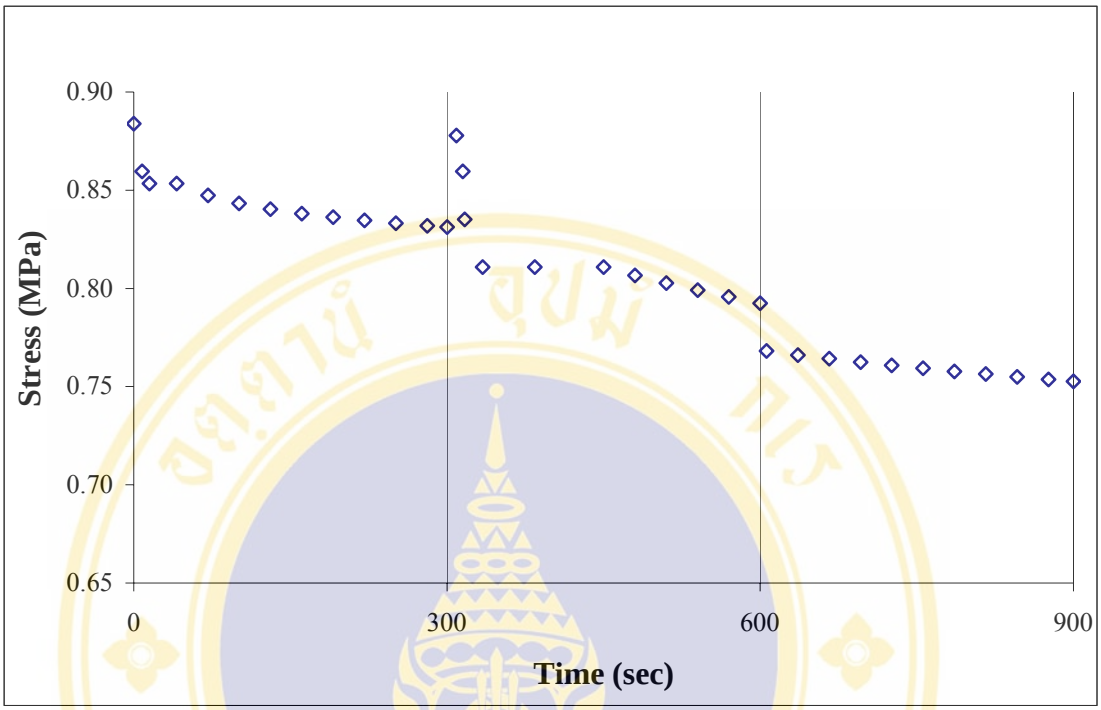

Figure 6.36: The stress relaxation of NR-Conv as a function of time under the temperature cycling condition.

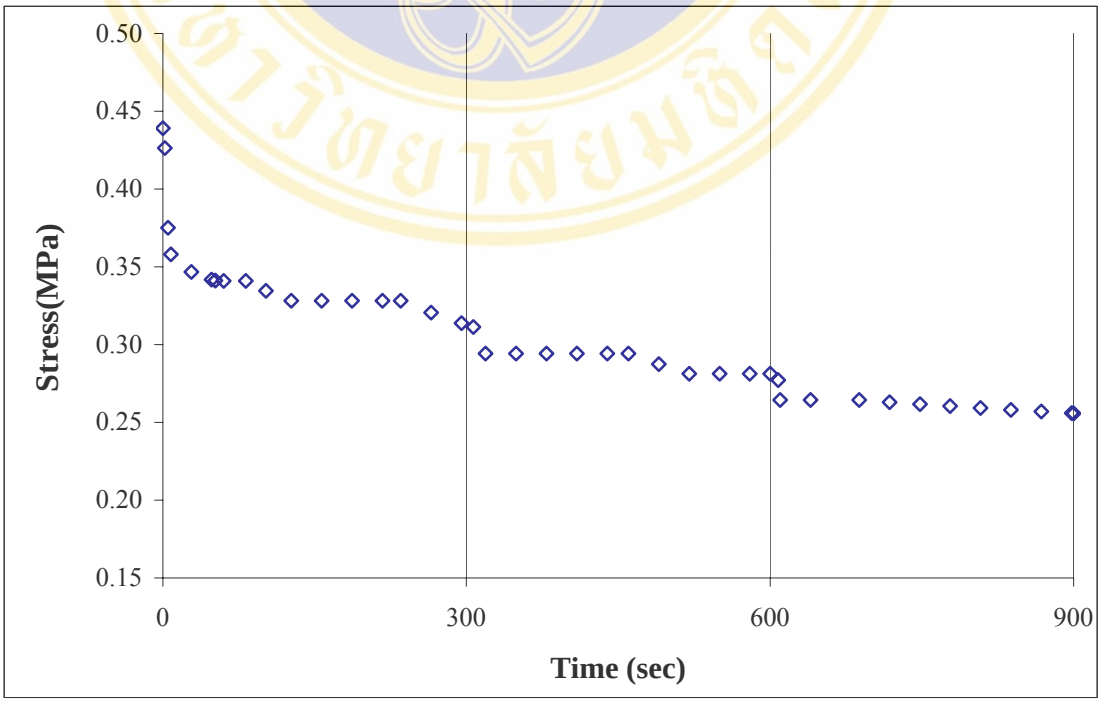

Figure 6.37: The stress relaxation of NR-Mast as a function of time under the temperature cycling condition.

Copyright by Mahidol University

The ratio between relaxation rate of carbon black filled NR prepared from both methods at each step of the temperature cycling and relaxation rate of unfilled NR at each step of the temperature cycling was calculated. The results are illustrated in Figures 6.38-6.40.

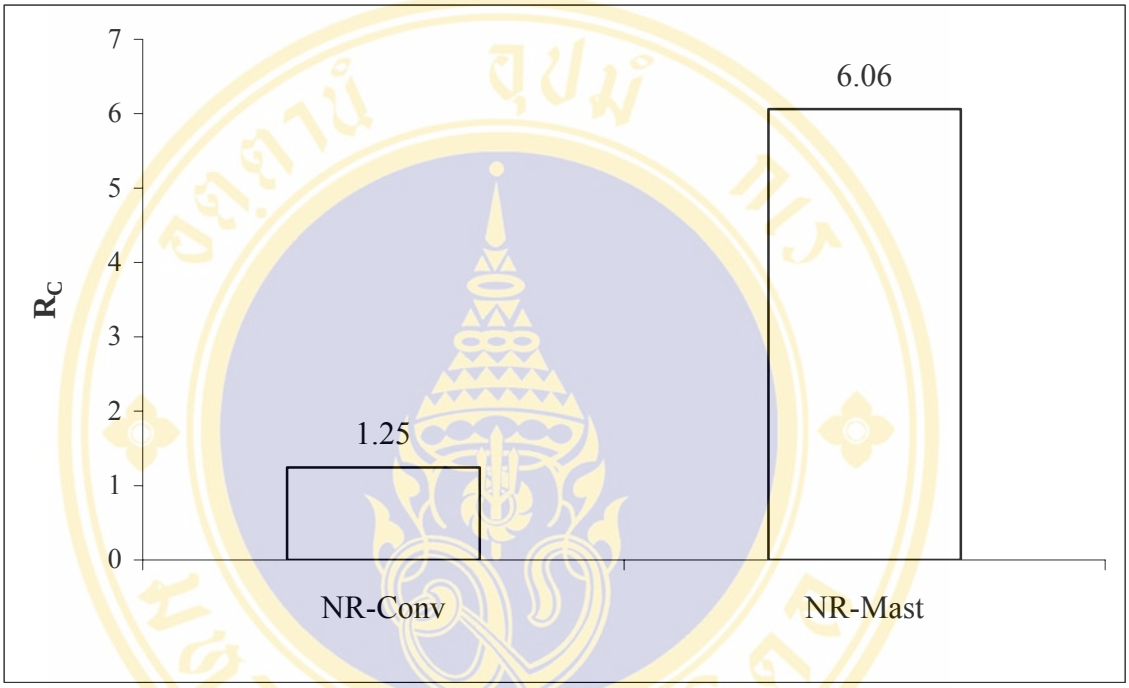

Figure 6.38: Comparison between the relaxation rate at 25°C in the first step of the temperature cycling condition and the different type of interaction between CB and rubber.

The calculated ratios (R_c) represented the stress relaxation fraction controlled by the reduction in elastomer-filler and filler-filler interaction. It can be noticed from Figure 6.38 that, the relaxation rate at 25°C of the NR-Mast was mostly governed by the elastomer-filler and filer-filler interaction compared to the value obtained from NR-Conv. However, this was not the case when this characteristic was measured in Figure 6.39 which the stress relaxation measurement was controlled at 50°C under the temperature cycling condition. The relaxation was controlled equally at high temperature by elastomer-elastomer, elastomer-filler and filler-filler. It could be noticed from Figure 6.40 represented the relaxation rate of carbon blacked filled NR in the third step of the temperature cycling at 25°C.

Copyright by Mahidol University

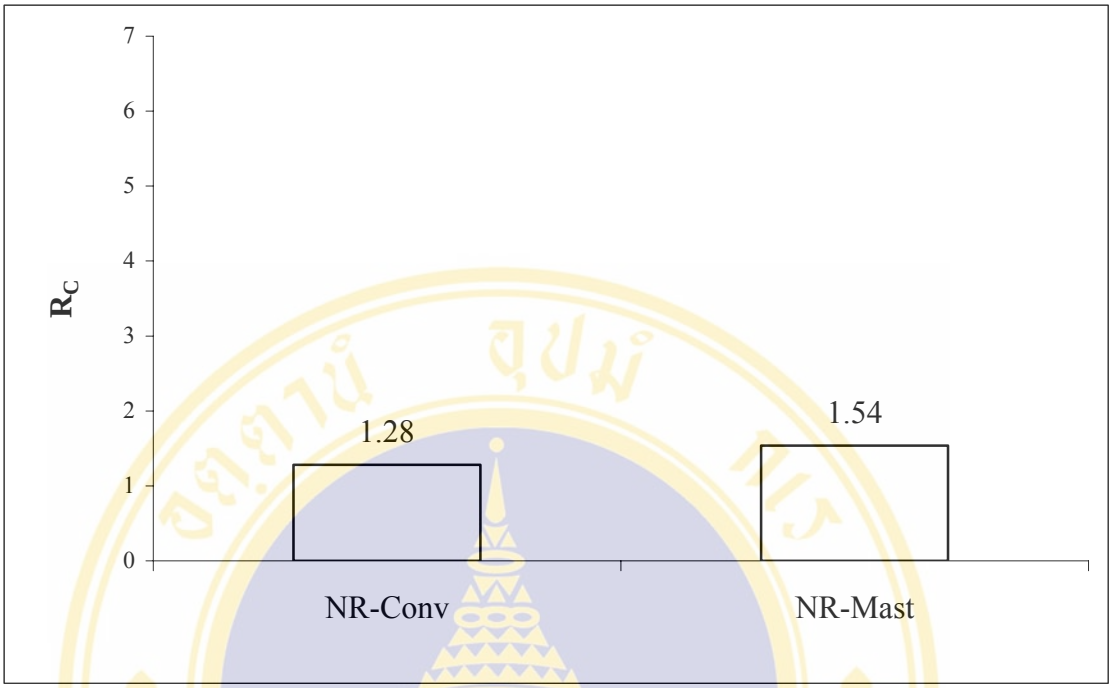

Figure 6.39: Comparison between the relaxation rate at 50°C in the second step of the temperature cycling condition and the different type of interaction between CB and rubber.

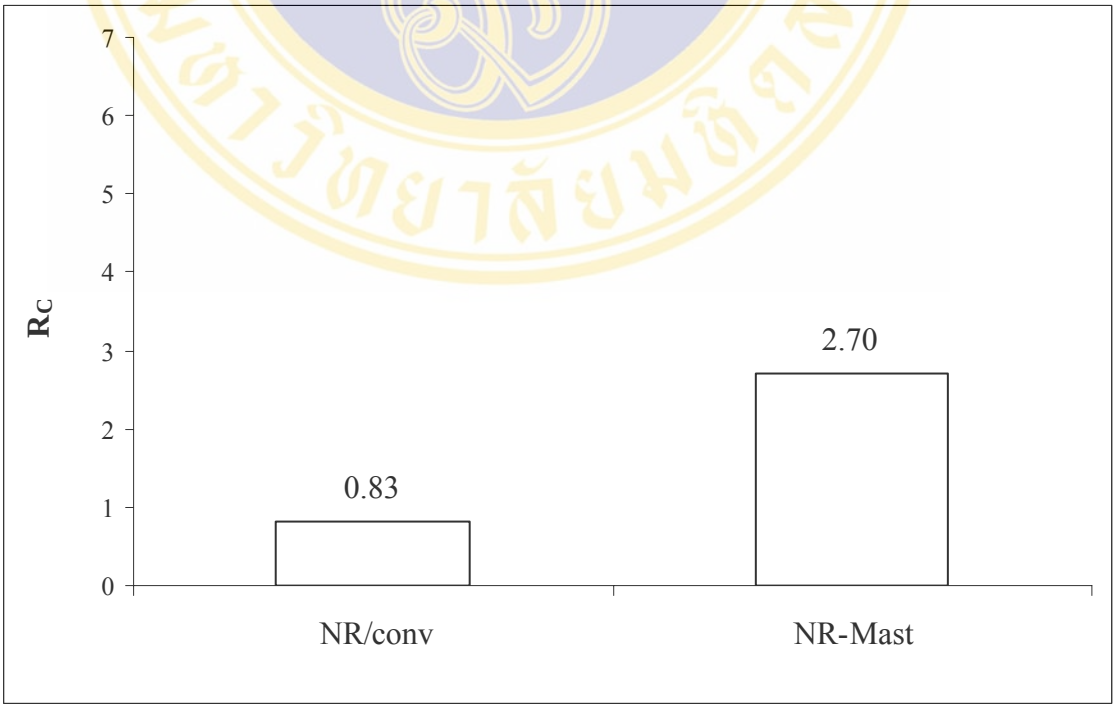

Figure 6.40: Comparison between the relaxation rate at 25°C in the third step of the temperature cycling condition and the different type of interaction between CB and rubber.

Copyright by Mahidol University

The ratio (R_c) between the relaxation rate at different type of the interaction between CB and rubber and the relaxation rate for unfilled NR indicated that the elastomer-filler interaction and filler-filler interaction were the dominate fraction controlling the reduction of the relaxation rate of the (NR-Mast) instead of elastomer-elastomer interaction found in NR-Conv. As stated thought out this study, the temperature cycling process could accelerate the reduction in the physical linkages. Therefore, it could be concluded that the interaction between elastomer and filler of (NR-Mast) was mostly physical interaction.

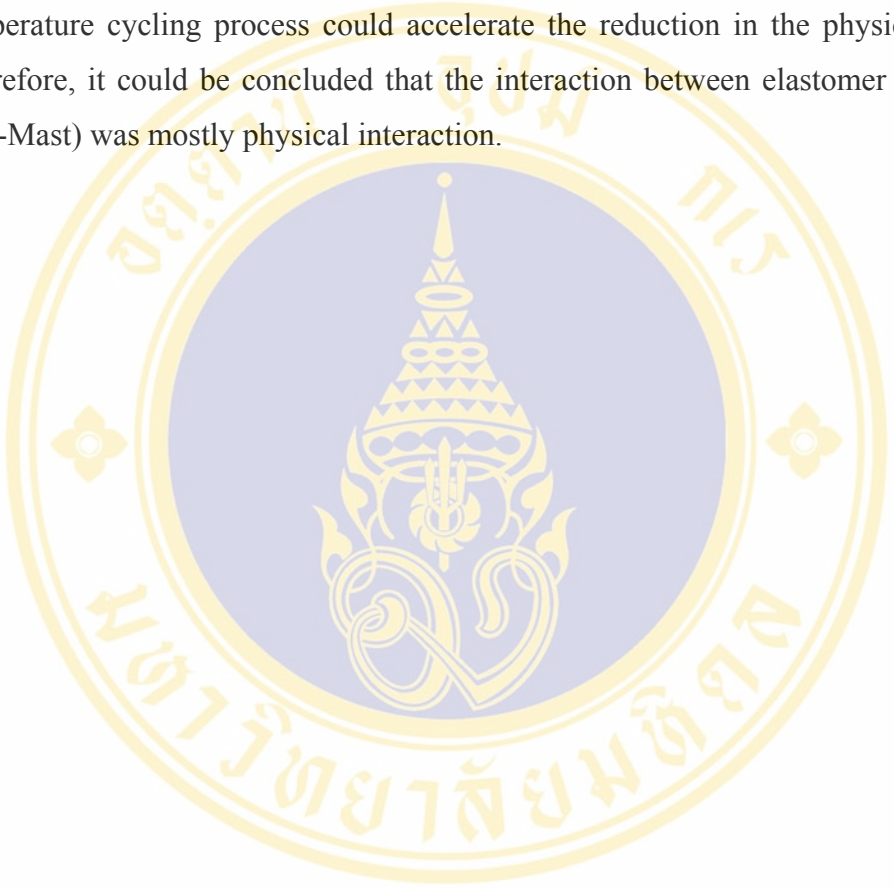

Copyright by Mahidol University

CHAPTER 7
CONCLUSIONS

The stress relaxation of elastomer under temperature cycling is the main topic of this dissertation. Temperature cycling condition which normally occurs in the temperature controlled chamber may affects mechanical properties and dynamic properties of the elastomer at high temperature. The temperature cycling condition can also be found in the practical applications such as rubber seal in the car engine.

Natural rubber, high relaxation rate, was chosen as a model in this study. Important factors such as initial strain, crosslink density were controlled in order to simplify the investigation because the relaxation behaviour could be altered by changing these two factors. The micro-tension apparatus was built in order to study the relaxation behaviour in the water environment. The heat conductivity in water is better than air and the relaxation behaviour of elastomer was not affected.

The relaxation behaviour of unfilled NR under the temperature cycling process was firstly investigated. WLF theory was employed in this study in order to verify that both changing in entropy and reduction in the internal viscosity could be considered as the explanation for the relaxation behaviour when the temperature was raised. However, the stress was dramatically decreased when the temperature was immediately reduced during the temperature cycling process. The difference in mobility of the rubber chains due to the non-equilibrium temperature over the rubber system caused a breakdown of physical interaction between elastomer-elastomer. Therefore, the stress relaxation behaviour could be accelerated by performing temperature cycling process. Cycling temperature repeatedly could reduce a large number of elastomer-elastomer interaction. Not only physical interaction between elastomer and elastomer was diminished but the chemical interaction might also be reduced when the temperature gradient of the temperature cycling was high enough. The effect of time interval of the temperature cycling on the relaxation behaviour was

Copyright by Mahidol University

also studied. Only time interval in the second step of temperature cycling was concerned when the rubber was operated under temperature cycling.

Furthermore, the relaxation behaviour of the carbon black filled NR under the temperature cycling was also studied. The proportional reduction in stress due to the temperature cycling process was equally associated with the break down of the elastomer-elastomer interaction, the elastomer-filler interaction and the filler-filler interaction.

The temperature cycling technique could also be employed to study the interaction between elastomer and filler in the carbon black filled NR prepared by conventional mixing method (NR-Conv) and incorporated carbon black into latex NR (NR-Mast). The relaxation rate of the carbon black filled NR after the temperature cycling condition was mostly controlled by the elastomer-filler and filler-filler interaction. The break down of the physical elastomer-filler linkage should happen at low temperature in the temperature cycling process. Therefore, it could be concluded that the linkage between elastomer and carbon black in (NR-Mast) presented in the physical form.

Copyright by Mahidol University

REFERENCES

1. Blow C. M. Rubber Technology and Manufacture. London: 1971.
2. Roberts A. D. Natural Rubber Science and Technology. 1st ed. New York: Oxford University press. 1988.
3. Burfield D. R. J. nat. Rubb. Res. 1986; 1(3): 202.
3. Tangpakdee J., Tanaka Y. J. nat. Rubb. Res. 1997; 12(2): 112-9.
4. Ichikawa N., Eng A.H., Tanaka Y. Inst. Rubb. Technol. Conf: Kuala Lumpur. 1993; 101.
5. Eng A. H., Ejiri S., Kawanhara S., Tanaka Y. J. Appl. Polym. Sci. Polym. Symp. 1994; 53: 5.
6. Eng A. H., Tanaka Y., GAN S. N. J. nat. Rubb. Res. 1993;8(2):109-13.
7. Eng A. H., Tanaka Y., GAN S. N. J. nat. Rubb. Res. 1992;7(2):152-5.
8. James E. M., Burak E., Frederick R. E. Science and Technology of Rubber, 2nd ed. Academic Press. 1994.
9. Wilett P. R. Rubber Chem. Technol. 1973; 46: 118.
10. Schuring D. J. Rubber Chem. Technol. 1980; 53: 601.
11. Medalia A. I. Rubber Chem. Technol. 1978; 51: 437.
12. Deeprasertkul C. Dynamic properties of carbon black filled elastomers containing liquids, Ph.D. Thesis ,Queen Mary and Westfield College, University of London.
13. Busfield J. J. C., Deeprasertkul C., Thomas A.G. Polymer. 2000; 41(26): 9219-25.
14. Treloar L. R. G. Trans. Faraday Soc. 1940; 36: 538.
15. Treloar L. R. G. The physics of Rubber Elasticity. 3rd ed. New York: Clarendon Press. 1980.
16. Gee R. Trans. Faraday Soc. 1946; 43: 585.
17. Rivlin R. S. Trans. Faraday Soc. 1947; 18: 444.
18. Treloar L. R. G. Trans. Faraday Soc. 1943; 39: 36.

Copyright by Mahidol University

19. Young R. J., Lovell P. A. Introduction to polymer. 2nd ed. London: Chapman & Hall.1991.
20. Kuhn W. Z. Phys. Chem.1939: B42.
21. Treloar L. R. G. Trans. Faraday Soc. 1954; 50: 881.
22. McCrum N. G., Buckley C. P., Bucknall C. B. Principles of Polymer Engineering New York: Oxford University Press. 1988.
23. Andre L., Gregory B. M. J. Polym. Sci. Pol. Phys. 1997; 35: 1167-74.
24. Andre L., Gregory B. M. Polymer. 1988; 29: 1812-17.
25. Kontou E. J.Appl. Polym. Sci. 1998; 67: 679-84.
26. Chasset R., Thirion P. Proceeding of the Conference on Physics of Non-Crystalline Solids. Amsterdam: North-Holl and Publishing Co. 1965: 345.
27. Plazek D. J. J. Polym. Sci. Pol. Phy. 1966; 70: 2594.
28. Flory P. J. Principles of Polymer Chemistry. New York: Cornell University Press. 1953: 458-64.
29. Ferry J. D. Viscoelastic Properties of Polymers. 2nd ed. New York: John Wiley & Sons.1970.
30. John G. C., Philip P. Macromolecules. 1983; 16: 559-62.
31. Naunton J. S., Waring J.R.S. Trans. Inst. Rubb. Ind. 1939;14: 340.
32. Medalia A. I. Rubber Chem. Technol. 1978; 51: 437.
33. Payne A. R. J. Appl. Polym. Sci. 1962; 6:57.
34. Voet A., Cook F.R. Rubber Chem. Technol. 1967; 40:1364.
35. Sircar A. K., Lamond T. G. Rubber Chem. Technol. 1975; 48: 79.
36. Davey A. B., Payne A. R. Rubber in Engineering Practice. London: MaClaren & Son. 1964.
37. Dannenberg E. M. Ind. Eng. Chem. 1952; 44: 813.
38. Boonstra B. B., Medalia A.I. Rubber Chem. Technol. 1963; 36: 115.
39. Donnet J. P. Rubber Chem. Technol. 1996; 71: 323.
40. Payne A. R. J. Appl. Polym. Sci. 1965; 9: 3245.
41. Medalia A. I., Laube S. G. Rubber Chem. Technol. 1978; 51: 89.
42. Donnet J. P. Rubber Chem. Technol. 1996; 71: 323.
43. Payne A. R. J. Appl. Polym. Sci. 1963; 7: 873.

Copyright by Mahidol University

44. Batschinski A. J. Z phys. Chem. 1913; 84: 643.
45. Fujita H., Kishimoto A. J. Chem. Phys. 1961; 34: 393.
46. Akutagawa K. The effect of liquids on the dynamic properties of natural rubber as a fuction of strain, Ph.D. Thesis , Queen Mary and Westfield College, University of London.
47. Paul S. B., M. Jahn R. L., Andrew J. T. rubber. Chem. Technol. 1992; 65(4): 744-60.
48. Tinker A. J. Rubber Chem. Technol. 1995; 68(3): 461-80.
49. Flory P. J. J. Chem. Phys. 1942; 10: 51.
50. Huggins M. L. J. Chem. Phys. 1950; 46: 151.
51. Flory P. J. J. Chem. Phys. 1950; 18: 108.
52. Shinyoug K., Donghwa G., Changwoon N. J Appl. Polym. Sci. 1997; 65: 917-24.
53. Mullings L. J.Appl. Polym. Sci. 1959; 2(4): 1-7.
54. Abd-El-Messieh S.L., Abd-El-Nour K.N. J.Appl. Polym. Sci. 2003; 88: 1613-21.
55. Gerard K. J.Appl. Polym. Sci. 1963; 7: 861-71.
56. Sally A.G. Rubber Chem. Technol. 1998; 71(5): 958-65.
57. Southern E. Thomas A.G. J. Polym. Sci.: Pol. Chem. 1965; 3: 641-46.
58. Flory P.J., Rehner J. J. Chem. Phys. 1943; 11: 521.
59. Porter M. Rubber Chem. Technol. 1967; 40: 866.
60. Bauer R. F., Crossland A. H. Rubber Chem. Technol. 1988; 61(4): 585-93.
61. Bauer R. F., Crossland A. H. Rubber Chem. Technol. 1991; 64(2): 234
62. Studebaker M. L., Beatty J. R. Rubber Chem. Technol. 1974; 47: 803.
63. Alan N. G. Engineering with Rubber. 1st ed. New York: Oxford University Press. 1992.
64. Shigeo A., Hiromune K., Masao S., Keizo M. J. Appl. Polym. Sci. 1991; 43: 1253-7.
65. Curro J. G., Pincus P. Macromolecules. 1983; 16(4): 559-62.
66. Ferry J. D. Viscoelastic Properties of Polymers. 3rd ed. New York: John Wiley & Sons.1980.
67. Williams M. L., Landel R. F., Ferry J. D. J. Am. Chem. Soc. 1955; 77: 3701.
68. Stratton R. A. Ferry J. D. J. Phys. Chem. 1963; 67: 2781.

Copyright by Mahidol University

69. Hotta A., Terentjev E. M. J. Phys. Condens. Matter. 2001; 13: 11453-64.
70. Dickie R. A., Ferry J. D. J phys. Chem. 1966; 70 : 2594-1600.
71. Ferry J. D., Mancke R.G., Maekawa E., Oyanagi Y., Dickie R. A. J. Phys. Chem. 1964; 68: 3414-8.
72. Vogel H. Phys. Z. 1921; 22: 645.
73. Clarke S. M., Elias F., Terentjev E. M. Eur. Phys. J. E. 2000; 2: 335-41.
74. Jonason K., Vinoent E., Hammann J. P., Bouchaud J. P., Nordblad P. Memery and Phys. Rev. Letter. 1998; 81(15): 3243-6.
75. Hess W. M., Ban L. L., Mcdonal G. C. Rubber Chem. Technol. 1977; 50: 842.
76. Stickney P. B., Falb R. D. Rubber Chem. Technol. 1964; 37: 1299.
77. Blow C. M. Polymer. 1973; 14: 309.
78. Funt J. M. Z. Phys. Chem. 1988; 61: 842.
79. Dannenberg E.M. Rubber Chem. Technol. 1976;49 : 410.
80. Wolff S., Wang M. J., Tan E. H. Rubber Chem. Technol. 1993; 66: 163.
81. Herd C. R., McDolnald G. C., Hess W. M. Rubber Chem. Technol. 1992; 65: 107.
82. Medalia A. I. J. Colloid Interf. Sci. 1970; 32: 115.
83. Krausb G. Rubber Chem. Technol. 1971; 44: 199.
84. Donnet J. B., Voet A. Carbon black-Physics, Chemistry and Elastomer Reinforcement. Marcel Dekker. 1976.
85. Pike M., Watson W. F. J. Polym. Sci. 1952; 9: 229.
86. Gessler A.M. Rubber Age. 1964; 94: 598.
87. Mullins L., Tobin N. R. J. Appl. Polm. Sci. 1965; 9: 2993.
88. Harwood J. A. C., Payne A. R., Smith J. Rubber Chem. Technol. 1970; 43: 687.
89. Mullins L. Rubber Chem. Technol. 1970; 43: 687.
90. Bueche F. J. Appl. Polm. Sci. 1961; 5: 271.
91. Boonstra B. B. J. Appl. Polm. Sci. 1967; 11: 389.
92. Harwood J. A. C., Mullins L., Payne A. R. J. Appl. Polym. Sci. 1965; B3: 119.
93. Harwood J. A. C., Payne A. R. J. Appl. Polym. Sci. 1966; 10: 1203.
94. Tangpakdee J., Mizokoshi M., Endo A., Tanaka Y. Rubber Chem. Technol.1998; 71: 795-802.

Copyright by Mahidol University

95. Tangboriboonrat P., Sirichaiwat C. Plast. Rubber. Compos. Process Appl. 1996; 25: 340.
96. Tangboriboonrat P., Rakdee C. J. Appl. Polym. Sci.2001; 82: 489-98.
97. ASTMD 1076-88. Standard specification for rubber-concentrated, ammonia preserved, creamed and centrifuged natural latex. In: Annual book of ASTM standards. 1997; 9.01: section 9.
98. Lee A., Mckenna B. G. J. Polym. Sci. B.: Polym Phys. 1997; 35: 1167-74.
99. Curro J. G., Salazar E. A. Rubber Chem. Technol. 1977; 50(5): 895-905.
100. Joseph T. S. Scott W. C., Kenneth L. R. Rubber Chem. Technol. 2003; 76(4): 785-802
101. Akinay A. E., Brostow W., Castano V. M., Maksimov R., Olszynski P. Polymer. 2002; 43: 3593-3600.
102. Yano S. Rubber Chem. Technol. 1980; 53(4): 944-49.
103. Isono Y., Ferry J. D. Rubber. Chem. Technol. 1984; 57(5): 925-943.
104. Meinecke E. A., Maksin S. Rubber Chem. Technol. 1981; 54(4): 857-870.
105. Morton M. Rubber Technology. 2nd ed. New York: Van Nostrand Reinhold Company. 1973.

Copyright by Mahidol University

APPENDIX

Copyright by Mahidol University

APPENDIX A
Cure Characteristic Measurement

The vulcanization characteristic of compounded rubber was measured by using Oscillating Disc Rheometer (ODR). It is shown in Figure 4.4. The curve from ODR indicated cure time (τ_{90}) which was used to control in Hydraulic Hot Press by using 1 mm. thickness mould at 160°C, air pressure as 15 atm. The cure time (τ_{90}) of rubber specimen used in this study are shown in Table 1A-3A.

Table 1A: The cure time (τ_{90}) with different amount of carbon black

Material	Cure time (min)
NR-0CB	3.44
NR-10CB	3.04
NR-30CB	2.31
NR-60CB	2.05

Table 2A: The cure time (τ_{90}) with different amount of sulphur.

Material	Cure time (min)
NR-1S	4.02
NR-1.5S	3.16
NR-2.5S	2.48

Table 3A: The cure time (τ_{90}) with different type of carbon black.

Material	Cure time (min)
NR-N2	2.42
NR-N3	2.52
NR-N5	3.04
NR-N7	3.07

Copyright by Mahidol University

APPENDIX B

Crosslink Density

In this study, a physical method was chosen to determine the crosslink density of vulcanized rubber. It was measured by using INSTRON extensometer apparatus. INSTRON extensometer apparatus was shown in Figure 4.8. Crosslink density could be calculated by using Equation 2.54-2.57. The cosslink density of rubber specimen used in this study are shown in Table 1B-4B.

Table 1B: Crosslink density (mol. g^{-1}) with different amount of carbon black

Material	Crosslink density (mol. g^{-1})
NR-0CB	7.32E-06
NR-10CB	8.79E-06
NR-30CB	5.85E-06
NR-60CB	6.88E-06

Table 2B: Crosslink density (mol. g^{-1}) with different amount of sulphur.

Material	Crosslink density (mol. g^{-1})
NR-1S	7.01E-06
NR-1.5S	9.79E-06
NR-2.5S	1.14E-05

Table 3B: Crosslink density (mol. g^{-1}) with different type of carbon black.

Material	Crosslink density (mol. g^{-1})
NR-N2	9.76E-06
NR-N3	8.48E-06
NR-N5	8.79E-06
NR-N7	9.56E-06

Copyright by Mahidol University

Table 4B: Crosslink density (mol. g^{-1}) with different type of interaction between carbon black and rubber.

Material	Crosslink density (mol. g^{-1})
NR-conv	8.21E-06
NR-mast	9.89E-07

Copyright by Mahidol University

APPENDIX C

Mooney Viscosity Measurement

The viscosity of compound rubber was used to confirm the mixing quality by using Mooney Shearing Disk Viscometer at 100°C for 7 min. It was shown in Figure 4.12. Mooney viscosity (MS1+4) of rubber specimens used in this study are shown in Table 1C-3C.

Table 1C: Mooney viscosity (MS1+4) with different amount of carbon black.

Material	Mooney viscosity (MS1+4)
NR-0CB	32.12
NR-10CB	32.90
NR-30CB	37.13
NR-60CB	46.56

Table 2C: Mooney viscosity (MS1+4) with different amount of sulphur

Material	Mooney viscosity (MS1+4)
NR-1S	28.23
NR-1.5S	29.40
NR-2.5S	28.24

Table 3C: Mooney viscosity (MS1+4) with different carbon black

Material	Mooney viscosity (MS1+4)
NR-N2	27.35
NR-N3	28.32
NR-N5	32.90
NR-N7	28.29

Copyright by Mahidol University

BIOGRAPHY

NAME	Ms. Chuleekorn Tangjai
DATE OF BIRTH	October 12, 1980
PLACE OF BIRTH	Bangkok, Thailand
INSTITUTIONS ATTENDED	Mahidol University, 1997-2000: Bachelor of Science (Chemistry) Mahidol University, 2001-2004: Master of Science (Polymer Science and Technology)
POSITION&OFFICE	Institute of Science and Technology for Research and Development, Salaya Campus, Mahidol University Nakhon Pathom, Thailand Position: Student Tel. 0-2889-3116 E-mail: iam_jor@hotmail.com
HOME ADDRESS	81/12 Bangkroy-Sainoi Road Bangbuathong, Nonthaburi, Thailand 11110 Tel: 0-2903-6035

Copyright by Mahidol University